(E75-10245) ARCTIC AND SUBARCTIC ENVIRONMENTAL ANALYSES UTILIZING ERTS-1 IMAGERY Final Report, Jun. 1972 - Feb. 1974 (Army Cold Regions Research and Engineering Lab.) 128 p HC $5.75

N75-21767

CSCL 08L G3/43

Unclas
00245

COVER PHOTO: Open pack ice in Norton Sound approximately 80 km south of Nome, Alaska. 4x enlargement from the southwestern quarter of Figure 42. ERTS MSS band 7 image 1205-21595, acquired 13 February 1973.

ARCTIC AND SUBARCTIC ENVIRONMENTAL ANALYSES UTILIZING ERTS-1 IMAGERY

Principal Investigator
Duwayne M. Anderson (DE 329)

Co-Investigators
Harlan L. McKim
Lawrence W. Gatto
Richard K. Haugen
William K. Crowder
Charles W. Slaughter
Thomas L. Marlar

Final Report
June 1972-February 1974

U.S. Army Cold Regions Research and Engineering Laboratory
Hanover, New Hampshire 03755

Prepared for
GODDARD SPACE FLIGHT CENTER
Greenbelt, Maryland 20771

ARCTIC AND SUBARCTIC ENVIRONMENTAL ANALYSES UTILIZING ERTS-1 IMAGERY

Principal Investigator
Duwayne M. Anderson (DE 329)

Co-Investigators

Harlan L. McKim
Lawrence W. Gatto
Richard K. Haugen
William K. Crowder
Charles W. Slaughter
Thomas L. Marlar

U. S. Army Cold Regions Research and Engineering Laboratory
Hanover, New Hampshire 03755

Final Report
June 1972-February 1974

Prepared for

GODDARD SPACE FLIGHT CENTER
Greenbelt, Maryland 20771

1. Report No.	2. Government Accession No.	3. Recipient's Catalog No.
4. Title and Subtitle ARCTIC AND SUBARCTIC ENVIRONMENTAL ANALYSIS UTILIZING ERTS-1 IMAGERY		5. Report Date February 26, 1974 6. Performing Organization Code
7. Author(s) Duwayne M. Anderson, et al.		8. Performing Organization Report No.
9. Performing Organization Name and Address U. S. Army Cold Regions Research and Engineering Laboratory P. O. Box 282, Hanover, NH 03755		10. Work Unit No. 11. Contract or Grant No. S-70253-AG
12. Sponsoring Agency Name and Address Technical Monitor - Edmund Szjana		13. Type of Report and Period Covered Type III June 1972-Feb 1974 14. Sponsoring Agency Code
15. Supplementary Notes		

16. Abstract

ERTS-1 imagery provides a means of distinguishing and monitoring estuarine surface water circulation patterns and changes in the relative sediment load of discharging rivers on a regional basis. Physiognomic landscape features were used as geologic and vegetative indicators in preparation of a surficial geology, vegetation, and permafrost map at a scale of 1:1 million using ERTS-1 band 5 imagery. The detail available from ERTS-1 imagery at 1:1 million scale compared favorably with the detail available on U.S. Geological Survey Miscellaneous Geologic Investigation Maps at a scale of 1:250,000. Physical boundaries mapped from ERTS-1 imagery in combination with ground truth obtained from existing small scale maps and other sources resulted in improved and more detailed maps of permafrost terrain and vegetation for the same area. Comparison of ERTS-1 and Mariner imagery has revealed that the thermokarst depressions found on the Alaskan North Slope, polygonal patterns on the Yukon River Delta, and the alas topography in the Yakutian region of Siberia are possible analogs to some Martian terrain features. Snowpack cover within a research watershed has been analyzed and compared to ground data. Large river icings

17. Key Words (Selected by Author(s))	18. Distribution Statement		
19. Security Classif. (of this report) Unclassified	20. Security Classif. (of this page) U	21. No. of Pages	22. Price*

*For sale by the Clearinghouse for Federal Scientific and Technical Information, Springfield, Virginia 22151.

No. 16 (continued)

along the proposed Alaska pipeline route from Prudhoe Bay to the Brooks Range have been monitored. Sea ice deformation and drift northeast of Point Barrow, Alaska have been measured during a four day period in March and shore-fast ice accumulation and ablation along the west coast of Alaska have been mapped for the spring and early summer seasons. These data will be used for route and site selection, regional environmental analysis, identification and inventory of natural resources, land use planning, and in land use regulation and management.

PREFACE

This report documents the results of research undertaken with support provided by the National Aeronautics and Space Administration under Contract S-70253-AG. The principal theme of the report is the evaluation of imagery aquired from a low altitude polar orbiting satellite in arctic and subarctic environmental analyses. This is a preliminary assessment representing an experience of approximately eighteen months duration. We have evaluated the potential of ERTS-1 imagery in: (1) mapping and analyzing sediment deposition and distribution in harbors, inlets, and docking facilities in Cook Inlet; (2) permafrost terrain mapping in Alaska as inferred from surficial geology, topographic and vegetative patterns; (3) identifying and locating terrestrial permafrost terrain analogs comparable to those found in Mariner imagery of Mars; (4) a correlation of the snowpack cover and snow melt regime of the Caribou-Poker Creeks watershed with stream runoff, and (5) the inventory of icings on the Chena River.

Photointerpretation procedures employed in this investigation were similar for all sections of the study. Direct analysis of bulk and precision processed positive transparencies and 9x9 prints was a common practice. Mapping was accomplished in several ways; in some instances it was done directly on the transparencies or prints, or on acetate overlays. In other instances a Bausch and Lomb Zoom Transfer Scope was used to project images derived from contrast enhanced photo products directly on a base map. Photo mosaics were sometimes produced from 9 x 9 prints supplied by NASA but more often a second generation print with controlled image density was produced as an enlargement at a consistent scale for use as the mapping base. Stereo viewing was used in most cases where image endlap and sidelap permitted and mapping uncertainties dictated. Preliminary maps based solely on image interpretation were prepared and subsequently compared with published maps and other reference data. In the end, most of the mapping and feature identification was done on the 1:1 million scale, single band ERTS prints or transparencies. However, false color composites were utilized near the end of the study as they became available. Activities to acquire "ground truth" included under-flight and post-flight oblique aerial photographic sorties and ground-based observations of selected phenomena.

The ERTS-1 system performance exceeded expectations. The 70 m resolution actually achieved makes possible the recognition and identification of a great many regional features and phenomena not previously feasible from lower altitude remote sensing platforms. We have found it possible to identify and map major estuarine circulation patterns, water masses, the distribution of tidal flats, and areas of sediment deposition in Cook Inlet. The areal distribution of four permafrost terrain units was mapped in a 153,400 km^2 test site in interior Alaska and in the area

south of Fairbanks. The results obtained were similar to those resulting from field observations but the regional map produced solely from the ERTS-1 imagery was more accurate in delineation. As a preliminary part of the permafrost mapping, surficial geology and vegetation maps were also made; these also were found to be more accurate in unit delineation than previously available versions. These results are immediately applicable to route and site selections for the Nome to Kobuk road in western Alaska. Permafrost maps prepared in this way will also be useful in regional environmental interpretation and urban and land use planning, in regulation and management in the areas of rapid development in Alaska.

ERTS imagery has been used to monitor snow accumulation and ablation and has been favorably compared to ground truth data. The inventorying and monitoring of large river icings in northern Alaska was also shown to be feasible. The need for information on ice patterns and movements for purposes of navigation and construction of offshore facilities to support development of the oil and gas fields of the north slope led to a quick analysis of sea and shore-fast ice in the Arctic Ocean. The synoptic, regional perspective of ERTS imagery was shown to be well suited for measurements of shore-fast ice and sea ice deformation. A two dimensional deformation analysis was done for a four day period in March 1973; this is the first application of satellite imagery for this purpose known to us. Shore-fast ice growth, the development of the shear zone and breakup along the western coast of Alaska was another mapping exercise accomplished during this investigation.

Based on the experience acquired during the preceding eighteen months, this investigation team considers it appropriate to formulate several recommendations: First, ERTS-1 should continue to be fully utilized so long as it remains operational. Second, there is a need to emphasize and improve provisions for technology transfer within user organizations. Greater awareness and participation from the operational personnel of user agencies is needed. This is primarily the responsibility of the user agencies but NASA can and should take the lead in stimulating a greater awareness of this requirement and aid in accomplishment. Third, a provision for a direct downlink for some users of DCP's would make the ERTS-1 system "operational" and enhance its utility for many present and potential users. Finally, the logical successors of the ERTS program would be the establishment of geostationary, operational satellites, as have been proposed in the GOES program and a family of operational, low altitude polar orbiting satellites of the ERTS type. These satellites should be specialized for distinct disciplines and carry active and passive sensors, have data relay and direct downlink capability and orbit at altitudes appropriate for separate or related disciplines.

ACKNOWLEDGMENTS

The authors express their appreciation to the following individuals at the U.S. Army Cold Regions Research and Engineering Laboratory: Fleetwood Koutz for acquisition of a ground truth data and low-altitude photography; Anthony Petrone for assistance in the analysis of the Cook Inlet imagery; Philip Splett for contributions in the comparisons between ERTS-derived and existing vegetation maps; Martha Greer for mapping shore-fast ice; Carolyn Merry for assistance in the analysis of snow cover-runoff data; Harold Larsen, Eleanor Huke, Carl Martinson and Matthew Pacillo for their assistance in layout and drafting; Robert Demars for photographic processing; Thomas Vaughan for cover design and graphics; Stephen Bowen and Mona McDonald for technical editing; and Connie Fish for reproduction of reports throughout this project.

Computer enhancement of ERTS imagery was accomplished with the assistance of several individuals at the Jet Propulsion Laboratory in Pasadena, California. Dr. Alexander Goetz provided computer time and suggested processing techniques to enhance features of interest. Mr. Peter Paluzzi of the Image Processing Laboratory spent several days in preparing computer programs, describing the processing techniques and acquiring enhanced photographs. Mr. Alan Gillespie made several useful suggestions for computer processing. Their assistance is greatly appreciated.

Ground truth data for the analyses in Cook Inlet were provided by Dr. Fredrick Wright, University of Alaska Marine Institute, Messrs Isiah Fitzgerald, Coastal Mapping Division and Robert Muirhead, Oceanographic Division, National Ocean Survey, National Oceanic and Atmospheric Administration.

TABLE OF CONTENTS

ILLUSTRATIONS

TABLES

Addenda

In general only one ERTS band is reproduced in this report. However, many of the conclusions are fully justified only by inspection of two or more spectral bands. In addition, the offset reproduction process has obscured some of the features discussed in the text or annotated on the photographs. This difficulty is particularly troublesome in the following figures:

5. The Cook Inlet mosaic was made with ERTS band 6 imagery acquired on 3 and 4 November 1972 when the sun angle was only 12^{o}. These were the first cloud-free images of the entire inlet but the low sun angle caused the patterns on the flat water surface to be subdued especially in bands 4 and 5. It was determined by inspection that band 6 provided the best rendition of coastline configuration and surface patterns. Interpretations of the features and patterns in figures 8, 11 and 13 were made utilizing all bands. However, to facilitate visualizing the relationships throughout the inlet the boundaries and features were superimposed on the band 6 mosaic and may not be distinguished in these representations.

8. The legend may be misleading to some. Actually, extensive tidal flats are shown as white areas and river plumes are outlined by white lines.

11 b. During final review it was pointed out that some confusion may result because the October boundary (small dots) was drawn from patterns observed on two successive days, not one as in November. This was necessitated because images were partially obscured by clouds. However, the observations on these two successive days were made at virtually identical tidal stages. In the areas of image overlap the two lines coincide, suggesting that the regional tidal changes from day to day were less significant than those over an 18 day period. This is in fact the conclusion illustrated in 11b.

p. 53, para. 2, lines 10-13 should read, "Alpine vegetation occurs in the highest, steepest areas. In the transition between the "m" and "u" units, black spruce and paper birch occur on north-facing slopes, and on south-facing slopes white spruce, paper birch, quaking aspen and alder are most common".

p. 104, line 7 should read, "as levied by the Congress on the Corps of Engineers".

1.0 Introduction

1.1 Background

In the research proposal leading to initiation of this project it was pointed out that two of the deficiencies inhibiting arctic and subarctic environmental research have been the absence of long-term observational data and its sparse geographical coverage. Synoptic studies of environmental topics have been either impossible or prohibitively expensive. Problems of resource utilization have recently been dramatized in Alaska, where the lack of basic environmental data and understanding has coincided with rapidly mounting pressures for extensive development of extractive industries, transportation systems, and population centers. Existing information on river, lake, and coastal hydrology, and on the distribution, properties and behavior of permafrost terrain, for example, is insufficient for a rational understanding of the various environments and their interrelationships. The history of construction and technological development in these areas contains many dramatic illustrations of failures due to difficulties caused by environmental extremes and the unforeseen consequences of disturbing established environmental equilibria.

Two examples were cited in that proposal to illustrate this. The proposal to construct a trans-Alaska pipeline several years ago created an urgent need for the acquisition of environmental data throughout the state. Voluminous data were obtained with great effort by many individuals but at a high cost. We now know that some of these data, especially data pertaining to route selection and regional patterns of soils, vegetation, and the distribution of permafrost, could have been acquired at considerable savings in time, money and manpower if ERTS imagery had been available then. Now that the decision to begin construction on the pipeline has been made, this need again is critical. As an illustration, the top three research topics recently identified to the National Science Foundation by the Alaska Oil and Gas Association are: 1) ice forces, features and movements, 2) permafrost distribution and behavior, and 3) landfast ice surveys. The need to develop remote sensing methods to rapidly map the distribution and properties of sea ice, permafrost and shore-fast ice in Alaska was given high priority at the Second International Conference on Permafrost held last summer in Yakutsk, Siberia. This need is also identified by the National Science Foundation CPR ad hoc committee on priorities in permafrost research. Accurate, up-to-date maps of permafrost and shore-fast ice would be very useful in final route selections, selection of pumping stations and offshore loading facility sites, and the planning and implementation phases of pipeline and facilities construction.

Another example of a situation where the availability of ERTS imagery could have resulted in cost savings and better utilization of resources is the harbor development in Dillingham. Only after construction was it discovered that the regional siltation patterns and rates were such that the rapid influx of sediment threatened to render the new facility useless within a short time. Continuous dredging is now required to maintain this harbor. A more favorable site could easily have been selected and a serious and expensive problem avoided, had better information on local circulation patterns been available. Similar projects in other localities now are in the planning stages. Based on our experience, imagery available from the ERTS system can help avoid these and many other difficulties.

1.2 Objectives

The specific objectives set for this investigation were as follows:

- Analyze and map the sediment deposition in harbors, inlets, and docking facilities in the Cook Inlet.
- Map the permafrost areas of Alaska as inferred by vegetative patterns. Compare major tonal and textural permafrost patterns with Mariner imagery.
- Correlate the snow pack cover of Caribou-Poker Creek with stream runoff.
- Map and inventory the icing on the Chena River.

1.3 Project history

This project was performed in three phases: Phase I - Data Analysis Preparation (23 June 1972 - 31 August 1972); Phase II - Preliminary Data Analysis (1 September 1972 - 31 October 1972); and, Phase III - Continuing Data Analysis (1 November 1972 - 26 January 1974). A chronological listing of the events that occurred and the milestones that were reached during the project is presented in Table 1. Reports published and presentations made during the project are summarized in Table 2. At the termination of Phase III in June 1973 a request for a no cost extension of Phase III was submitted; approval was made on 15 August 1973. The basis for requesting this extension was outlined in the Second Type II, Semi-annual Progress Report submitted 13 November 1973. During this six month, no cost extension, additional surficial geology, vegetation and permafrost terrain maps were prepared for an area near Fairbanks Alaska; a more detailed investigation was made of Martian terrain analogs in northern Alaska and Yakutsk, Siberia; the results of an earlier analysis of surface circulation and sediment distribution in Cook Inlet were verified, and, the correlation of snow ablation and stream runoff in the

Caribou-Poker Creeks watershed was accomplished. In addition, a measurement of sea ice movement and deformation in the Beaufort Sea for a 4 day period and the mapping of shore-fast ice on the northwest coast of Alaska were accomplished as ancillary investigations.

As the new completion date for the project, 26 January 1974, approached, pressures for rapid development of the Alaskan North Slope petroleum reserves during the latter part of 1973 were mounting. Recognizing the possibility of immediate application of the data and procedures developed during this project, we were encouraged to submit a proposal to continue our effort in mapping permafrost, surveying shore-fast ice and monitoring stream icings. This proposal was submitted on 8 January 1974. Completion of this report was delayed until we received official notification on 6 May 1974 that it was not possible to approve a further extension. We submitted our outline for a NASA Type III Final Report for approval on 13 May 1974; approval of the outline was received on 11 June.

Table 1. Project history, chronological listing of events and milestones.

Milestones	1972*			1973						1974					
	4	5	6	1	2	3	4	5	6	1	2	3	4	5	6
PHASE I: Data Analysis Preparation (23 June - 31 August)	▬														
Literature search and survey	▲														
Acquisition of supportive reports, data and photography	▲														
Acquisition of specialized equipment	▲														
Antech A-12 planimetric color densitometer															
Spectral Data Corporation multispectral viewer															
Bausch and Loom zoom transfer scope															
Stereoscopes															
Mapping/drafting equipment															
Launch ERTS-1	▲	23 July													
Test analyses with U-2 imagery	▲														
Development of USACRREL data handling procedures	▲														
Initial scene verification mission-satellite under flights	▲	1-10 August													
Development of interpretive keys															
Acquisition of low altitude, aerial photography															
Coordinate with Gilmore Creek Tracking/Data Acquisition															
Facility															
Submission of abstract for Eighth International Symposium on Remote	▲	26 July													
Sensing of Environment, 2-6 October at University of Michigan															
Submission of 1st Type 1, Bimonthly Progress Report (23 June -23Aug	▲	23 August													
Receipt of first ERTS images		▲ 31 August													
PHASE II: Preliminary Data Analysis (1 Sep - 31 Oct)		▬													
Evaluation of imagery and data analysis plan (DAP) as proposed		▲													
Processing of first two months of imagery and ancillary data		▬													

Remarks

*Calendar year divided into bimonthly periods

Table 1 (con't)

Milestones	1972*			1973						1974					
	4	5	6	1	2	3	4	5	6	1	2	3	4	5	6
Preparation of a DAP with slight changes in analysis plan															
Preliminary thematic mapping on first images															
Presentation of a "Quick Look" report at First ERTS-1 Symposium				29 September											
Presentation at Eighth Remote Sensing Symposium				2-6 October											
Preparation of north central Alaska photomosaic for thematic mapping															
Submission of 2nd Type I, Bimonthly Progress Report (23 Aug - 23 Oct)				23 October											
PHASE III: Continuing Data Analysis (1 Nov 72 - 30 Jun 73)															
"In-House" presentation of progress at USACRREL Colloquium				November											
Submission of abstract for University of Tennessee Symposium				1 December											
Submission of DAP				5 December											
DAP approval: official start of Phase III				26 December											
Thematic mapping in north central Alaska															
Article on USACRREL ERTS investigation published in Army R/D Magazine				December											
Submission of 1st Type II, Semi-Annual Progress Report (23 June - 23 Dec)				23 December											
Preliminary surficial geology, vegetation and permafrost terrain maps for north central Alaska completed				January											
Identification and interpretation of geologic, geomorphic, vegetative and cultural features															
Thematic mapping in Cook Inlet															
Analysis of Mars terrain analogs															
Presentation of ERTS results at Dartmouth College meeting of the Society of Sigma Xi				17 January											

Remarks

*Calendar year divided into bimonthly periods

Table 1 (con't)

Milestones	1972* 4	5	6	1973 1	2	3	4	5	6	1974 1	2	3	4	5	6
Submission of abstract for Second ERTS-1 Symposium				▲ 9 February											
Submission of 3rd Type I, Bimonthly Progress Report (23 Dec - 23 Feb)				▲ 23 February											
Presentation of research progress at Dartmouth College Dept. of Earth Sciences				▲ 28 February											
Correlation of snow cover and runoff in Poker-Caribou Creeks				▬▬											
Inventory of icings on Chena River and north slope				▬▬											
Presentation at Second ERTS-1 Symposium				▲ 5-9 March											
Presentation at Office of Chief of Engineers (OCE), Washington, D. C.				▲ 9 March											
Presentation at the University of Tennessee Symposium				▲ 26-28 March											
Presentation at New England Junior Science Symposium				▲ 5 April											
Submission at 4th Type I, Bimonthly Progress Report (23 Feb - 23 Apr)				▲ 23 April											
USACRREL Technical Report 241 published				▲ June											
Ancillary investigation - National Dam Inventory				▬▬											
Presentation at Water Resources International Symposium				▲ 11-14 June											
USACRREL Special Report 183 published				▲ June											
Request of 6 month, no cost extension of Phase III				▲ 29 June											
Discontinue receipt of ERTS imagery				▲ 27 July											
Submission of chapter for the OCE Remote Sensing Handbook				▲ July											
Renewal of ERTS imagery delivery				▲ 7 August											
Approval for no cost extension				▲ 15 August											
EXTENSION OF PHASE III: Continuing Data Analysis (1 Jul 73-26 Jan 74)							▬▬	▬▬	▬▬						
Submitted proposed changes in reporting dates for extension								▲ 12 September							
Ancillary investigation- Analysis of Sea Ice Movement and Deformation							▬▬	▬▬							

Remarks

***Calendar year divided into bimonthly periods**

Table 1 (con't)

Milestones	1972* 4	5	6	1973 1	2	3	4	5	6	1974 1	2	3	4	5	6
Thematic mapping in Fairbanks area, Alaska							■	■	■						
Verification of results in Cook Inlet analysis							■	■	■						
Continue investigation of Mars terrain analogs							■	■	■						
Correlate ground truth with ERTS imagery							■	■							
Mapping of icings/collaborate with Canadian and University of Alaska Investigators								■							
Monitor shorefast ice accumulation/ablation								■	■						
Submission of 5th Type I, Bimonthly Progress Report (23 Jun-23 Aug)								▲	5 October						
Presentation at meeting of Committee on Polar Research, National Academy of Sciences								▲	26 October						
Project status review for Environmental Research Panel, Goddard Space Flight Center								▲	30 October						
Submission of 6th Type I, Bimonthly Progress Report (23 Aug-23 Oct)									▲ 13 November						
Submission of 2nd Type II, Semi-Annual Progress Report (23 Dec 72-23 June 73)									▲ 13 November						
Presentation at U.S. Army Remote Sensing Symposium									▲ 23-30 November						
Presentation at Interdisciplinary Symposium on Advanced Concepts + Techniques in Study of Snow/Ice Resources									▲ 3-7 December						
Request for acquisition of winter ERTS imagery									▲ 8 December						
Presentation at Third ERTS-1 Symposium									▲ 10-13 December						
Approval for changed reporting requirements										▲ 4 January					
Submission of 7th Type I, Bimonthly Progress Report (23 Oct-23 Dec)										▲ 7 January					
Submission of proposal (cost estimates included) for extension of ERTS-1 investigation										▲ 8 January					
Approval for acquisition of winter ERTS imagery										▲ January					

Remarks

*Calendar year divided into bimonthly periods

Table 1 (con't)

Milestones	1972*			1973						1974					
	4	5	6	1	2	3	4	5	6	1	2	3	4	5	6
ERTS image enhancement with ERTS CCT at J. P. L. - Mars analogs										▲	21-25 January				
Letter requesting clarification of ERTS-1 project extension proposal										▲	25 February				
Submit requested clarification										▲	7 March				
Extension proposal refusal											▲	6 May			
Submission of outline for Type III, Final Report											▲	13 May			
Approval of outline												▲	11 June		
Submission of Draft of Type III, Final Report (23 Jun 72 - 31 Aug 74)									9 September					▲	
Approval of draft for Type III, Final Report									3 October					▲	
Submission of Type III, Final Report									3 December						▲

Remarks

*Calendar year divided into bimonthly periods

Table 2. Reports prepared and presentations made during the project.

Reports Published

Army Research and Development News Magazine, Vol. 13, No. 8, December 1972 "ERTS-1 Imagery.....Arctic and Subarctic Environmental Analysis"

USACRREL Special Report 183, June 1973, "The Use of ERTS-1 Imagery in the National Program for the Inspection of Dams"

USACRREL Technical Report 241, June 1973, "An ERTS view of Alaska: Regional Analysis of Earth and Water Resources Based on Satellite Imagery"

Oral Presentations

Goddard Space Flight Center symposium, 29 September 1972, "Delineation of Permafrost Boundaries and Hydrologic Relationships" *

8th International Symposium on Remote Sensing of Environment, University of Michigan, 2-6 October 1972 "Cold Regions Environmental Analysis Based on ERTS-1 Imagery"*

USACRREL Colloquium, November 1972, "Preliminary Findings Utilizing ERTS-1 Imagery of Alaska"

Meeting of the Dartmouth College Chapter of the Society of the Sigma Xi, January 17, 1973, "Satellite Technology at USACRREL"

Dartmouth College Department of Earth Sciences meeting, 28 February 1973, "Arctic and Subarctic Environmental Analysis Utilizing ERTS-1 Imagery"

Second ERTS-1 Principal Investigator's Symposium, Goddard Space Flight Center, 5-9 March 1973, "Sediment Distribution and Coastal Processes in Cook Inlet, Alaska"*

Office of Chief of Engineers Review, sponsored by Systems Analysis Branch, 9 March 1973, "Land Use and Pollution Patterns on the Great Lakes"; "Sediment Distribution and Coastal Processes in Cook Inlet, Alaska"; and, "The Utility of ERTS-1 Imagery in Mapping Geology, Vegetation and Permafrost Distribution in Alaska"

* Written report appears in the published volume for the symposium

Second Annual Remote Sensing of Earth Resources Conference, sponsored by the University of Tennessee Space Institute, 26-28 March 1973, "The Use of ERTS-1 Imagery in the Regional Interpretation of Geology, Vegetation, Permafrost Distribution and Estuarine Processes in Alaska"*

New England Junior Science and Humanities Symposium sponsored by the University of Massachusetts Department of Engineering, 5 April 1973, "The Use of ERTS-1 Imagery in the Analysis of Cold Regions Environments"

Remote Sensing of Water Resources International Symposium in Burlington, Ontario, Canada, 11-14 June 1973, "The Use of ERTS-1 Imagery in the National Program for the Inspection of Dams"*

Meeting of the Committee on Polar Research, National Academy of Sciences, convened at the National Center for Atmospheric Research (NCAR), Boulder, Colorado, 26 October 1973, "The Use of ERTS-1 Imagery in Arctic Research"

Project status review of the ERTS-1 investigation, "Arctic and Subarctic Environmental Analysis Utilizing ERTS-1 Imagery" given before the Environmental Research Panel, convened by NASA at Goddard Space Flight Center, 30 October 1973.

U.S. Army Corps of Engineers Remote Sensing Symposium, 26-30 November 1973, L.B. Johnson Space Center, Houston, Texas, "Coastal Processes" and "Discrimination of Water Boundaries" session.

Interdisiplinary Symposium on Advanced Concepts and Techniques in the Study of Snow and Ice Resources, 3-7 December 1973, "Mesoscale Deformation of Sea Ice from Satellite Imagery."*

Third ERTS-1 Principal Investigator's Symposium, Goddard Space Flight Center, 10-13 December 1973, "Applications of ERTS-1 imagery to terrestrial and marine environmental analyses in Alaska".*

2.0 Approach

2.1 Test sites

The distribution of the several categories of permafrost in central Alaska, where its occurrence is discontinuous, in general is not well known. Small area studies of permafrost distribution and seasonal thaw regime based on large scale air photo interpretation have been accomplished, but the methods employed require extensive ground examination and are not readily applicable to rapid surveys of large areas. To test the feasibility of detailed regional analysis, a 10 scene photo mosaic was constructed of a 153, 400 km^2 area in north central Alaska (area 18, Fig. 1). Surficial geology, vegetation and permafrost terrain units were mapped from this photo mosaic. Seven surficial geology, eight vegetative cover, and four permafrost terrain units were defined and delineated. Permafrost units were mapped from textural and tonal patterns related to surficial geology and vegetation. The mapping techniques developed during the feasibility study were then used to extend the mapping of surficial geology, vegetation, and permafrost terrain in an area of approximately 4200 km^2 south of Fairbanks, Alaska (in area 19, Fig. 1) from a 4X enlargement of MSS image 1103-20502, band 5.

Accurate maps of permafrost including shore-fast ice are valuable in route selection, selection of pumping stations and offshore loading facility sites, and in the planning and implementation phase of pipeline and facilities construction. To augment permafrost mapping, shore-fast ice was identified, delineated and monitored along the Alaskan coast from Point Barrow to Cape Krusenstern (area 29, Fig. 1) from imagery acquired during the late winter, 1973 and the early spring of 1974.

The Caribou-Poker Creek watershed (in areas 19 and 53, Fig. 1) was designated as the study site for a test of a possible correlation between the extent of snowpack cover and stream runoff. This watershed is situated in the Yukon-Tanana Uplands of Central Alaska. It is considered typical of the intermountain plateau physiographic province of this region. The complete catchment area is only 103 km^2 and constitutes a very small portion of a 34,225 km^2 ERTS scene. Thus it must be considered as a single point of reference for the purpose of this comparison.

The Chena River watershed (in areas 19 and 53, Fig. 1) was selected as a site for testing the feasibility of using ERTS imagery for identification and inventory of stream icings. Beginning in January, the Chena watershed was monitored for the formation of icings on a monthly basis by surface vehicles and light aircraft. No major icings were observed until late March during the 1972-1973 season. However, on the North Slope, icings were observed and monitored along the proposed Alaskan pipeline route from Prudhoe Bay to the Brooks Range.

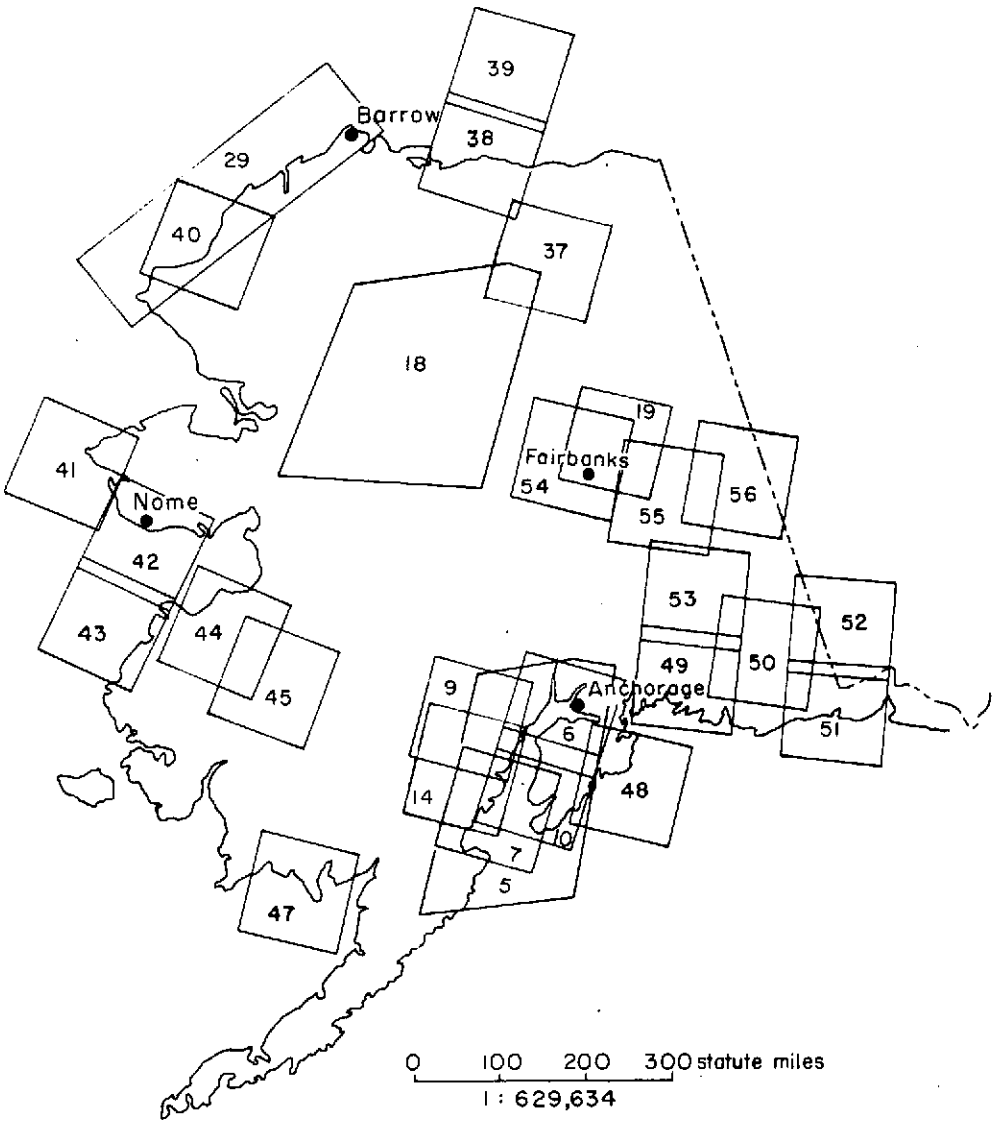

Figure 1. Site locations (the numbers refer to figures in this report).

A 6 scene photo mosaic was constructed of the Cook Inlet region (area 5, Fig. 1) to aid in the hydrologic and oceanographic analyses of this cold water, tidal estuary in south central Alaska. Surface circulation patterns, tidal flat configuration, suspended sediment distribution and water mass boundaries were delineated and interpreted on this mosaic. Oceanographic processes have also been observed on several ERTS scenes of other coastal areas in Alaska.

A need for a rapid method of assessing sea ice deformation and drift has been generated by the development of the North Slope oil reserves, subsequent construction of offshore docking facilities and increased utilization of northern sea transportation routes. As an ancillary investigation, sequential deformation and drift of 14,000 km^2 of the Arctic pack ice, approximately 90 km northeast of Point Barrow, Alaska were followed during a four day period from 19-22 March 1973. A quantitative analysis was performed illustrating that valuable, detailed deformation and drift data are available from sequential ERTS imagery at favorable locations and times.

All the ERTS imagery was searched for terrestrial analogs of Martian terrain and compared to Mariner 9 imagery. Detailed examinations were made of the thermokarst depressions of the Alaskan north slope, the polygonal patterns on the Yukon Delta, the pingos of the Yukon-Tanana Uplands and a preliminary examination was made of the alas topography in the Yakutian region of Siberia.

The identification and interpretation of other physical and cultural features was accomplished on a large number of individual scenes of selected areas throughout Alaska (Table 3). A number of these scenes were chosen as representative of the major physiographic provinces of the state (Wahrhaftig 1965); some are annotated and reproduced in this report.

Table 3. Selected scenes of physiographic provinces in Alaska.

Physiographic provinces	Figure numbers in this report
Arctic coast and foothills	37, 38,
Seward Peninsula	41, 42
Yukon-Kuskokwim coastal lowland and Nulato Hills	43, 44, 45
Ahklun Mountains and Nushagak-Bristol Bay lowland	47
Kenai-Chugach Mountains	5, 6, 7, 10
Gulf of Alaska coast	48, 49, 51
St. Elias Mountains	51, 52
Wrangell Mountains	50, 53
Yukon-Tanana Upland and Tanana-Kuskokwim lowland	19, 54, 55, 56

2.2 USACRREL data handling and analysis

Bulk (system corrected) 70 mm and 9.5 in. imagery was received from NASA and a preliminary screening performed. Following the initial screening, precision and special processed data of certain carefully selected scenes were requested from the NASA Data Processing Facility. Imagery was indexed and filed in a systematic way to facilitate rapid accessibility and retrieval throughout the investigation. The cataloging procedure (code given in Fig. 2) was as follows:

1. "Footprints" of all images received during each 18 day cycle were plotted on a base map of Alaska (scale 1:2,500,000). A separate map thus resulted for each cycle.

2. An alphabetical designation was assigned to each orbit in a cycle.

3. A numerical designation was given to each scene.

4. The cycle number, orbit designation, scene number, product type, product format, and sensor band for each scene were then written on the "Footprint" map and on each image.

5. All imagery was filed sequentially according to cycle, orbit, and scene numbers.

The techniques and procedures used for interpretation and analysis of the ERTS imagery were similar in all sections of the investigation (Fig. 3). Bulk and precision processed data, photo mosaics produced from NASA products and in-house reproductions were used in direct analysis and mapping. Stereo viewing was used when image endlap and sidelap permitted. Ground truth activities included acquisition of under flight and post-flight oblique aerial photography and measurement of temperature, salinity and suspended sediment concentration in the marine studies. Data from all phases of the study have been published in reports, symposium proceedings and journal articles.

As a demonstration to illustrate the feasibility of rapidly producing accurate thematic maps directly from ERTS-1 imagery, surficial geology, vegetation and permafrost terrain maps were prepared on acetate overlays over bulk imagery at a 1:1,000,000 scale. Mapping was accomplished without reference to published maps or other available ground truth. In addition, six sequential maps of shore-fast ice distribution were prepared with a Bausch and Lomb Zoom Transfer Scope to project the ERTS image directly on a base. These maps illustrate the accumulation and ablation of shore-fast ice along the northwest coast of Alaska from March to July 1973. The movement and deformation of sea ice was also monitored and deformation diagrams prepared directly on ERTS 9"x9"

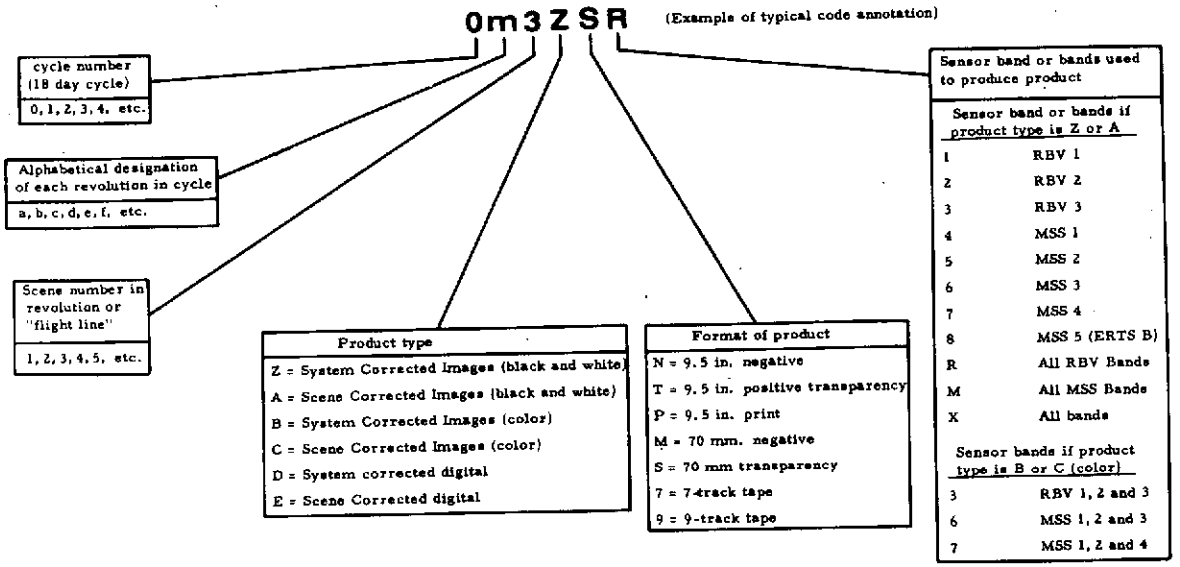

Figure 2. Alphanumeric code for cataloging ERTS-1 imagery.

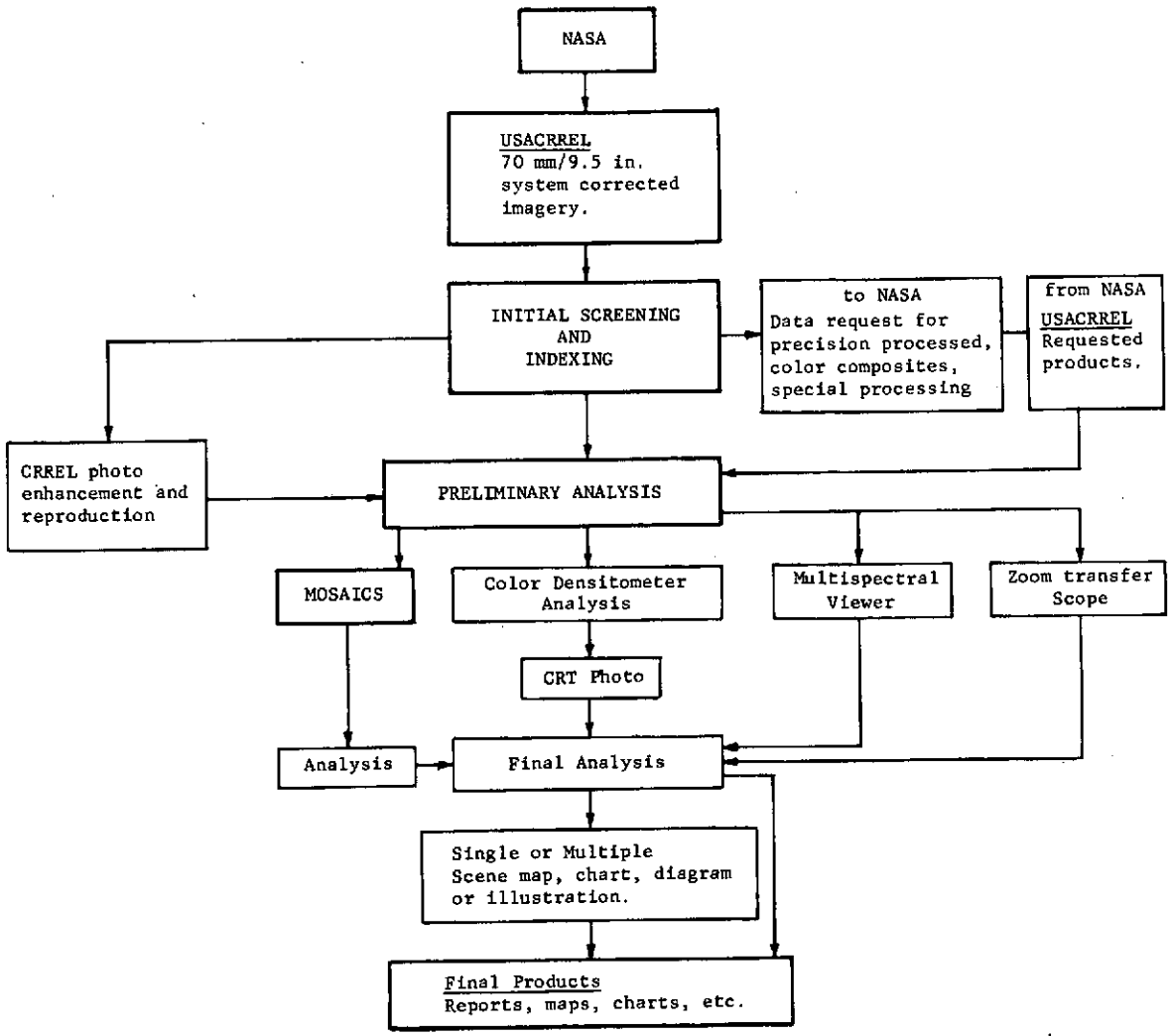

Figure 3. ERTS imagery analysis flow chart.

images. The movement of water masses, sediment distribution and circulation patterns in Cook Inlet were mapped directly from bulk, 9"x9", black and white prints and color composites. The thematic maps based strictly on ERTS imagery interpretations were subsequently compared with published maps and other references.

Imagery analysis was facilitated by several laboratory techniques and specialized equipment. Reproductions and enlargements were prepared from 70mm and 9.5 in. positive transparencies. Image enhancement by high contrast printing techniques was necessary to accentuate the information content of low contrast, low sun angle ERTS imagery. Vegetation mapping based mainly on tonal identifications was facilitated by the production of false color composites using a Spectral Data Corporation Multispectral viewer and an Antech color densitometer, used also for area measurements. A Bausch and Lomb Zoom Transfer Scope was utilized for sea ice mapping as described above.

3.0 Results

3.1 Surface circulation and sediment deposition in Cook Inlet.

Cook Inlet is a large tidal estuary in south central Alaska (Fig. 4). It is oriented in a northeast-southwest direction and is approximately 330 km long, increasing in width from 37 km in the north to 83 km in the south. The inlet is bordered by extensive tidal marshes, lowlands with many lakes, and mountains (Fig. 5). Tidal marshes are prevalent around the mouth of the Susitna River, and in Chickaloon, Trading and Redoubt Bays. The Kenai Lowland separates the inlet from the Kenai Mountains on the upper southeast side. The Susitna Lowland lies between the Talkeetna Mountains on the northeast and the southern Alaska Range on the northwest. The Kenai Mountains are adjacent to the inlet mouth on the southeast; the Alaska-Aleutian Range forms the western border.

Many of these natural features and the major cities, towns and some previously unmapped developments south of the mouth of the Drift River and on the southern shore of the West Lowlands are identifiable on the image shown in Figure 6. Anchorage (1), the state's most populated city, is the center of transportation, commerce, recreation and industry and is situated between Knik (2) and Turnagain (3) Arms in the northern portion of the inlet. Fire Island (4) is located approximately 8 km off the coast west of Point Campbell. The Susitna River (5) with an average discharge of approximately 918 m^3/sec (Wagner et al. 1969) is a major contributor of sediment to the inlet. Note the well-defined tidal channels that have formed at the river mouth. Chickaloon Bay (6) and other areas around the border of the northern inlet have extensive tidal flats (7) that are exposed during low tide. McArthur River (8), a glacial stream originating in the Chigmit Mountains to the west, drains into the inlet in Trading Bay (9). Trading Bay has 14 oil producing platforms around Middle Ground Shoal and is the major site of active petroleum production in the Cook Inlet area. An oil refinery and a tanker terminal are located at Nikiski (10) 24 km across the inlet. Kenai (11), at the mouth of the Kenai River, is a fishing and oil and gas processing center. Numerous submarine pipelines across the inlet and several crude oil gathering facilities are located along the coast in this area. Additional offshore platforms, coastal facilities and tanker terminals will be constructed as petroleum production increases and as the southern portion of the inlet is developed. The Kenai Lowland (12) located east of Kenai is a flat, glaciated plain marked by numerous lakes and swampy areas. The Kasilof River (13) begins at Tustumena Lake and discharges into the inlet approximately 21 km northeast of the lake. Kalgin Island (14) is located in the central portion of the inlet and separates the two deep channels found between Harriet Pt. and Kasilof. Near the mouth of the Drift River is a tanker terminal, an oil storage area, and a landing strip (15). Sediment patterns and a tongue of oceanic water (16) with a lower suspended sediment

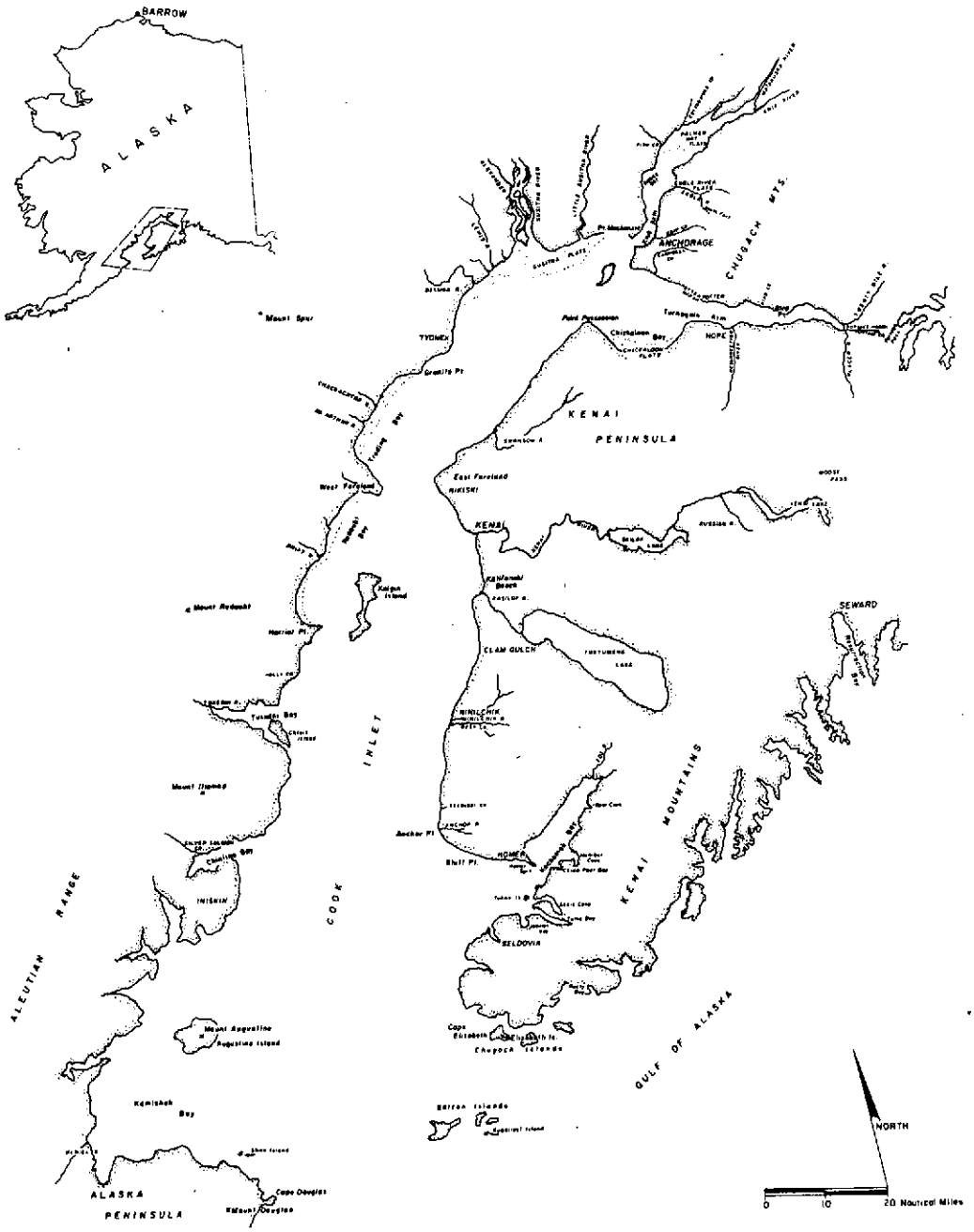

Figure 4. Regional map of Cook Inlet.

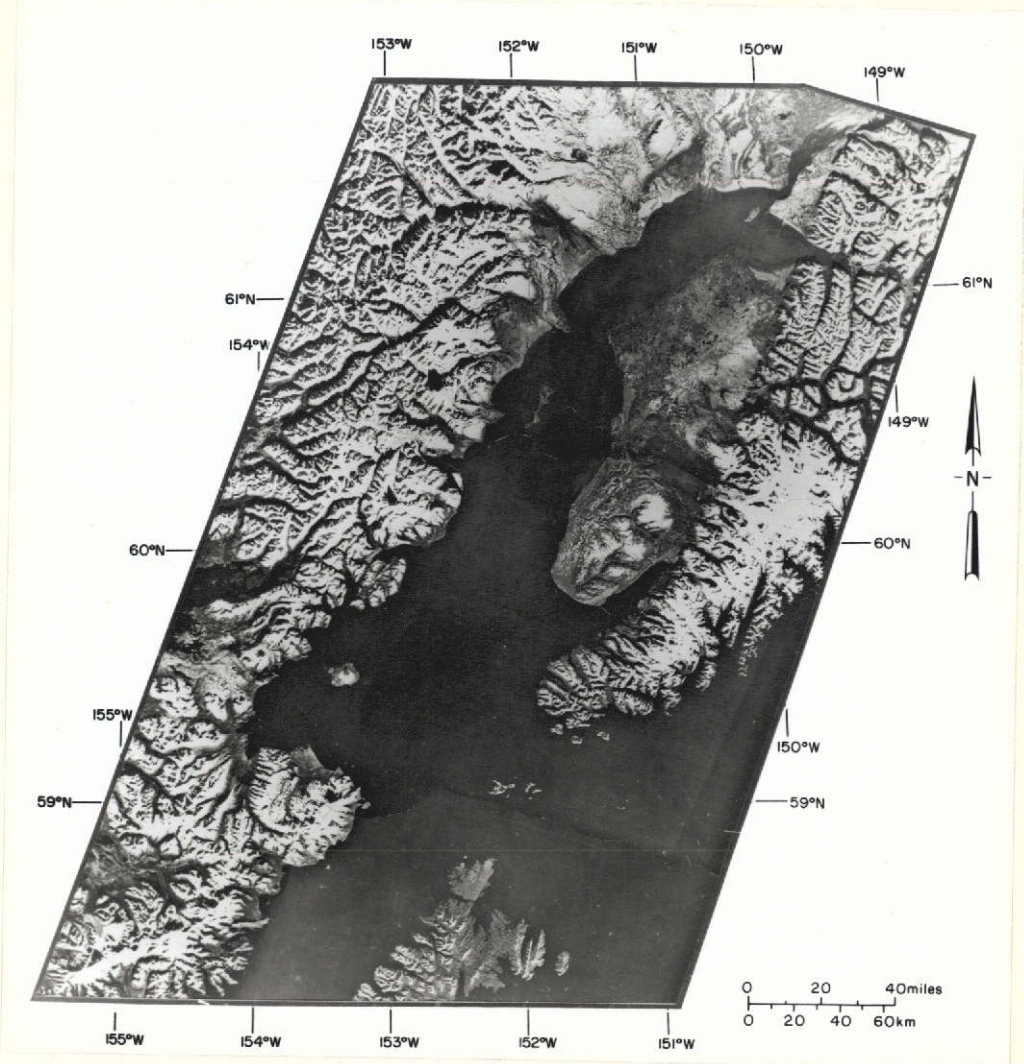

Figure 5. Geographic setting of Cook Inlet. Mosaic made from MSS band 6, images 1103-20513, 1103-20520, 1103-20522, 1104-20572, 1104-20575, 1104-20581.

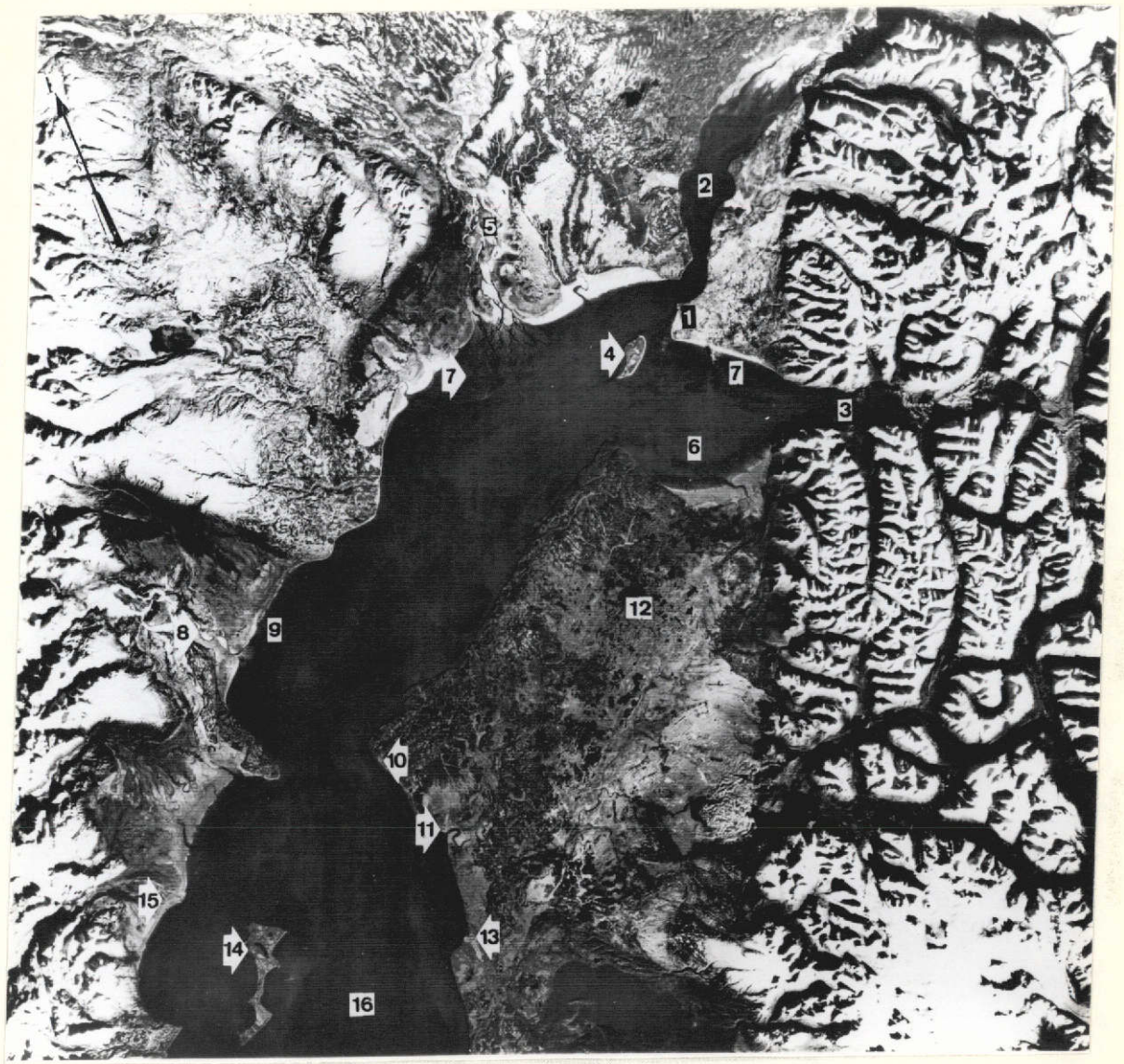

Figure 6. Northern portion of Cook Inlet. MSS band 6, image 1103-20513, acquired 3 November 1973.

concentration are discernible in the inlet. The higher concentration of sediment elsewhere in the inlet waters is discernible because the sediment laden water produces more reflection of visible light and appears lighter.

In view of present acute energy requirements rapid development of the petroleum resources in the Cook Inlet area and subsequent industrial expansion along the coast are inevitable. The estimated petroleum and gas reserves of the Cook Inlet area are 7.9 billion barrels (bbl) and 14.6 trillion cubic feet, respectively (Crick 1971). Coal deposits in the Beluga River region north of Trading Bay are estimated at more than 2.3 billion tons (equivalent to approximately 7 billion barrels of oil) (Evans et al. 1972). The effects on the inlet environment likely to result from future development must be assessed in order to formulate a rational coastal management plan for the Cook Inlet region. The present types and amounts of pollutants in the inlet will increase, therefore it is important to evaluate the dispersion and flushing capability at an early date. Glacial sediment is currently the dominant pollutant in the inlet. It is estimated that in developing areas as much as 20,000-30,000 times more sediment is produced than in natural undisturbed areas (Environmental Currents 1972). The Knik, Matanuska, Susitna, Beluga, McArthur, Drift and Tuxedni Rivers presently contribute the dominant amounts of sediment to the inlet; future development in these watersheds will increase their annual deposition.

Other sources of pollutants in the inlet are the coastal towns. With completion of the Asplund Water Pollution Control Facility the sewage from the Greater Anchorage Area Borough is treated prior to being discharged into the inlet near Point Woronzof. This project is the single most important environmental protection measure so far undertaken in the Anchorage area (Alaska Construction and Oil 1973). The remaining cities and villages, however, discharge untreated sewage directly into the inlet. Petroleum pollution originates from numerous sources: oil producing offshore wells; the Drift River, Arness or Nikiski tanker terminals, submarine and coastal pipelines; the gathering and handling facilities along the coast; and, wastewater effluent from the Standard Oil and Tesoro refineries. Approximately 9500-17500 bbl/yr or 0.3% (Kinney et al. 1970a) of the total crude oil produced is accidentally spilled, but, to date, the spills have not been noticeably detrimental to the coastal areas. From January through April 1972, 5 spills occurred in the inlet as a result of accidental disconnects at tanker terminals. Evidence of these spills had disappeared in 3-4 days (Evans et al. 1972). This is typical. Because of the high surface turbulence and mixing, oil spills rarely reach shore; they simply evaporate and disperse as they move up and down the inlet with the exceptionally high tidal fluctuations.

Petro-chemicals from the Phillips liquified natural gas plant and the Collier Chemicals ammonia plant at Nikiski presently are discharged directly into the inlet. The effluent outfalls from these plants are located in a region of high turbulence, however, and dilution of the wastes is rapid. As a result, concentrations remain below harmful levels even during the low runoff winter months (Rosenberg et al. 1967).

The southern portion of Cook Inlet (Fig. 7) is less populated than the northern area. Nevertheless, there are numerous small towns and settlements. Ninilchik (1), Anchor Point (2), Homer (3), and Homer Spit, approximately 5 km long, are located along the southern shore of the inlet. Homer, at the mouth of Kachemak Bay (4), is a fishing town and is often used as a haven for ocean vessels caught in foul weather in the Gulf of Alaska. Seldovia (5) and English Bay (6) are small fishing villages on the northern side of the Kenai Range at the inlet mouth. The Chugach Islands (7) are clearly seen on the south side of the Kenai Mountains. The mountainous west shore of the inlet is marked by many varied embayments. Tuxedni (8), Chinitna (9), and Kamishak (11) Bays are the largest along this shoreline. The general geologic structure of the Iniskin Peninsula (10) is recognizable in this image. Augustine Island (12) is an active composite volcano (strato volcano) with a classic conical shape. It has a history of violent eruptions typical of an andesitic type volcano (Selkregg et al. 1972). Cape Douglas (13) is located at the western edge of the inlet mouth, and between the Barren Islands (14) and the Kenai Peninsula to the north is the Kennedy Entrance to the inlet. Differences in sediment concentration between the oceanic water intruding into the inlet on the east and the inlet water moving out on the west are visible in this image. The shear zone between the northerly and southerly moving water masses is approximately in the middle of the inlet.

3.1.1 Tidal flat distribution.

The high sediment load in glacial rivers is the source of material rapidly building the tidal flats throughout the upper inlet. MSS bands 5 and 7 images were found to be ideal for a regional analysis of these tidal flats. Because most of the sediment deposited in the inlet is carried by the Susitna and Knik Rivers (Wagner et al. 1969) the largest areas are north of the forelands (Fig. 8). In the lower inlet tidal flats usually occur as bayhead bars in the numerous embayments along the western shore and northeast of Homer in Kachemak Bay. The high current velocities and frequent changes in current direction of the inlet water produce great variation in configuration. The migration of some of the major tidal channels and the configurations of some tidal flats in Knik and Turnagain Arms can be substantiated by comparing Figure 6 with National Ocean Survey Navigational Chart 8553. A better understanding of these changes would be useful in maintaining the navigation channels and harbor facilities in this area.

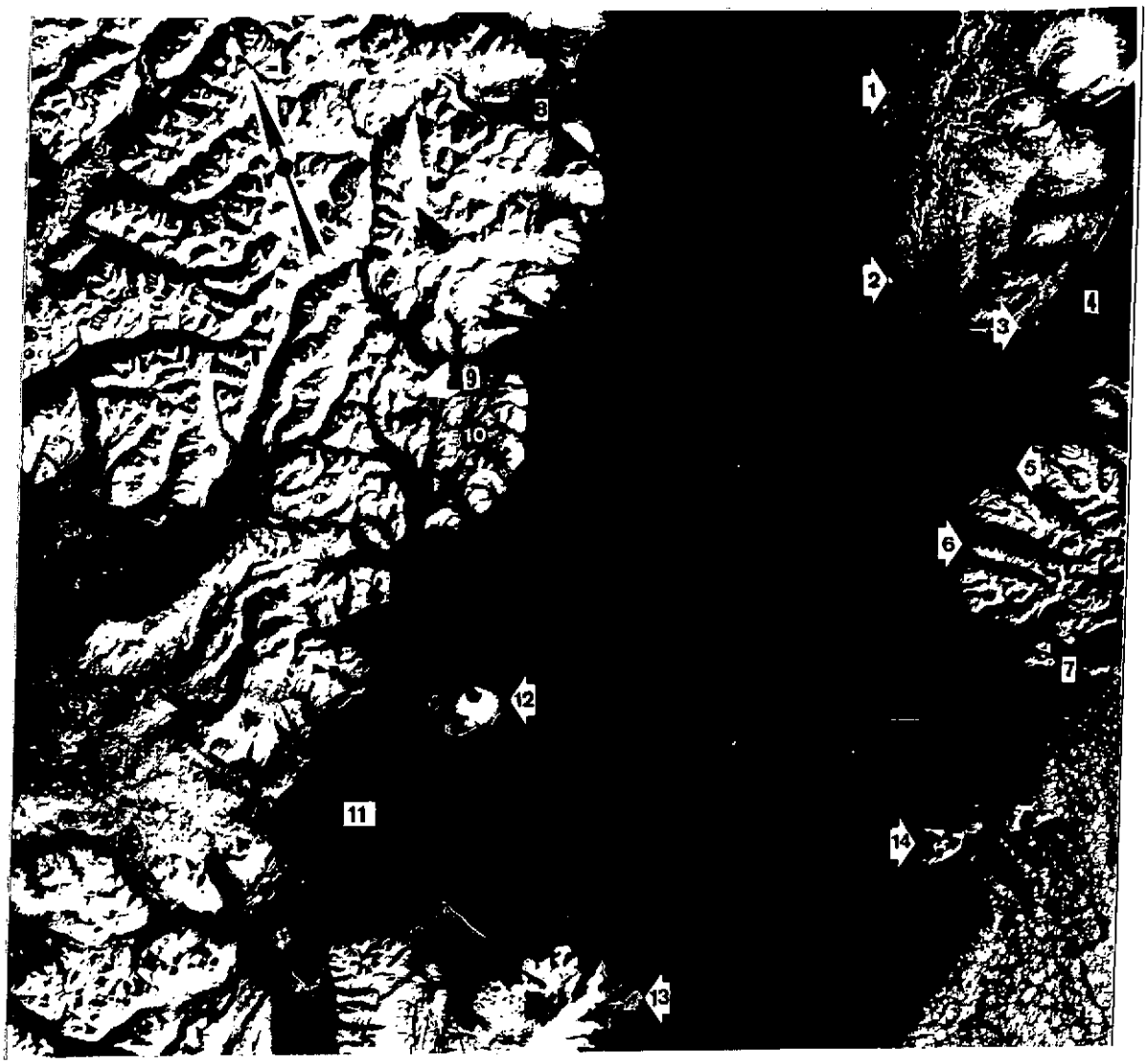

Figure 7. Southern portion of Cook Inlet. MSS band 6, image 1104-20574, acquired 4 November 1972.

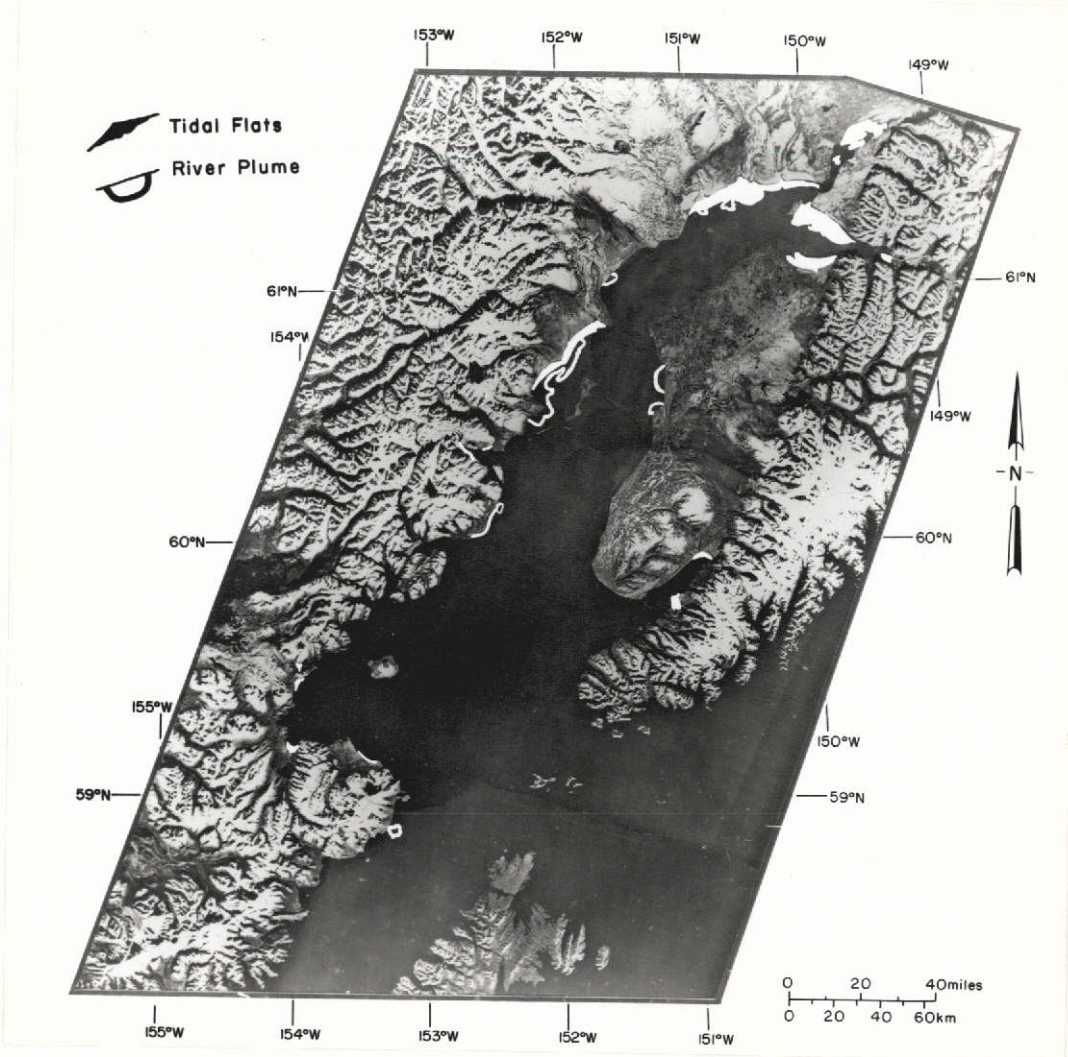

Figure 8. Tidal flat distribution and river plumes.

3.1.2 River plumes.

The sediment laden rivers discharging into the inlet produce sediment plumes that are easily visible in MSS bands 4 and 5. Figure 8 shows the distribution of plumes from some of the major rivers entering the inlet. Although the Knik and Matanuska Rivers at the head of Knik Arm contribute most of the sediment deposited in the inlet (Wagner et al. 1969) these rivers do not produce distinct sediment plumes. The river borne sediment is dispersed so quickly in this high energy area and the sediment concentration of the inlet water is so high (approximately 1350 mg/liter; Kinney et al. 1970b) at this location that a distinct plume is not formed. The Susitna River, another major sediment contributor, has only a small plume because the river discharge is reduced during the winter months (Wagner et al. 1969). In addition, this plume is rendered indistinct because the inlet water itself at the mouth of the Susitna river has a very high suspended sediment concentration (approximately 1540 mg/liter; Kinney et al. 1970b). Figure 9, taken on 7 August, shows the sediment plumes from the Drift (3) and Big (4) Rivers during flood tide. The shape and location of the plumes are convenient markers from which one can determine current directions along the west shore between McArthur River (1) and Tuxedni Bay (2); they appear clearly to be moving in a northerly direction. Relict sediment plumes from earlier tidal changes are visible far offshore and serve to indicate integrated water movement through several tide cycles. Relative differences in sediment concentration of the inlet water also can be distinguished. Lighter gray tones occur farther from shore and indicate deposition, mixing and dilution due to rapid transport. Tidal flats (5) are seen as a gray border along the coastline. Mt. Spurr (6), one of the many volcanoes in the Chigmit Mountains, Lake Chakachamna (7) and numerous glaciers (8) are also visible.

Changes in sediment plume patterns of the Big (5) and Drift (6) Rivers are shown in Figure 10. This scene was taken on 10 September 1972. The southerly direction of the near shore current during ebb flow in Redoubt Bay (7) is indicated by the shape of these river plumes. Sediment laden water from the Tuxedni River (12) is being transported along the coast in a southerly direction between Chisik Island (13) and the mainland. The shapes of the sediment plumes of the Kenai (15) and Kasilof (14) Rivers also indicate a southern current along the east shore in this location. Other features of interest in this scene are: the snowcapped Kenai Mountains (1), the Kenai Lowland (2), the East (3) and West (4) Forelands, a sediment pattern indicating a counterclockwise current (8) around Kalgin Island (9), tidal flats (10), Harriet Point (11), and sediment laden Lake Tustumena (16).

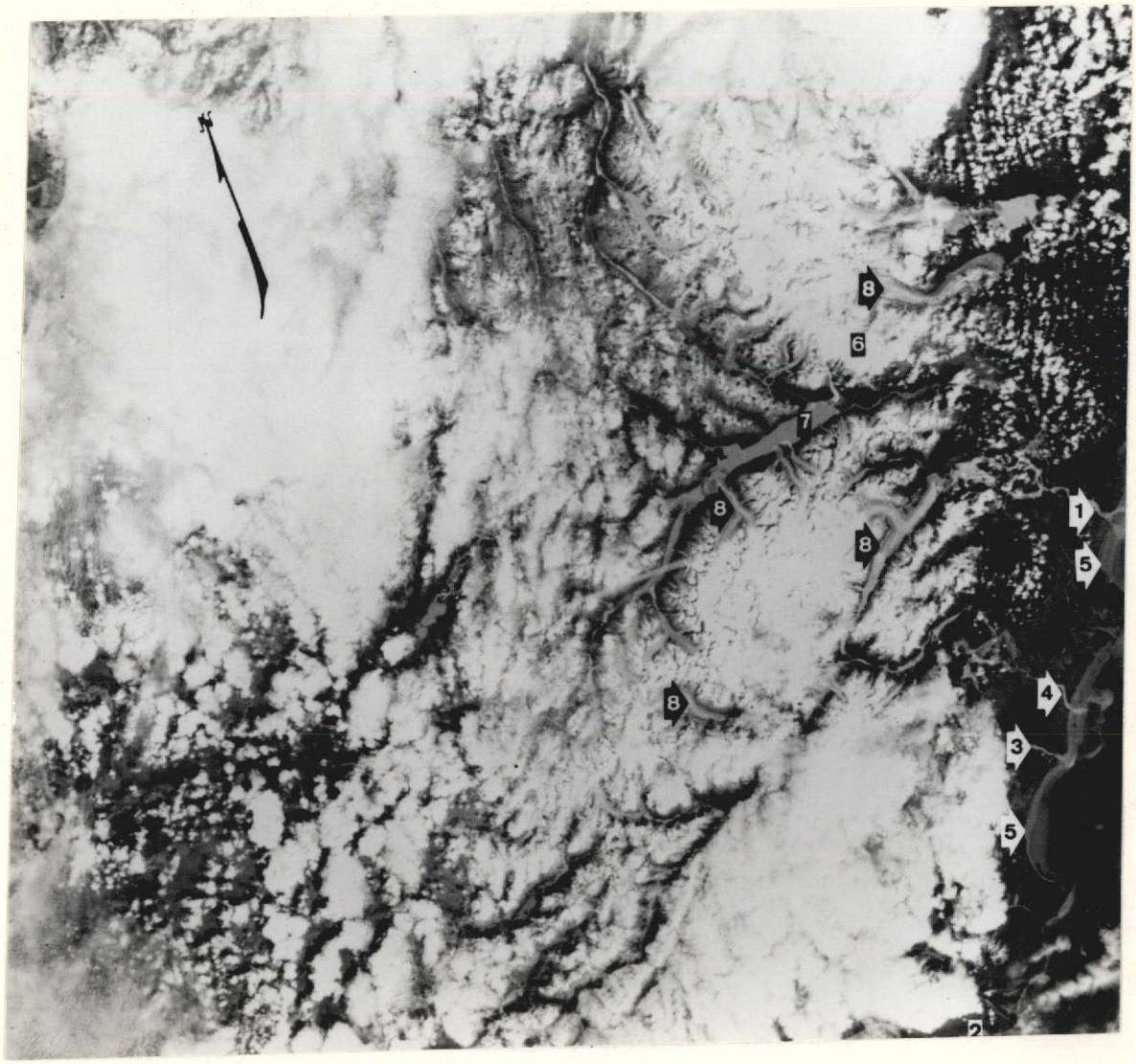

Figure 9. West shore of Cook Inlet between McArthur River and Tuxedni Bay. MSS band 5, image 1015-21022, acquired 7 August 1972.

Figure 10. Central portion of Cook Inlet. MSS band 5, image 1049-20512, acquired 10 September 1972.

3.1.3 Water types.

MSS bands 4 and 5 clearly show the distinction between the relatively clear, saline, oceanic water in the southeastern portion of the inlet and the fresher sediment laden inlet water in the northern and southwestern portions. Again, recognition of the boundary is possible because of the sediment in the inflowing fresh water which functions as a tracer, marking water masses and making current patterns visible. Daily changes and changes occurring during the 18 day ERTS cycle can be seen. Figure 11a shows differences in the main boundary between the oceanic and fresh water in the southern inlet on two successive days. The boundaries separate the two major water types during low tide in Anchorage and high tide in Seldovia. The irregularity of the western portion of these lines may be due to the upwelling of cold, saline oceanic water thought to occur in the western portion of the inlet (Kinney et al. 1970b; Evans et al. 1972). The northern portion of the 4 November boundary is also quite irregular, possibly due to a similar upwelling effect. Some estuaries are characterized by a salt wedge that moves headward along the bottom while the fresh water outflow moves over this wedge and out the estuary (Bowden 1967). In Cook Inlet this subsurface tongue of oceanic water may progress headward and move up the shoaling bottom of the inlet to the latitude of Tuxedni Bay where it may rise to the surface south of Kalgin Island during flood tide (Kinney et al. 1970b). The upwelling waters would appear as a large, distinct area of clear water surrounded by more turbid water. This process may produce a zone of high nutrient concentration in the photic zone at this location which may be significant to the local fishing industry. Changes in the boundary over an 18 day cycle are shown in Figure 11b. The boundary is generally comparable to that shown in Figure 11a, although some differences appear, and the general positions of the two water types would appear from these observations to remain fixed with time.

3.1.4 Surface circulation.

The regional circulation patterns in the Cook Inlet are governed by interactions between the semidiurnal tides, Coriolis force, and the counterclockwise Alaska current, primarily. Local currents are influenced by local bathymetry, morphometry and fresh water influx (Evans et al. 1972). The water in the upper inlet is well mixed due to the very large tidal fluctuations in this shallow, narrow basin. During summer, when surface runoff is high, there is a net outward movement of water from the upper inlet. With reduced runoff in the winter there is virtually no net outflow (Murphy and Carlson 1972). The middle inlet has a net inward circulation of cold, saline oceanic water up the eastern shore and a net outward flow of warmer and fresher inlet water along the western shore (Evans et al. 1972). The two water types are

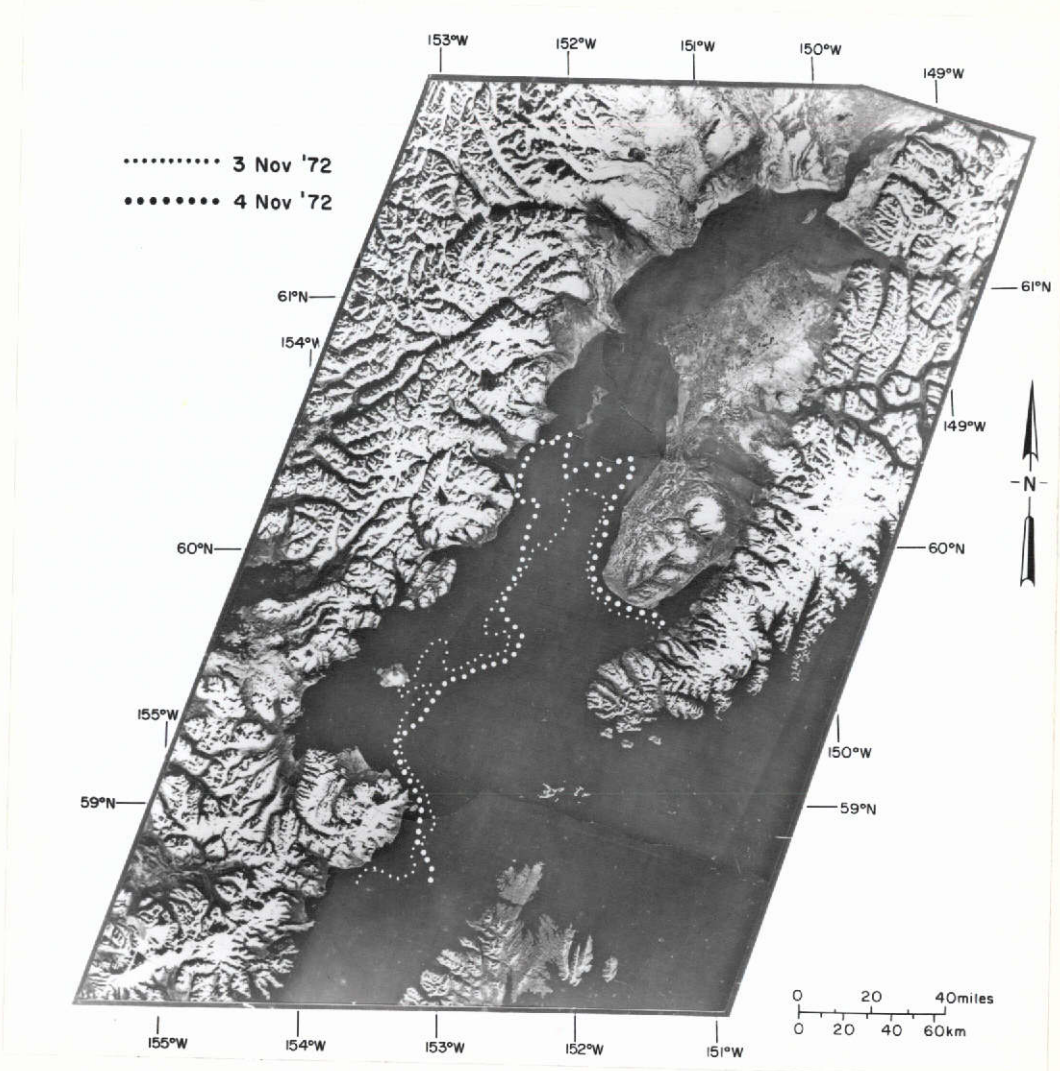

Figure 11. Boundaries separating oceanic and inlet water (from Anderson et al. 1973). a. Daily changes.

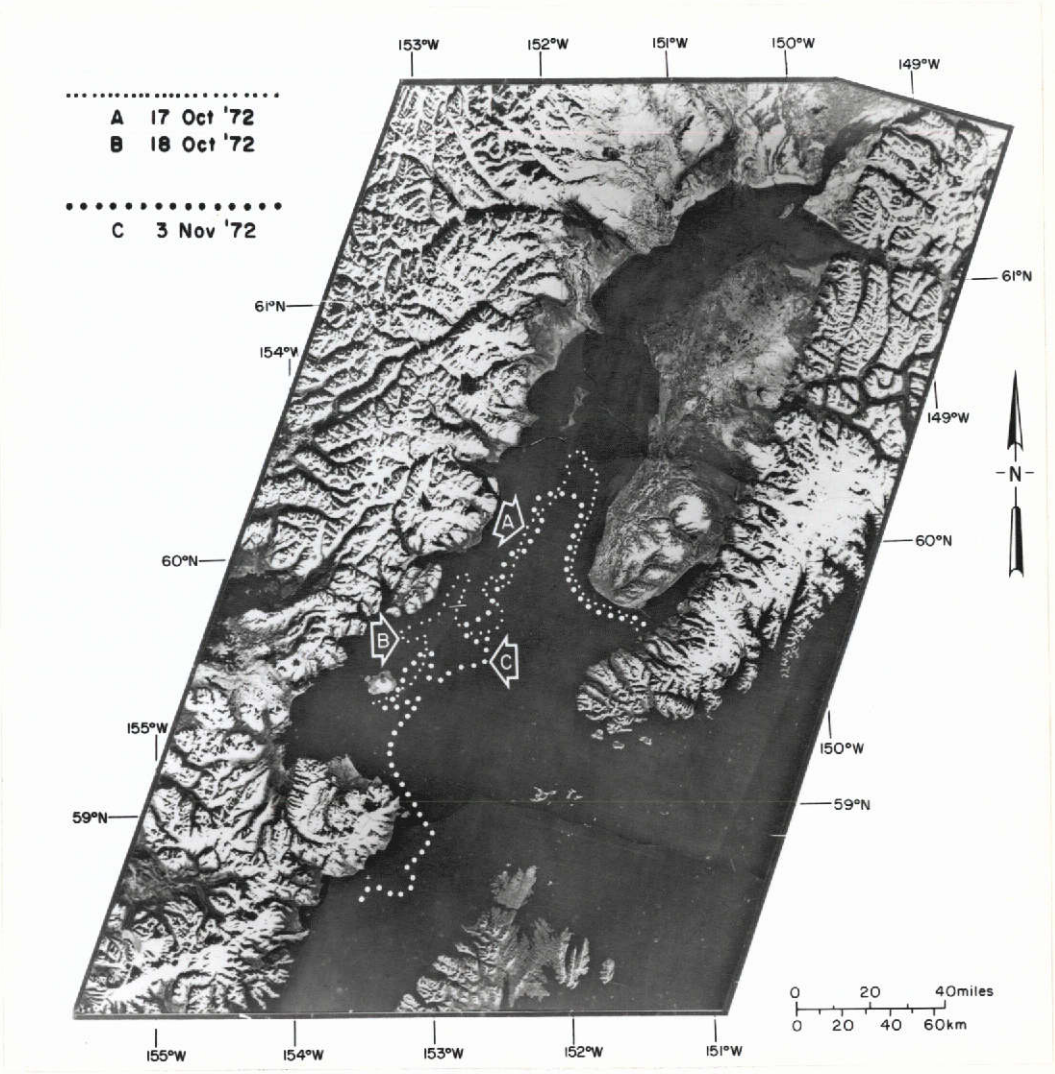

Figure 11 (continued). b. Changes over 18-day period.

well mixed vertically along the eastern shore but they are separated laterally by a well defined shear zone. In the lower inlet this lateral temperature and salinity separation is still maintained, but in the western portion vertical stratification occurs with colder, saline oceanic water underlying warmer, less saline inlet water. During tidal inflow the deeper oceanic water may rise to the surface at the latitude of Tuxedni Bay and mixes with the inlet water (Kinney et al. 1970b).

Bathymetry is varied throughout the estuary. Depths in the upper inlet north of the forelands are generally less than 36 m. The deepest portion, 82 m, is located in Trading Bay just off the mouth of the McArthur River (Sharma and Burrell 1970). Turnagain and Knik Arms are the shallowest areas with much of the bottom exposed at low tide. South of the forelands two channels, one between Kalgin Island and Harriet Point and the other between Kalgin Island and the southeast shore, extend southward in the inlet and join in the area west of Cape Ninilchik. The deepest portion of the western channel, located between Kalgin Island and Harriet Point, is approximately 130 m. The eastern channel is deepest just south of a line between the forelands; it is 135 m in this area but rapidly shoals to approximately 55 m as it merges with the western branch to form a single broad channel. South of Cape Ninilchik this channel gradually deepens to approximately 145 m and widens to extend across the mouth of the inlet between Cape Douglas and Cape Elizabeth.

The semi-diurnal tides in Cook inlet consist of two unequal high tides and two unequal low tides per tidal day (24 hours, 50 minutes). Because of the size of the inlet, high tide in Anchorage occurs 4-1/2 hours later than at the inlet mouth (Fig. 12). Mean diurnal tide range varies from 4.2 m at the mouth to 9.0 m at Anchorage. It varies within the lower portion of the inlet from 5.8 m on the east side to 5.1 m on the west side (Wagner et al. 1969). The extreme tidal range produces tidal currents of 4 knots (2.2 m/sec) typically, and occasionally 6 to 8 knots (Horrer 1967). The high Coriolis force at this latitude, and the strong tidal currents combined with the inlet geometry produce strong cross currents and turbulence throughout the entire water profile during both ebb and flood tides (Burrell and Hood 1967). The turbulence is especially high along the eastern shore of the inlet.

As observed above, the high concentration of suspended sediment in the fresh water influx functions as a natural, semi-opaque "tracer" by which the surface circulation of tidal and long shore currents are made visible. The currents are most easily seen in MSS bands 4 and 5. Figure 13 shows the generalized surface circulation in the inlet based on published data (Evans et al. 1972) and as inferred from ERTS-1 imagery. The regional circulation of the inlet water previously deduced was observed and verified with few changes in the ERTS images. Clear

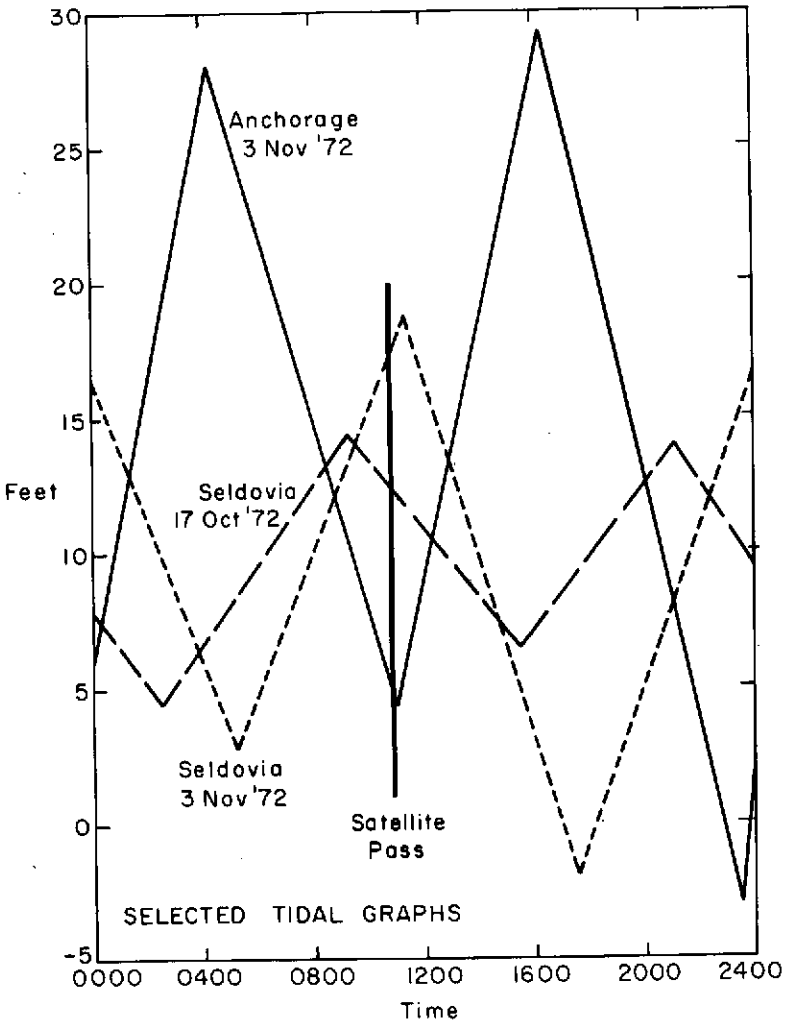

Figure 12. Selected tidal graphs.

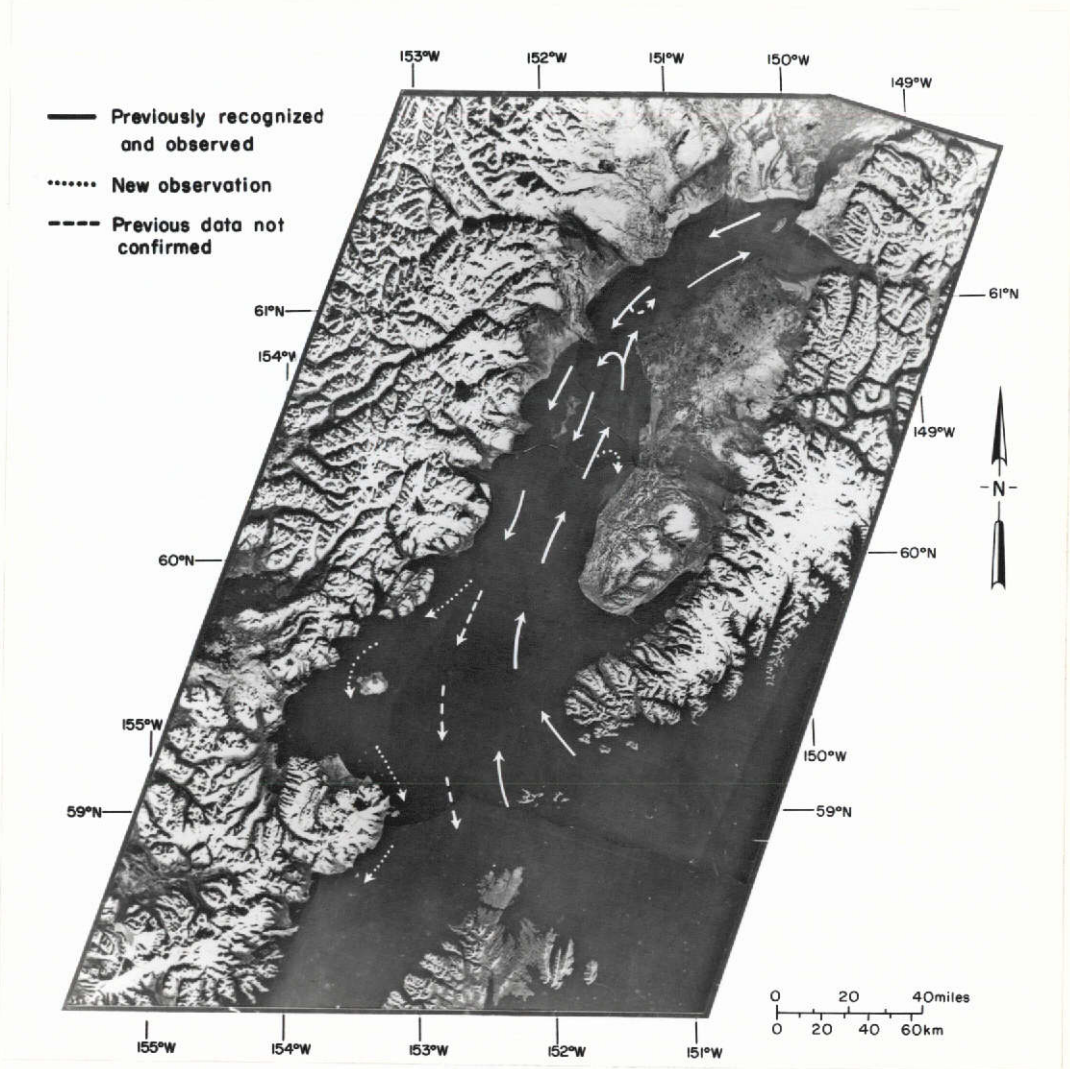

Figure 13. Generalized surface current patterns. Patterns were visible on MSS bands 4 and 5, images 1103-20513, 1103-20520, 1103-20522, 1104-20574, 1104-20581.

oceanic water enters the inlet at flood tide along the east side around the Barren Islands. A portion is forced into the inlet by the counterclockwise Alaska Current in the Gulf of Alaska. A tongue of this oceanic water (Fig. 11) occupies the southeastern portion of the inlet, and gradually becomes less distinct in the northeast direction because of mixing with the more turbid upper inlet waters around Ninilchik. The tide front progresses from the mouth of the inlet to Anchorage in approximately 4-1/2 hours. It moves faster along the east shore, being diverted in that direction by the Coriolis force. A back eddy not previously reported (dotted arrows) was visible forming in the slack water area northeast of Cape Ninilchik during flood tide on MSS frames 1103-20513-5, 1103-20520-5 and 1104-20574-5.

As the tidal front continues past the East Foreland, a large peninsula protruding some 16 km into the inlet, it is partially diverted across the inlet and abuts the West Foreland. At this point the front splits; part of it moves south of the West Foreland and the remainder moves north. This circulation pattern is repeated twice daily during the two daily flood tides. The result is a counterclockwise circulation pattern around Kalgin Island (Fig. 10). This pattern was verified by direct observation from 1800 m altitude during an aircraft underflight at the time the satellite passed and this image was acquired. The circulation of surface water north of the forelands appears to be similar to that previously reported (Evans et al. 1972). The ebb flow in the inlet moves predominantly along the northeastern shore past the forelands. This general pattern was also discernible on the imagery except for a previously reported counterclockwise pattern (dashed arrow) north of the forelands which was not seen. A characteristic pattern is formed as the ebbing waters run into the West Foreland and some are diverted across the inlet and move headward with the flood current along the east shore. As the sediment laden ebbing water moves past the area of Chinitna Bay it appears to flow along the shoreline and circulate around the west side of Augustine Island in Kamishak Bay. It continues to parallel the coast past Cape Douglas and progresses through Shelikof Strait. This pattern in Kamishak Bay west of Augustine Island has not been previously reported but it is clearly visible on the MSS imagery.

The currents and circulation patterns are important in determining the distribution of suspended and bottom sediments throughout the inlet. The suspended sediment is mostly of glacial origin with the highest concentrations in the northern portion of the inlet, a well mixed turbulent zone of strong tidal currents. Suspended sediment is nearly absent in the waters of the central and eastern portions at the inlet mouth. Bottom sediments have been grouped into three facies: a predominantly sand facies in the upper inlet, a sandy gravel with minor silt and clay facies in the middle inlet, and a gravelly sand and minor interspersed silt and clay facies in the lower inlet (Sharma and Burrell 1970).

The movement and strength of ice in Cook Inlet is an important aspect of the inlet environment to be considered; it is particularly critical in planning offshore construction. The inlet ice is seasonal; it is present for approximately 4 months of the year. The ice is fine- to medium-grained (1mm-4mm) with a salinity of .4-.6% and a ring tensile strength of 10-20 kg/cm^2. The inlet ice exists as large floes which are commonly greater than 320 meters across with individual blocks generally less than 1 meter thick. Pressure ridges up to 6 meters in depth occasionally form (Blenkarn 1970). Large floes move up and down the inlet with the 6-8 knot tidal currents.

ERTS imagery acquired during the winter months has been compiled for use in monitoring the formation, movement and ablation of inlet ice. Although an image acquired on 14 February 1974 is 80% cloud covered, ice floes are nevertheless visible. Most of the ice on that day was concentrated in the area around Kalgin Island and in the northern Inlet. A 15 February image is also cloud covered but it shows the western shoreline between the West Foreland and the Iniskin Peninsula. Surface circulation patterns are made apparent because of the high surface density of frazil ice. Cloud-free imagery acquired on 29 January 1974 (Fig. 14) shows the distribution of ice floes and frazil ice along the western coast of Cook Inlet from Chenik Head north to Redoubt Bay. Offshore winds are moving the ice out of Kamishak Bay while the interplay between winds and tidal currents creates complex circulation patterns along the inlet coast farther north. The presence of the mobile ice cover is useful in making comparisons between summer and winter circulation patterns. In general, the circulation patterns are similar to the summer patterns made visible by waters of variable turbidity. The highest concentrations of sea ice were seen to occur in the western portion of the inlet while the eastern portion was generally ice free to the latitude of Kenai. The intrusion of ice free sea water progresses to this latitude in agreement with conclusions deduced from the summer imagery. Although large ice floes move up and down the inlet between the forelands during flood and ebb tide, respectively, and ice is a navigation hazard, extensive damage to shipping generally has been avoided.

3.2 Permafrost

3.2.1 Definition and worldwide distribution

Permafrost is formally defined solely on a temperature basis. It is rock or soil material, with or without moisture or organic matter, that has remained continuously below 0°C for two or more years (Ferrians 1969). It occurs wherever the depth of winter freeze exceeds the depth of summer thaw and is classified in two broad categories: continuous and discontinuous. In the continuous permafrost zone (Fig. 15), permafrost lies beneath all land areas, but it is often absent directly beneath large water bodies which provide enough of a heat reservoir to

Figure 14. Distribution of ice floes and frazil ice along the west coast of Cook Inlet. MSS band 5, image 1555-20591, acquired 29 January 1974.

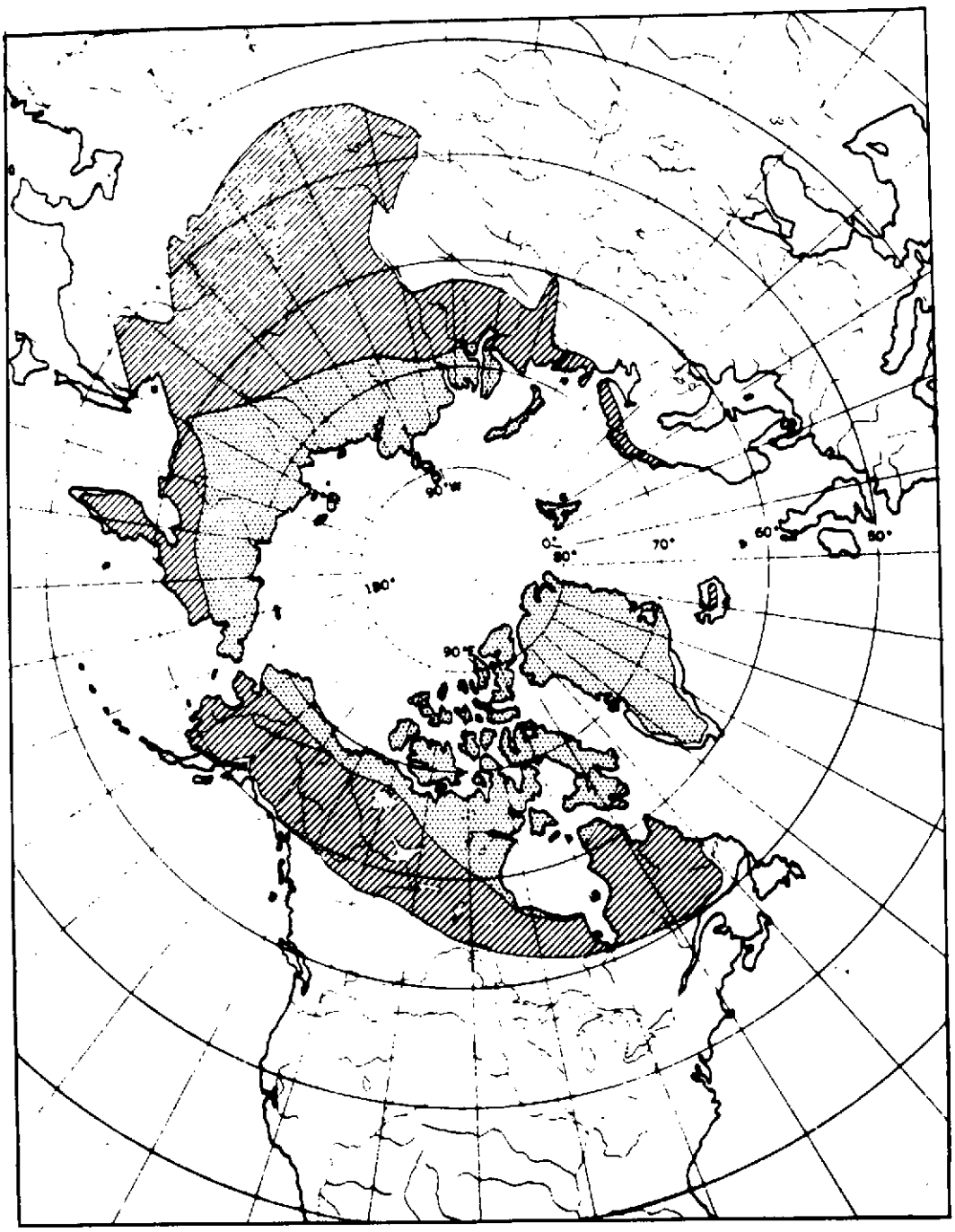

Figure 15. Geographic distribution of permafrost; stippled area is continuous permafrost zone, lined area is discontinuous permafrost zone (from Ferrians 1969).

prevent underlying materials from freezing (Williams 1970). The thickness of permafrost in the continuous zone ranges from greater than 50 m in the south to an extreme of more than 600 m in northern Alaska. The boundary that separates these two zones is theoretically distinct but it is imperfectly located. Climatically, it approximates the mean southern position of arctic air in summer (Bryson 1966); it is close to the southern limit of the tundra (MacKay 1972) and is the effective limit of active ice wedges and pingos (Péwé 1966). The discontinuous permafrost zone is a complex mosaic of frozen and unfrozen ground with permafrost thickness decreasing in a southerly direction.

Permafrost is a major environmental factor in Alaska and other high latitude regions. The existence of permafrost is the result of complex interactions among environmental factors such as local microclimate, plant cover, the insulating qualities of the organic and vegetative layers, texture and moisture content of the soil, surficial geology and topographic position (Péwé 1967, Brown 1969). Figures 16 and 17 illustrate typical permafrost settings and the nomenclature in current use.

In central Alaska the distribution of permafrost is discontinuous because the present climate in this area is near the threshold values for the continued existence of permafrost. Only in well-protected locations such as north facing slopes, shaded valley bottoms, or high elevations within the region does permafrost exist. Minor changes in the thermal regime, whether natural or man-induced, can produce major alterations in permafrost landscapes.

3.2.2 Surficial geology, vegetation and permafrost terrain mapping

The first usable ERTS-1 images of interior Alaska were obtained during orbit 30 on 25 July 1972. In the intervening period more than 3000 individual multispectral scanner (MSS) scenes have been reviewed. Those images that are relatively cloud free and with acceptable sun elevations have been compiled for interpretation and to construct photo mosaics of selected areas for the permafrost mapping experiments.

As a prelude to permafrost mapping, surficial geology was mapped on a 1:1 million scale photo mosaic (Fig. 18) of north central Alaska and on a 1:250,000 scale, 4x enlargement of a portion of ERTS image 1103-20502 of the Fairbanks, Alaska area (Fig. 19). Mapping was accomplished with the aid of stereo pairs and available ground truth data in the form of published maps and reports. Seven recognizable units ultimately were defined and mapped in the 153,400 km^2 area of north central Alaska (Fig. 20). Five of these were recognized and subsequently mapped in the area south of Fairbanks, Alaska (Fig. 21). The bedrock (b) unit defined consists of bedrock and very coarse, rubbly bedrock-derived colluvium, scree, talus, etc. It is primarily confined to steep slopes and mountain crestlines. The bedrock-colluvium (bc) unit includes coarse-to

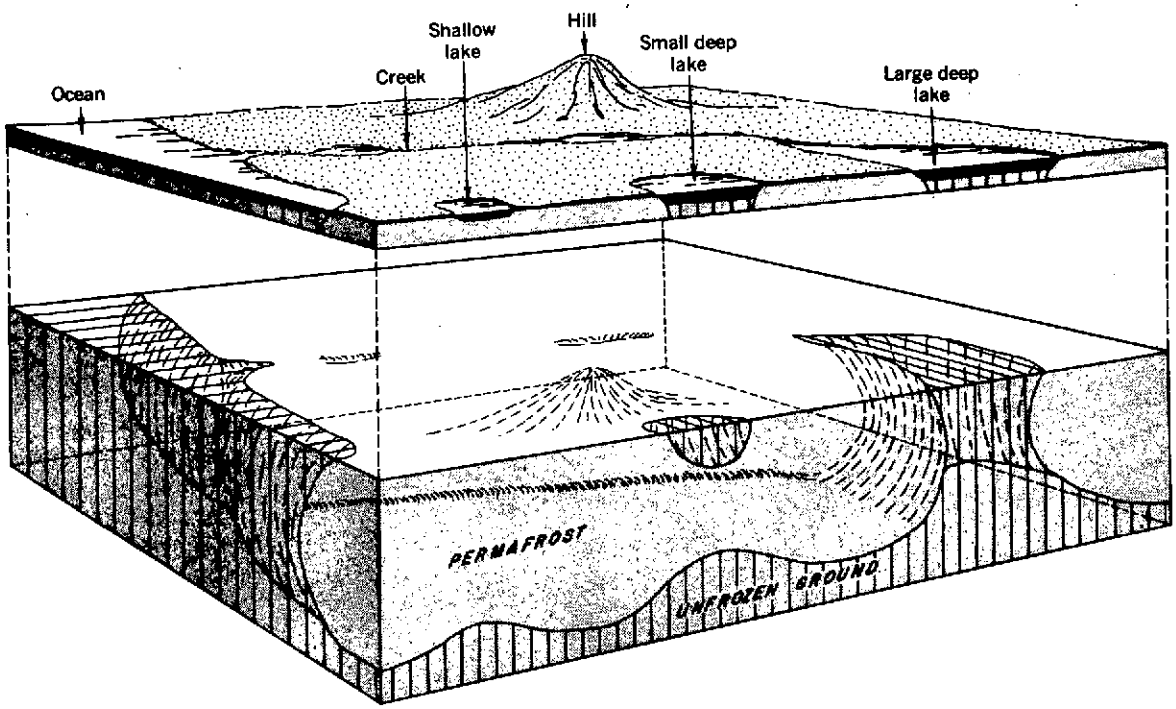

Figure 16. The effect of surface features on the distribution of permafrost in the continuous permafrost zone (after Lachenbruch 1968, p. 837).

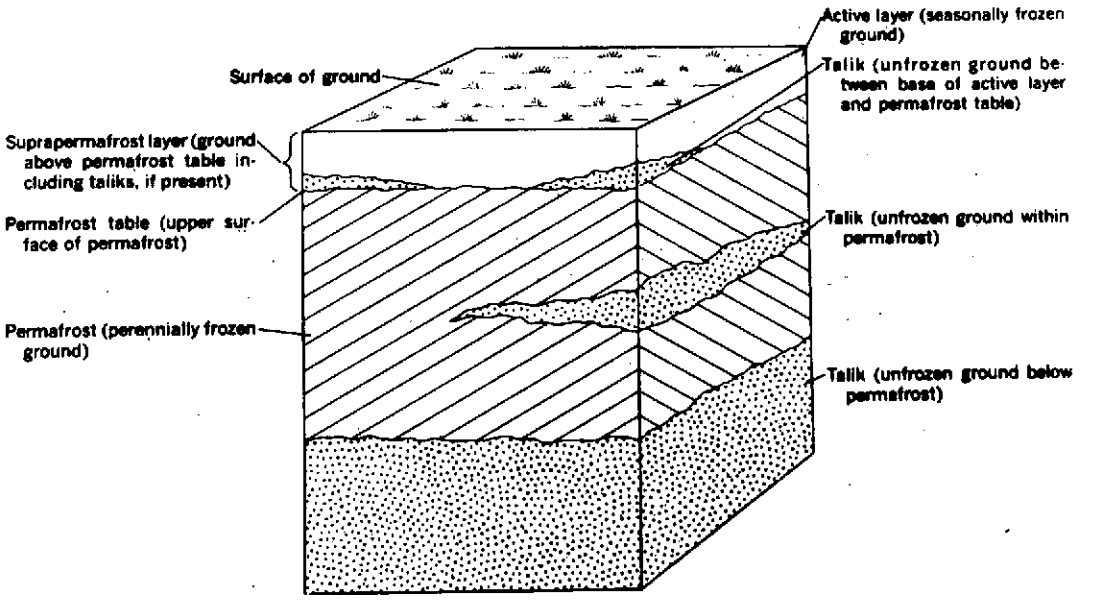

Figure 17. Occurrence of taliks in relation to the active layer, supra-permafrost zone, permafrost table and permafrost (from Ferrians et al. 1969).

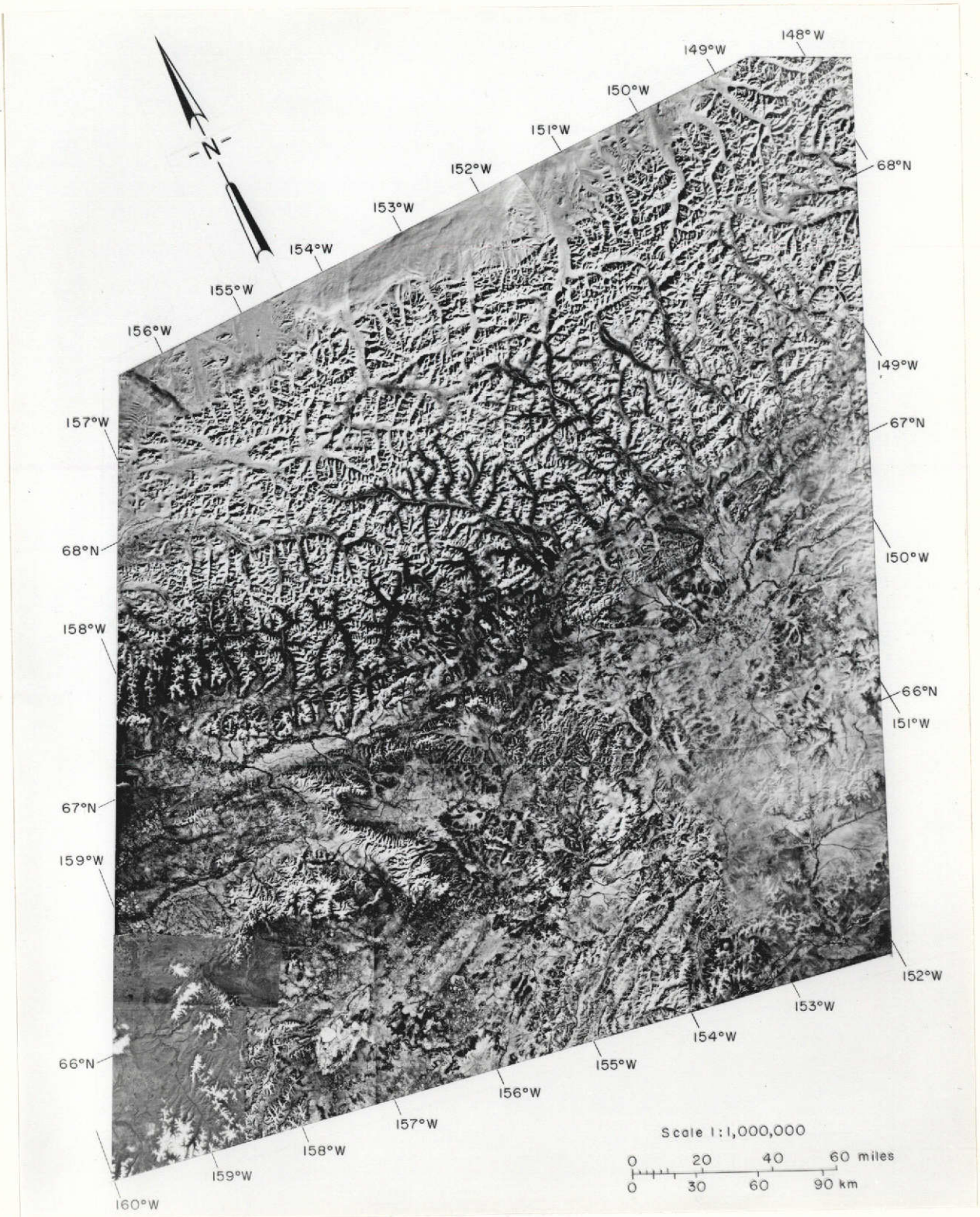

Figure 18. Uncontrolled photo mosaic of 153, 400 km^2 area in north central Alaska made from MSS band 5 images.

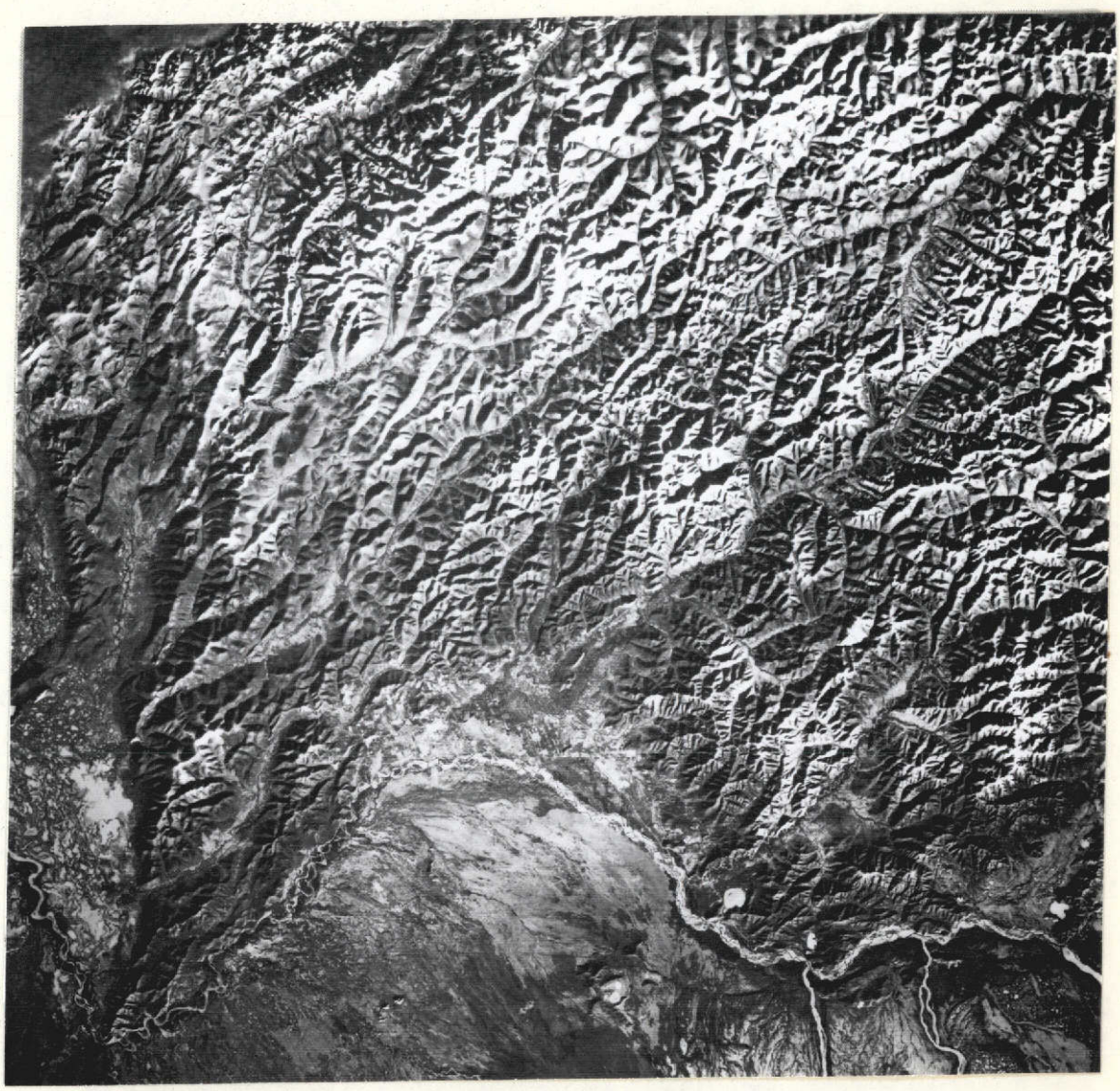

Figure 19. Fairbanks, Alaska area. MSS band 5, image 1103-20502, acquired 3 November 1972.

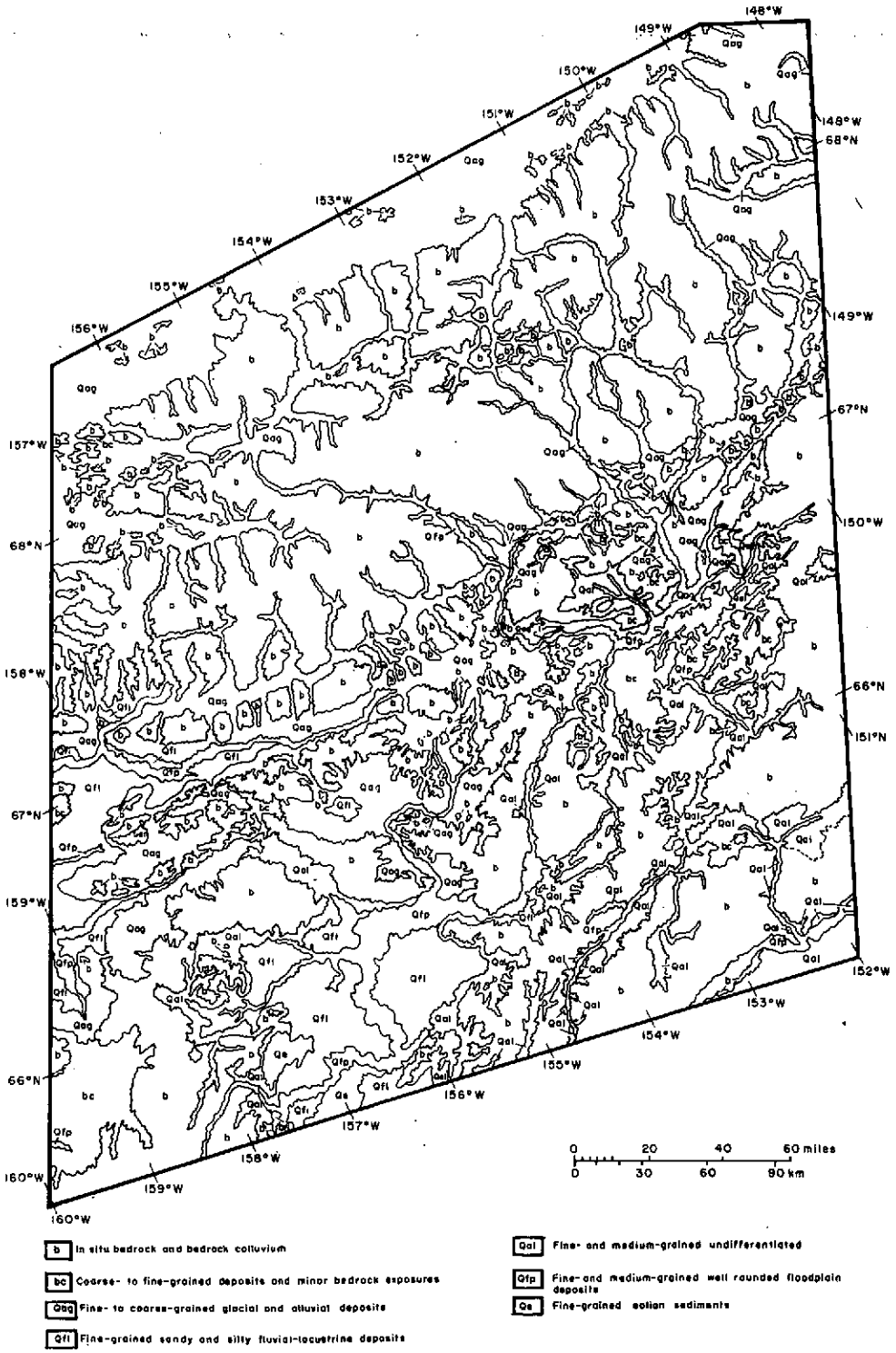

Figure 20. Surficial geology of north central Alaska from ERTS-1 imagery.

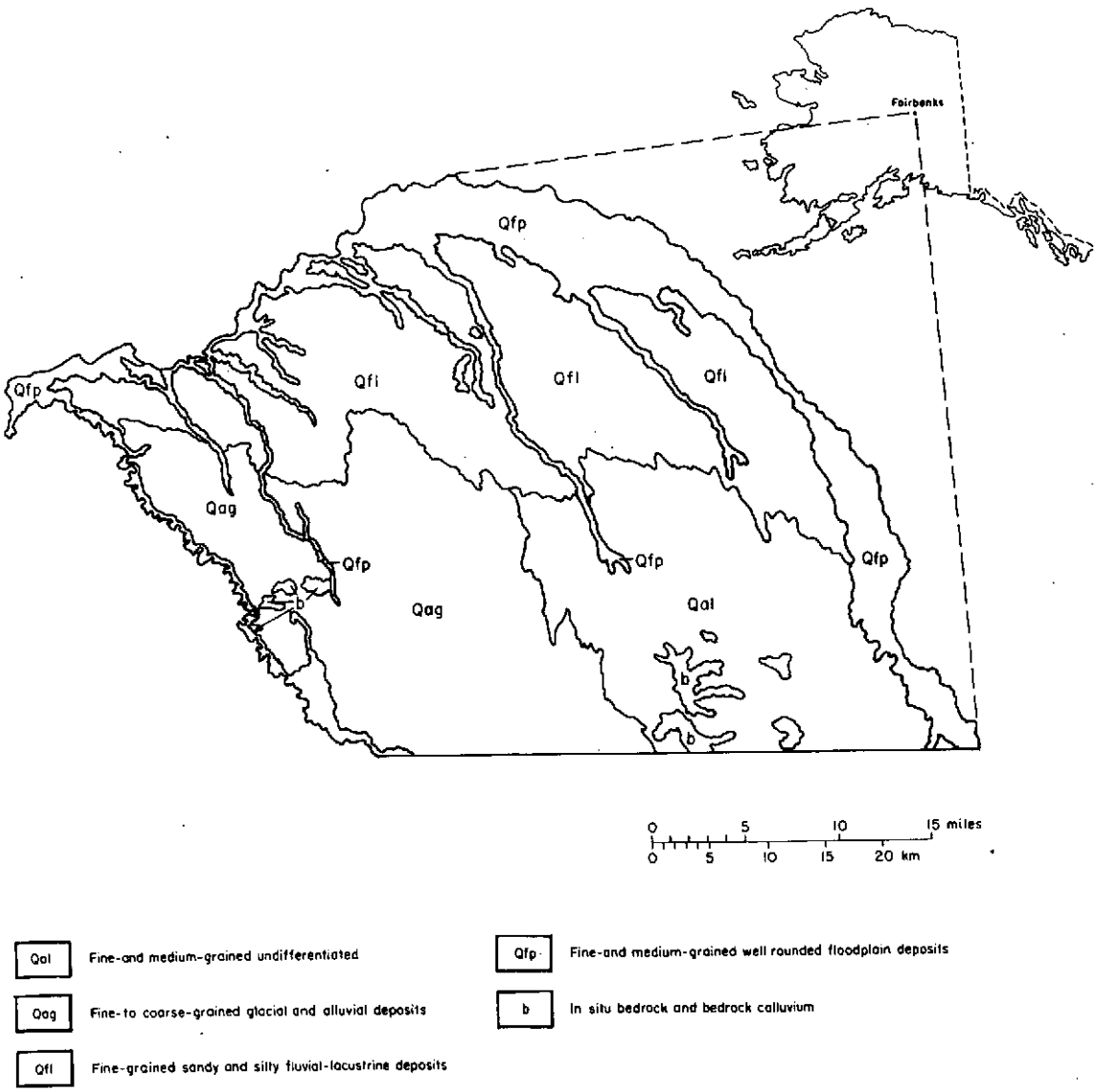

Figure 21. Surficial geology of area south of Fairbanks from ERTS-1 imagery.

fine-grained deposits occurring on moderate to steep slopes in mountainous terrain and rolling uplands which have minor scattered bedrock exposures restricted to the uppermost slopes and crestlines. Alluvial-glaciofluval deposits (Qag) are fine-to coarse-grained sediments derived from reworked glacial and alluvial deposits, morainal deposits, till, and outwash gravels and sands. This unit occurs in part on modified morainal topography and on large alluvial terraces. Fluvial-lacustrine deposits (Qfl) consist of fine-grained sands and silts associated with abandoned floodplains and low-lying terraces. They may include some windblown sands and silts. Undifferentiated alluvium (Qal) includes fine- and medium-grained alluvial fan, terrace, and stream and eolian deposits. The floodplain unit (Qfp) consists of fine-and medium-grained silts and sands associated with modern floodplains and low-lying terraces. Eolian deposits (Qe) are fine-grained windblown sediments, massively deposited on gently to moderately sloping hills and low-lying flatlands including areas of actively drifting dunes.

The resulting surficial geology map at the 1:1 million scale was subsequently compared to USGS Miscellaneous Geologic Investigations Maps at a scale of 1:250,000 (Cass 1959, Patton 1966, Patton and Miller 1966, Patton et al. 1968, Weber and Péwé 1970) and the 1:1.5 million scale Surficial Geology of Alaska Map (Fig. 22). It was established that the surficial geology map made from ERTS-1 imagery compares favorably with the published 1:250,000 maps and is clearly superior to the existing 1:1.5 million map.

Vegetation is a most important indicator of permafrost characteristics and type, but the relationship is complex (Hopkins et al. 1955). Vegetation actually influences permafrost stability by governing thermal exchange at the atmosphere-lithosphere boundary and also the soil moisture regime (Trytikov 1959). Vegetation retards soil warming in the summer and cooling in the winter. However, the depth of the active layer also depends on other variables, such as the depth of winter snow and drainage conditions during summer. Vegetation type and density in a permafrost region are most directly related to soil type and drainage conditions. The value of a map of vegetation patterns lies in its relationship to the depth of seasonal thaw. The vegetation association - depth of thaw relationship where permafrost is present in the discontinuous permafrost zone is generalized in Table 4.

Table 4. Relationship between vegetation association and depth of thaw (Hopkins et al. 1955).

Vegetation	Depth of Thaw (m)
Tall willows on floodplain	2.4
Mixed alder, willow, white birch	1.2
Mixed stands of white spruce and white birch	0.6 - 0.9
Black spruce in tundra or muskeg	0.3

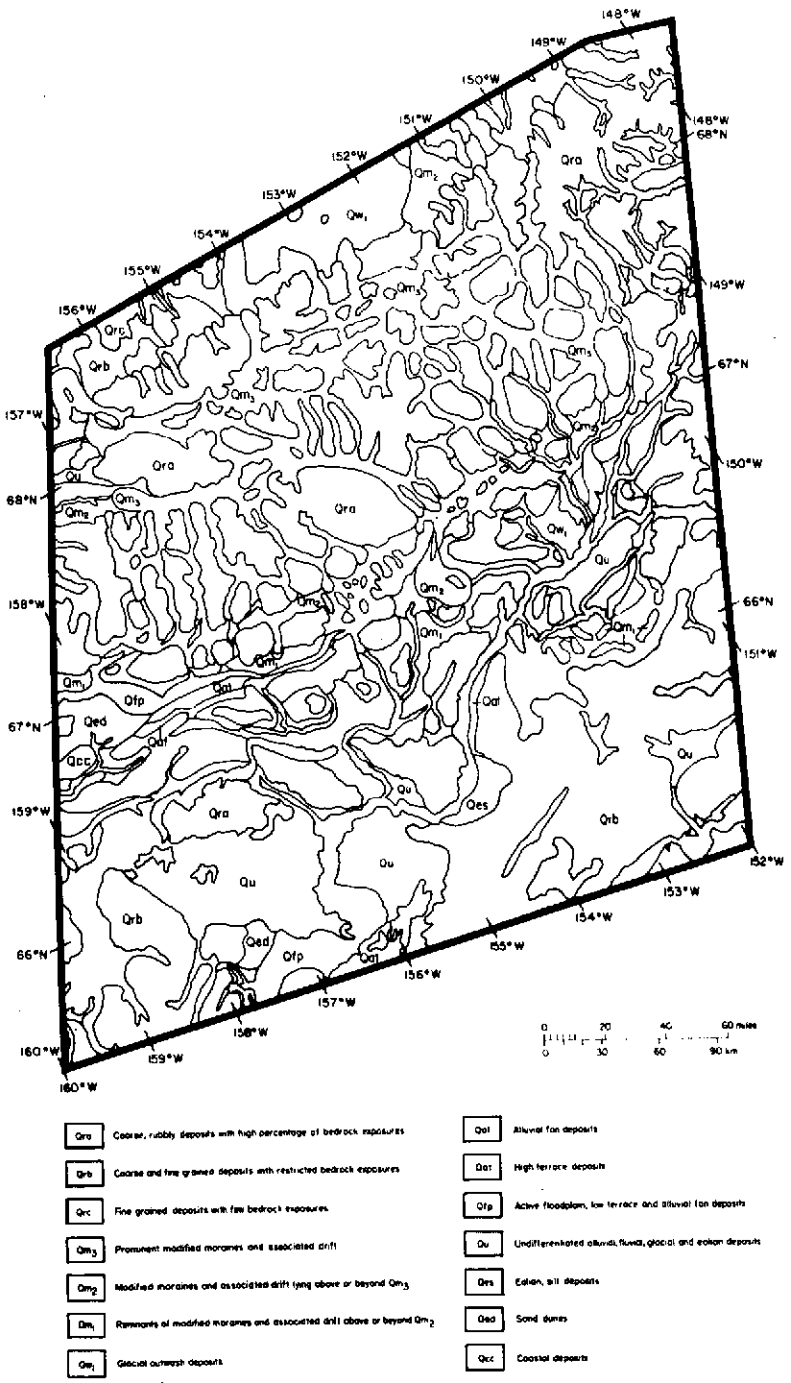

Figure 22. Surficial geology of north central Alaska from Karlstrom and others (1964).

The principal aims in mapping vegetation patterns were: to demonstrate that ERTS imagery could be used to prepare a detailed vegetation map of a remote area with minimal ground truth data, effort and expense as compared to conventional vegetation mapping approaches; and, to provide a delineation of vegetation associations at a level of detail comparable with the surficial geology maps in Figures 20 and 21. Mapping was done on an acetate overlay of the ERTS MSS 1:1 million, band 5 mosaic and the enlargement of the area south of Fairbanks. The primary source of supplementary data was Spetzman's (1963) vegetation map of Alaska. This provided most of the information on vegetative composition within the mapping units defined. Valuable data was also obtained from a series of oblique aerial color photographs taken during an aircraft overflight of the area during September 1972. Additional information was obtained from narratives and photographs contained in several USGS area reports (Cass 1959, Patton 1966, Weber and Péwé 1970). To aid in the interpretation process, a false color composite was constructed with a multispectral viewer from MSS bands 4, 5 and 7 of ERTS image 1037-21234 acquired on 29 August 1972 and located approximately in the center of the mosaic area.

Because of the relatively coarse resolution of the MSS imagery, vegetation differences are apparent primarily through tonal rather than textural patterns. The tonal differences are related both to vegetation density and species composition; textural differences are related primarily to terrain features, but they, nevertheless, provide indirect information on vegetation. Eight vegetation association units were mapped in the north central area (Fig. 23). Fc (Forest, closed) is a tall to moderately tall, closely spaced spruce-hardwood forest, consisting of white and black spruce with paper birch, aspen, and balsam poplar on moderately to well drained sites such as active floodplains, mountain slopes (especially south facing) and highland areas. Fc appears on the mosaic as a solid dark tone. Fo (Forest, open) consists of stunted open tree growth dominated by black spruce; also includes tamarack, white birch, and white spruce; thick mosses, grasses and heath comprise the principal ground cover. This association is widespread on poorly drained lowlands throughout the southern two thirds of the mosaic area and appears as a slightly mottled, medium gray tone. Fou (Forest, open, upland) is an intermediate mapping unit having a species composition similar to Fc, but identified by a lighter tone than Fc indicating a more open forest. Its occurrence is primarily on poor to moderately well drained uplands. Fod (Forest, open, dunes) is an open, dominantly black spruce forest with a lighter and smoother tone than the Fo unit. This mapping unit is confined to several isolated areas where the forest has overgrown and stabilized sand dunes. The brighter tonal signature could be accounted for by open areas of sand within the association. Tm (Tundra, moist) occupies vast areas of poorly to moderately drained topography. The unit contains some scattered and stunted black spruce

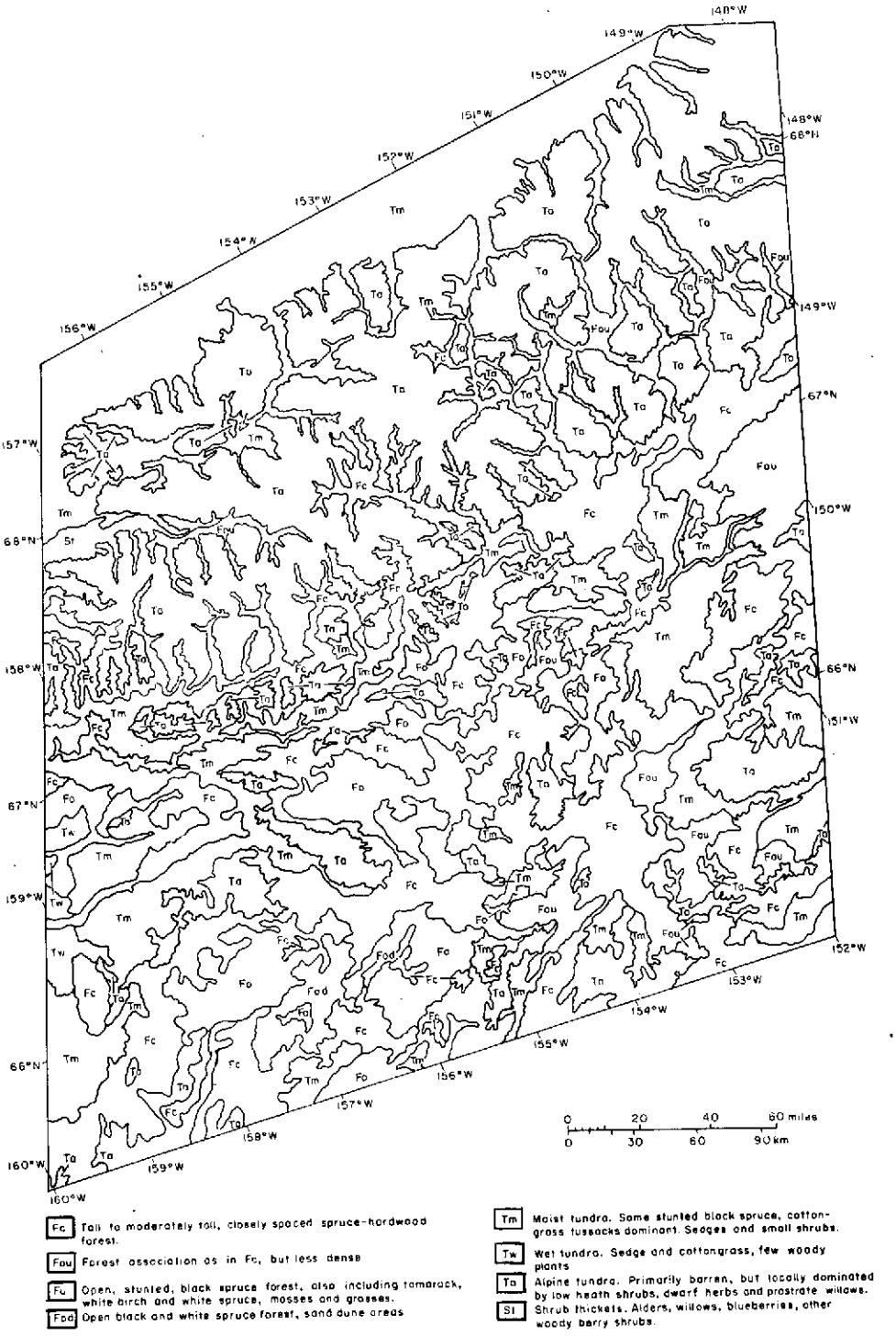

Figure 23. Vegetation of north central Alaska from ERTS-1 imagery.

within the southern two thirds of the study area. Cottongrass tussocks are the dominant vegetation form, with sedges and dwarf shrubs where tussocks are absent. It is represented on the ERTS mosaic as a smooth medium gray tone which darkens slightly near stream channels. Tw (Tundra, wet) consists of sedge and cottongrass with a few woody plants. This association is similar to, or the same as, Tw in its tonal signature, and is distinguished by the presence of many thaw lakes and wet areas. St (Shrub thickets) consists of dense thickets of alders, willows, blueberries and other woody berry shrubs found in coastal areas and floodplains north of the timberline. Extensive areas of this association in the northern foothills of the Brooks Range appear on existing vegetation maps. Except for a small area in the northwest portion of the mosaic, the signature of this St unit was obscured by snow and was not mapped. Ta (Tundra, alpine) is primarily barren, but is locally dominated by low heath shrubs, prostrate willow, and dwarf herbs. In the mosaic area, this association is generally found at elevations over 600 m. The alpine tundra was snow covered when mapping was begun. Analysis of summer imagery differentiates the alpine tundra as a smooth, medium gray pattern readily distinguishable from the Fc association which forms its lower boundary on mountain slopes.

The tonal signatures indicated in the interpretation of the vegetation mapping units are characterized only by relative density. The overall density of the ERTS imagery varies from scene to scene and also within scene. Therefore the vegetation association patterns and tones must in all cases be interpreted relative to each other and to topographic position. Snow in the central and northern parts of the mosaic and in the alpine areas has the effect of emphasizing some patterns, such as the Fc - Ta boundary, but it obscures the distinction between the tundra and shrub associations.

The vegetation map prepared from ERTS imagery (Fig. 23) was compared to the existing vegetation map by Spetzman (1963)(Fig. 24). It is clear that the boundary detail of the mapped vegetation associations is greater on the ERTS derived map than on the previously available map of the area. It is recognized, however, that Spetzman's map was deliberately generalized in keeping with its original 1:2,500,000 scale; but it is also true that considerably more detail could have been achieved from the ERTS imagery had the project objectives warranted.

A vegetation map at a 1:250,000 scale was also prepared for an area south of Fairbanks (Fig. 25). The mapping units were generally the same as those in north central Alaska; however, several associations were not present in the Fairbanks area because of its lower topography and interior location. In addition, shrub thicket or brush unit, St, which was largely masked by a deep snow cover in the northern and western part of the north central Alaska mosaic, was readily distinguishable in the Fairbanks area. The thin snow cover in Fairbanks was approximately

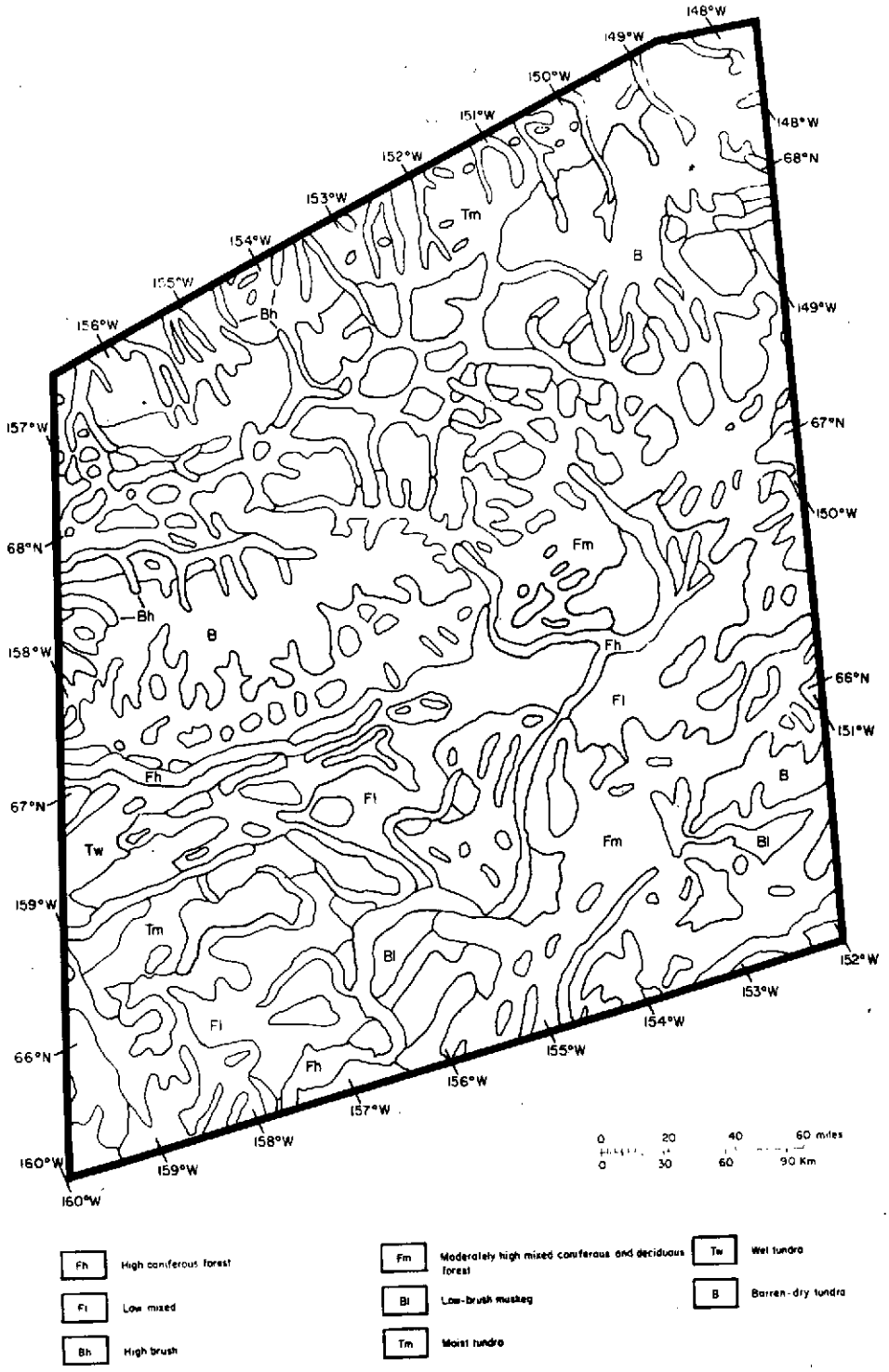

Figure 24. Vegetation of north central Alaska from Spetzman (1963).

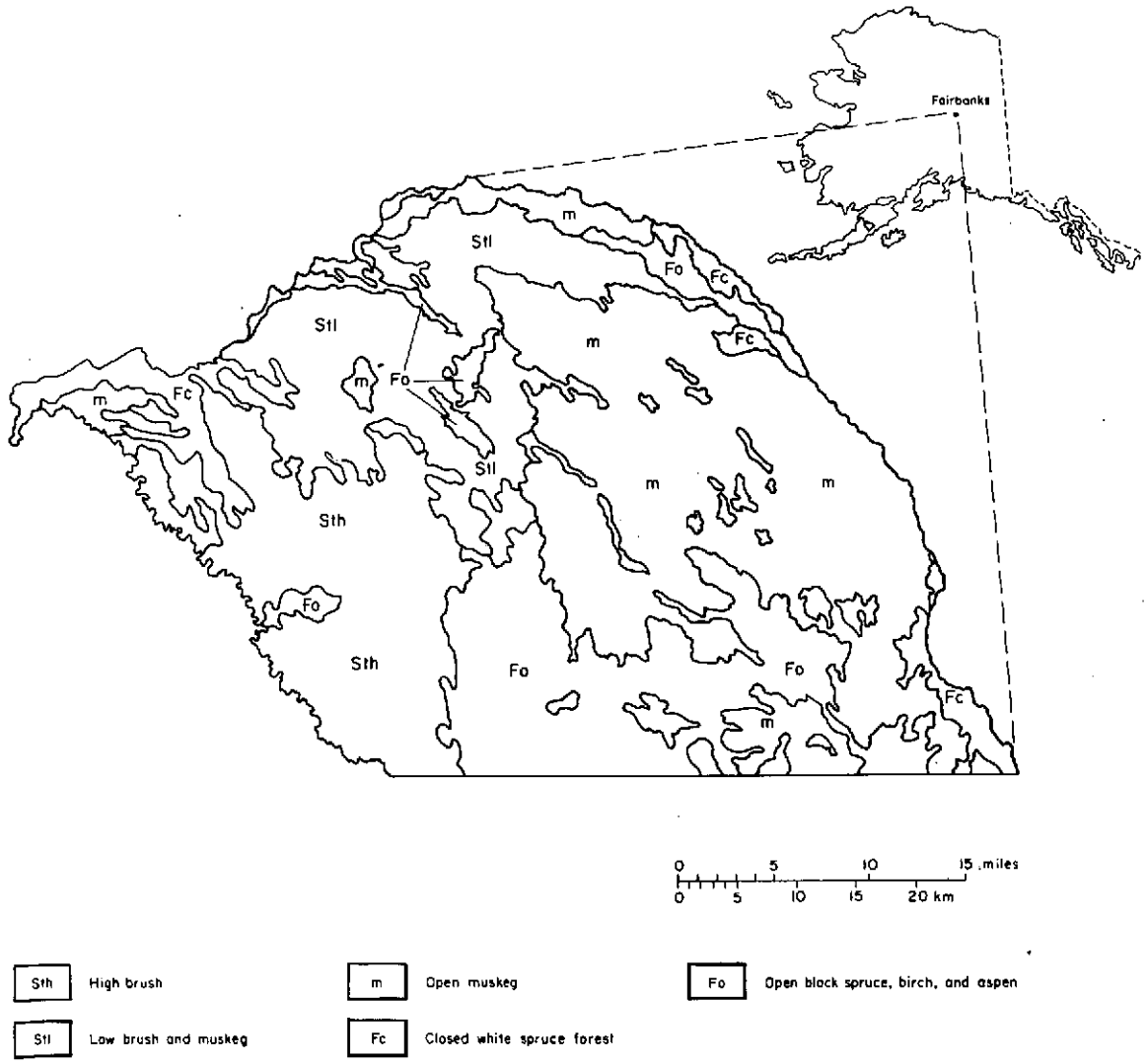

Figure 25. Vegetation of area south of Fairbanks from ERTS-1 imagery.

5 cm thick (as measured at the Fairbanks FAA) at the time of image acquisition and served to enhance the St association and two distinct units were differentiated, Sth (high brush) and Stl (low brush and muskeg). The Sth association had a darker mottled gray signature than Stl on the November 3 scene (Fig. 19). The boundary between the Sth and Stl units approximates the boundary between the surficial geology units, Qfl and Qag, which suggests that drainage influences the height and density of vegetation in this area.

Existing maps of permafrost distribution are general, primarily because of the lack of extensive, detailed data (Ferrians 1969). The delineation of permafrost boundaries from conventional aerial photography has been found to be difficult, requiring extensive ground studies to confirm. There is no precedent study in which permafrost terrain has been classified utilizing imagery of the scale and resolution available with ERTS. Consequently, it could not be known in advance the extent to which the more subtle tonal and textural changes on the MSS images might show large scale patterns not discernible in aerial imagery and useful in differentiating among the various types of permafrost terrain. The ERTS-1 MSS imagery exceeded expectation in this respect. Large scale patterns easily identifiable on the imagery include thermokarst topography, icings (naleds, aufeis), beaded drainage, and permanent ice fields. Smaller features, such as pingos/palsas, ice wedge polygons, solifluction lobes, nivation terraces, and stone polygons and stripes could not be identified at the resolution afforded by the multispectral scanner system.

Four permafrost terrain units have been defined and mapped in north central Alaska (Fig. 26) and the Fairbanks area (Fig. 27) based on interpretations of surficial geology and the probable depths of thaw inferred from the vegetation. Other mapping criteria, such as temperatures and permafrost properties, are not observable on the ERTS imagery and, hence, were not used in the permafrost terrain mapping. The bedrock (m) terrain is characterized by a thaw depth of 0.3 - 1.0 m except on south-facing slopes where thaw depths may exceed 2 m. It also contains a few scattered taliks. Soils are coarse-textured and shallow. Alpine vegetation occurs on the highest, steepest area with black spruce and paper birch on the north-facing slopes. The principal trees on south-facing slopes are white spruce, paper birch, quaking aspen and alder. The alluvium-colluvium (u) permafrost terrain unit has relatively high ice contents and a thaw depth of <0.5 m in areas of poor drainage and 0.5 - 2.0 m and numerous taliks on moderately to well-drained slopes. Fine-grained, shallow soils occur on steep slopes and medium - to fine-grained, deep soil on gentle slopes. Alpine vegetation occurs on summit positions and black spruce and paper birch on north-facing slopes. White spruce, quaking aspen and alders are found on the south-facing slopes. Moist tundra occurs on poorly drained footslope

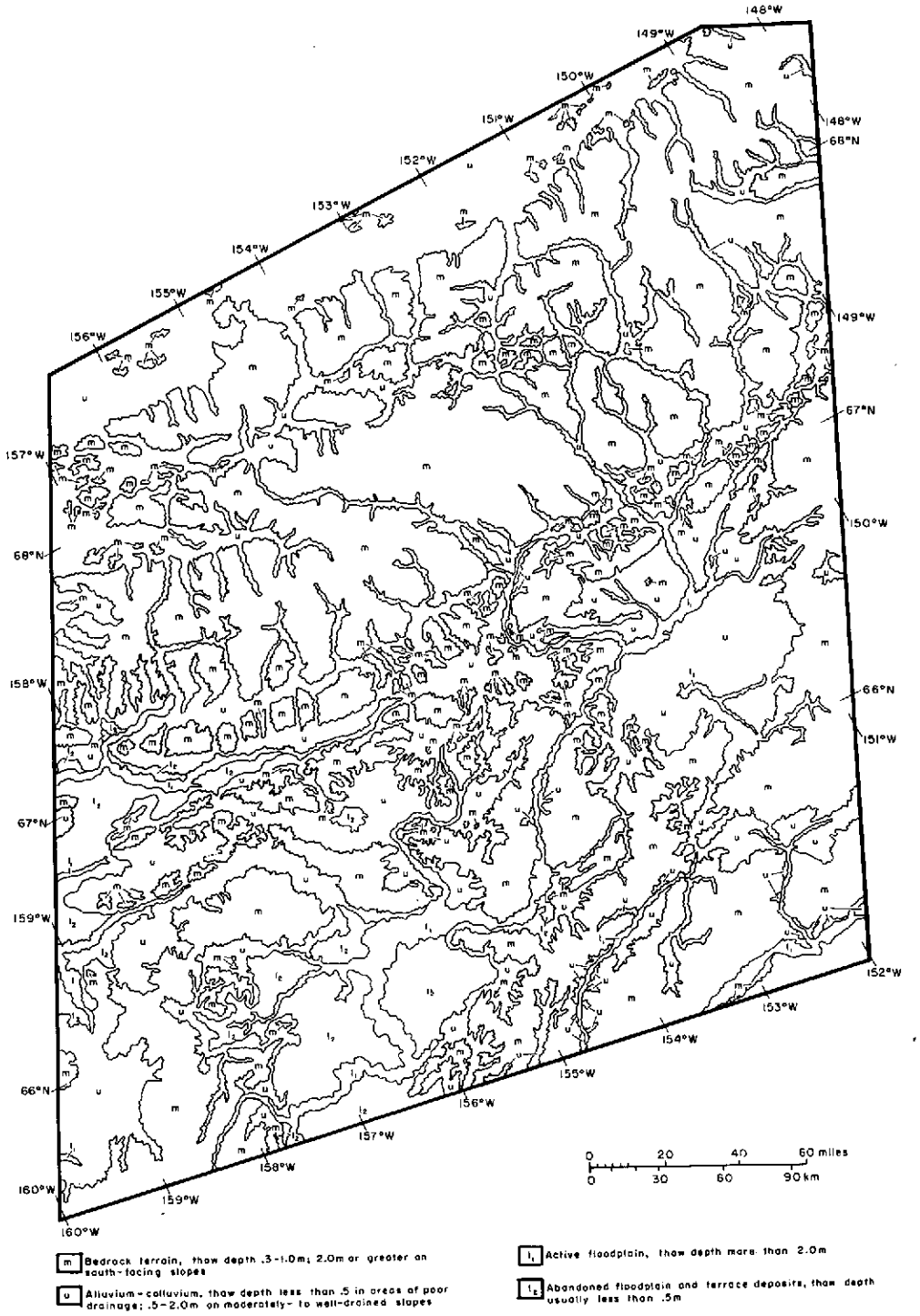

Figure 26. Permafrost terrain of north central Alaska from ERTS-1 imagery.

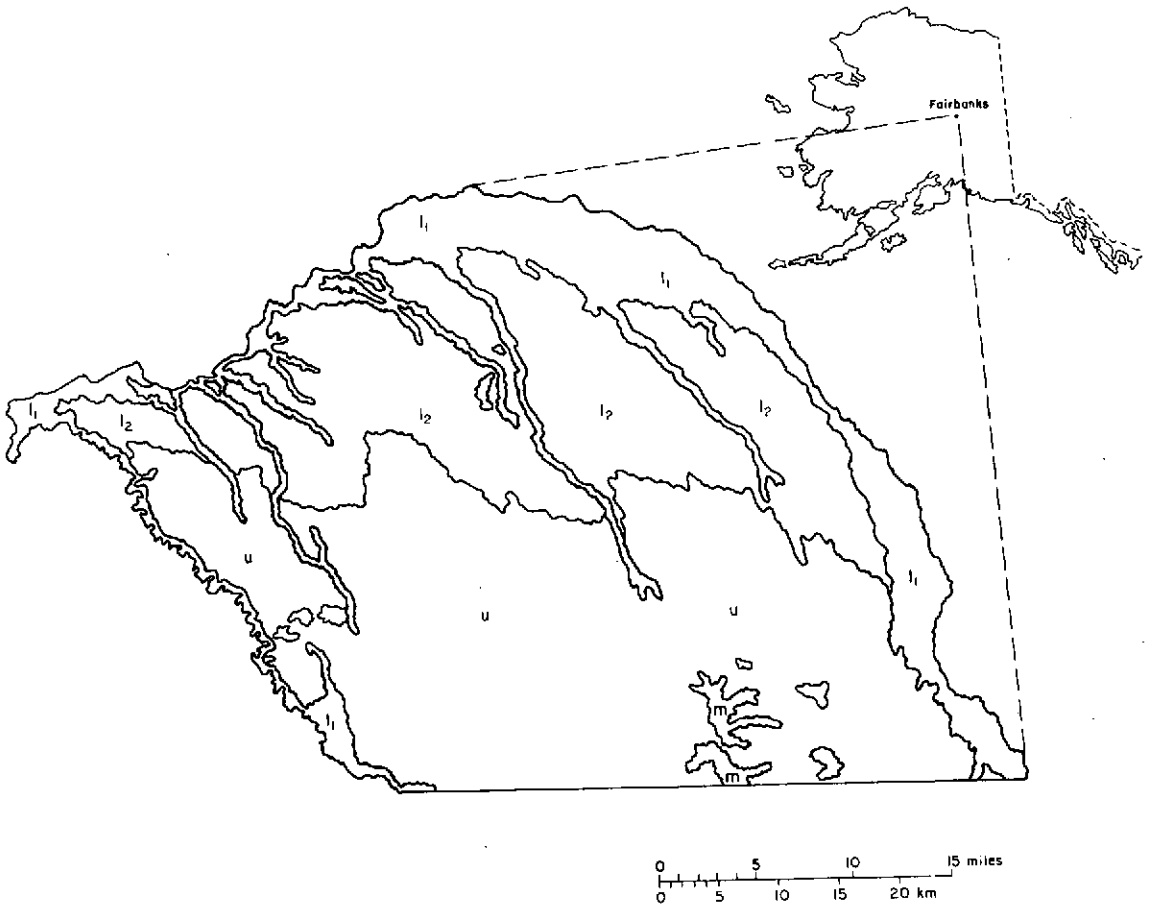

Figure 27. Permafrost terrain of area south of Fairbanks from ERTS-1 imagery.

positions. The active floodplain (l_1) terrain is characterized by numerous taliks, a thaw depth of more than 2.0 m, and fine-grained, deep soils. Balsam poplar, paper birch and white and black spruce predominate. The fourth permafrost terrain unit, abandoned floodplain and terrace (l_2), is also characterized by numerous taliks but in addition contains many small thaw lakes. Soils are fine-grained and shallow with permafrost occurring at depths usually less than 0.5 m. Vegetation includes moss, lichens, low lying shrubs and black spruce. Using these criteria, a permafrost terrain distribution map was prepared in considerably greater detail than any previously available (Fig. 28). It is quite feasible by extending these techniques, to rapidly produce improved permafrost maps more detailed than any presently in existence.

3.2.3 Shore-fast ice survey

Among the top three research topics recently identified by the Alaska Oil and Gas Association is the development of a rapid method to map the distribution and properties of sea and shore-fast ice in Alaska. The need for a remote sensing technique to accomplish this was also given high priority at the Second International Conference on Permafrost held in 1973 at Yakutsk, Siberia. More recently it has been highlighted by a National Science Foundation ad hoc committee on priorities in permafrost research. Accurate, up-to-date maps of permafrost including shore-fast ice now are needed in final route selections, selection of pumping station and off-shore loading facility sites, and the planning and implementation phases of the Alaska pipeline and facilities construction. Mapping of permafrost related features was therefore extended to a large portion of the Alaskan Coast where permafrost continues below the continental shelf. The distribution of shore-fast ice has been charted along the west coast of Alaska from Point Barrow to Cape Krusenstern in an attempt to relate its occurrence with the distribution of offshore permafrost. Accumulation and ablation of shore-fast ice was mapped from imagery acquired from March to July 1973 for the spring and early summer seasons (Fig. 29). It is clear that the shore-fast ice regime is easily monitored by means of sequential ERTS imagery. When compiled in an atlas as a function of season, shore-fast ice distribution will be valuable in guiding the planning and construction of navigational and shore facilities.

3.2.4 Terrestrial analogs of Martian permafrost terrain

Prior to the launch of Mariner 9 it was widely speculated that patterned ground, exceptionally large pingos and large scale thermokarst depressions might be seen on Mars. The resolution of the ERTS multispectral scanner and Mariner 9, Camera B (narrow angle) imagery is comparable. Therefore Martian permafrost features similar in appearance

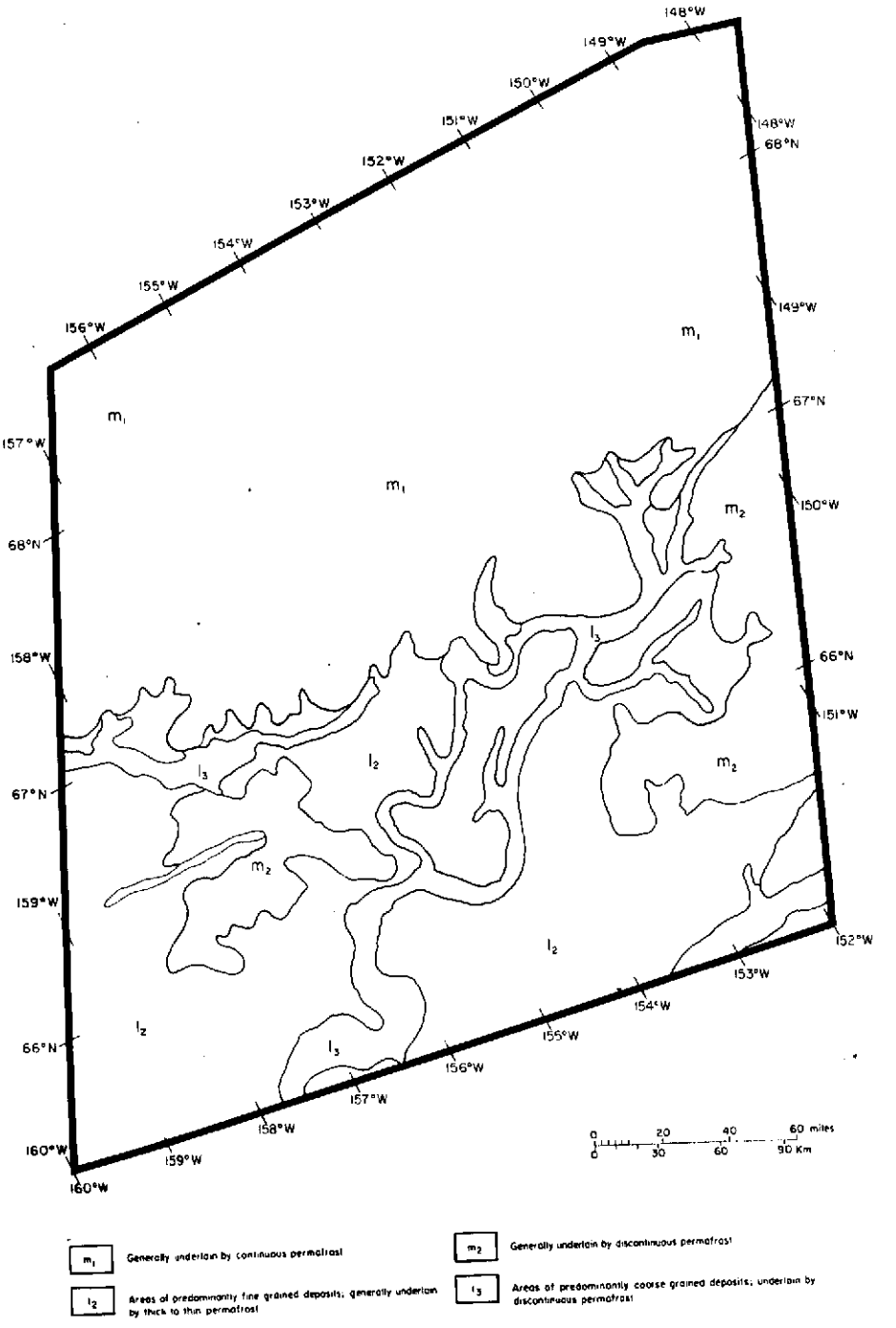

Figure 28. Permafrost map of north central Alaska from Ferrians (1969).

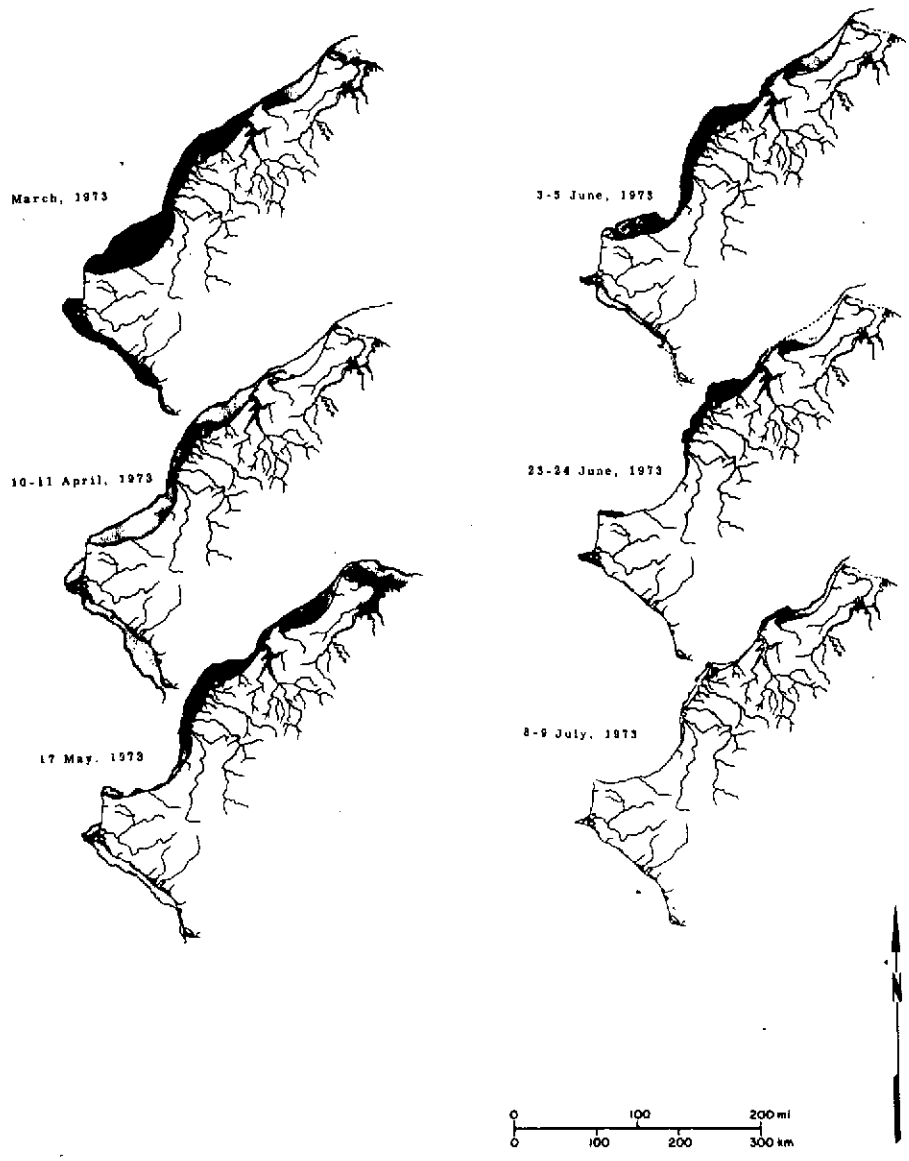

Figure 29. Distribution of shore-fast ice from Cape Krusenstern to Point Barrow from March to July 1973.

and size to terrestrial permafrost features resolved by ERTS would also be expected to be resolved in the Mariner 9 B-frames. Several ERTS-1 scenes of Alaska show terrestrial permafrost terrain features in permafrost areas large enough to be seen if present on Mariner B-images. In Figure 44, along the south coast of Norton Sound, interesting polygonal patterns can be seen in the lowlands of the Yukon River Delta. Ice wedge polygons are less than 100 m across and therefore are too small to be detected by either the Mariner 9 or ERTS satellite imagery. The polygonal patterns in this scene, however, are some 300-500 m across. Their unusually large size is thus quite remarkable. They occur in a region generally underlain by thin to moderately thick permafrost. Aerial photography (Fig. 30) of this area permits an interpretation. It reveals that this polygonal network results from the superposition of old beach ridges (1), old distributary channels (2) and thaw lakes (3) (Shepard and Wanless 1971). A superficial comparison to the polygonal patterns on Mars shown in Mariner 9 image number PLYBK P177, picture 35B is possible. However, although the processes of formation of these polygonal patterns on Mars are not known, it is unlikely that the processes are truly comparable. It is, however, likely that the presence of ice-rich permafrost on Mars would result in a number of surface expressions and that polygonal ground is one of them.

Pingos are generally too small to be clearly resolved on the ERTS imagery; however, in cases in which the location of a pingo field is known, tones and textures accompanying the presence of pingos generally can be distinguished on close inspection. An example is the Yukon-Tanana Uplands of interior Alaska where numerous pingos previously identified by ground and aerial observations are barely visible (Figure 56). There the pingos are conical, elliptical, oval or irregular mounds and are found singly as well as in clusters. They vary from 3 to 30 m in elevation and from 8 to 364 m in diameter (Holmes et al. 1963). Clearly, unless analogous features present on Mars are very much larger, they would not be identifiable on the Mariner imagery.

During this portion of the investigation, a photo mosaic of Alaska north of latitude 68° from the Canadian border to the Chukchi Sea was prepared from 17 MSS band 7 images taken in March 1973. The region was blanketed with snow at this time. The snow cover coupled with a low sun angle enhanced topographic features. As a result many small scale depressions not normally visible are apparent. When seen from this perspective, the topography of the North Slope between the White Mountains and the Titaluk River is particularly interesting. In a number of respects it is similar to chaotic and fretted terrains in the northern part of Zanthe-Cryse region on Mars shown in Mariner 9 B-frames. This terrestrial analog consists of pits, basins, valleys, and closed depressions with small hummocks often containing lakes. It is characteristic of degrading permafrost areas with high subsurface ice contents; as the

Figure 30. Photo mosaic made from aerial photographs of the southern coast of Norton Sound (photographs courtesy U.S. Navy). Outline of the mosaic on Figure 44.

ice melts, the surface subsides. Eventually individual depressions coalesce to form shallow elongated valleys. Local forms of thermokarst topography depend on the amount and forms of subsurface ice and the balance between thermal, mechanical, and fluvial erosion.

The north slope thermokarst terrain is similar in some respects to the alas topography of the Yakutian loess deposits of Siberia (Czudek and Demek 1970) which we have advanced also as a terrestrial analog of some Martian terrains. A photo mosaic of the Siberian thermokarst region was prepared from 12 MSS band 7 images. A linear contrast stretch and geometric corrections identical to those performed on the Mariner 6, 7 and 9 imagery were performed on the ERTS computer compatible tape of a portion of these areas by the Image Processing Laboratory (IPL) of the Jet Propulsion Laboratory. The contrast stretch enhanced tonal differences of these uniformly high albedo scenes and aided in comparing the ERTS and Mariner imagery. The geometric correction merely compensated for the Earth's motion under the satellite during image acquisition and was of negligible importance in this investigation. Contrast stretching was applied to bands 4, 5, 6, and 7. In this case enhancement of band 7 resulted in the best rendition for recognition and definition of thermokarst terrains. These preliminary findings have led to plans to continue the investigation. ERTS imagery of other polar and subpolar terrain will be obtained and examined for terrestrial analogs of Martian permafrost terrains under the NASA-CRREL Viking and Planetary Programs Investigations during the period 1974-77. In addition to providing a useful basis of interpretation and analysis of satellite imagery of Mars, these comparisons also will provide new insights and perspectives in terrestrial geomorphology of the polar regions.

3.3 Snow cover-runoff relationships

3.3.1 Location and description of Caribou-Poker Creeks watershed

The Caribou-Poker Creeks research watershed (Fig. 31) is well suited for an investigation of the utility of ERTS imagery in analyzing snow cover-runoff relationships: it is recognized as typical of the intermountain plateau physiographic province of this region; it is completely vegetated by a "natural" plant cover that has been unaffected by the activities of man for more than 40 years, and, snow cover, water equivalent and stream discharge data are readily available, a unique situation for Alaska where such data generally are sparse.

The watershed is a 103 km^2 catchment area located in the Yukon-Tanana Uplands of central Alaska. It has a dendritic drainage pattern formed in the Birch Creek Schist which underlies most of this area. Local elevations range from 212 m to 769 m (Caribou Peak). Valley floors are occupied by riparian shrub-tree complexes; south-facing slopes support extensive stands of aspen and birch, with admixtures of alder,

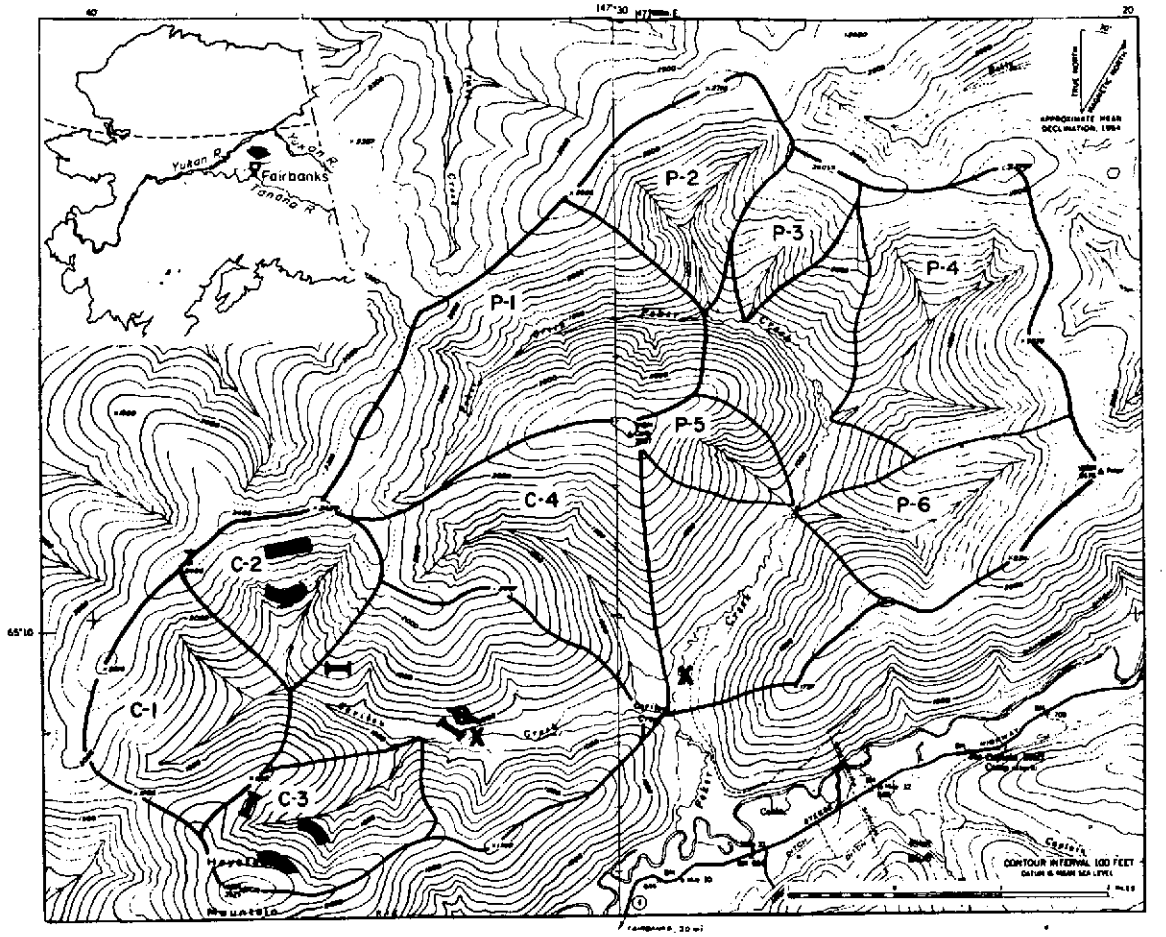

Figure 31. Location, instrumentation and data acquisition sites, Caribou-Poker Creeks research watershed.

and lesser areas of both white and black spruce; north-facing slopes support a predominantly black spruce cover. A thick (2.4-6.0 cm) ground cover of moss and duff overlies virtually all north-slope and valley sites.

3.3.2 Snow course and snow pillow data collection

Snow observations were made at eight locations in the Caribou Creek branch of the watershed (Fig. 31). The measurements included: (1) three standard Soil Conservation Service (SCS) snow courses (Haystack Mountain #102; Caribou Creek #103; and, Snow Pillow #104); (2) four transects, each with 40 points, 25 m apart, on the contour at elevations 485 m and 636 m in both subdrainage C-2 (south-facing) and subdrainage C-3 (north-facing); and (3) a recording liquid-filled snow pillow located at 311 m in the Caribou Creek valley. The SCS snow courses were measured monthly from December through June. Measurement of snow depth and water equivalent (the amount of liquid water in area-inches which would be yielded by melting a unit area sample of the existing snowpack) was accomplished with a Federal snow sampler at predetermined points. The snow transects were measured once at the time of maximum accumulation. At each sampling point (marked by a 5 cm x 5 cm stake with a measurement tape attached) snow depth was recorded and the water equivalent measured (normally) at six representative points on each transect. Snow accumulation/ablation (snow water equivalent) was recorded continuously by the snow pillow which consists of a flexible neoprene bladder, 1.8 m in diameter, filled with ethylene glycol antifreeze and hydraulically connected to a stilling well located in a nearby instrument shelter. The weight of increments of snow accumulated on or ablated from the pressure pillow causes fluctuations of the fluid level in the stilling well where changes are recorded on a conventional water level recorder (Leupold-Stevens, Type F 1).

Snow accumulation/ablation (snow water equivalent) data for the '72-'73 season as recorded at the snow pillow in the Caribou Creek Valley is shown in Figure 32. The data show that the snowpack in the watershed during the winter of 1972-73 was lighter than the previous year. Results of snow surveys at SCS snow courses in the watershed are given in Table 5. These data are mean values of five measurements from each snow course and date acquired according to standard snow surveying procedures. The data show little change (≈5.1 cm) in snow accumulation in March, although the snow pillow record shows an increase of 1.27 cm water equivalent in early March. Ablation at the snow pillow was rapid in late April, but was considerably slower on north-facing slopes and at higher elevations as indicated by data from the Haystack snow course (Table 5). These data show a net decrease in snowpack depth but an increase in total water content (hence, an increase in mean snowpack density) in April at this location. Data from snow transects taken approximately at the time of maximum snow depth are given in Table 6. These data were acquired on different dates because of difficulties in reaching the C-3 sites in early April. The maximum snow pack occurred

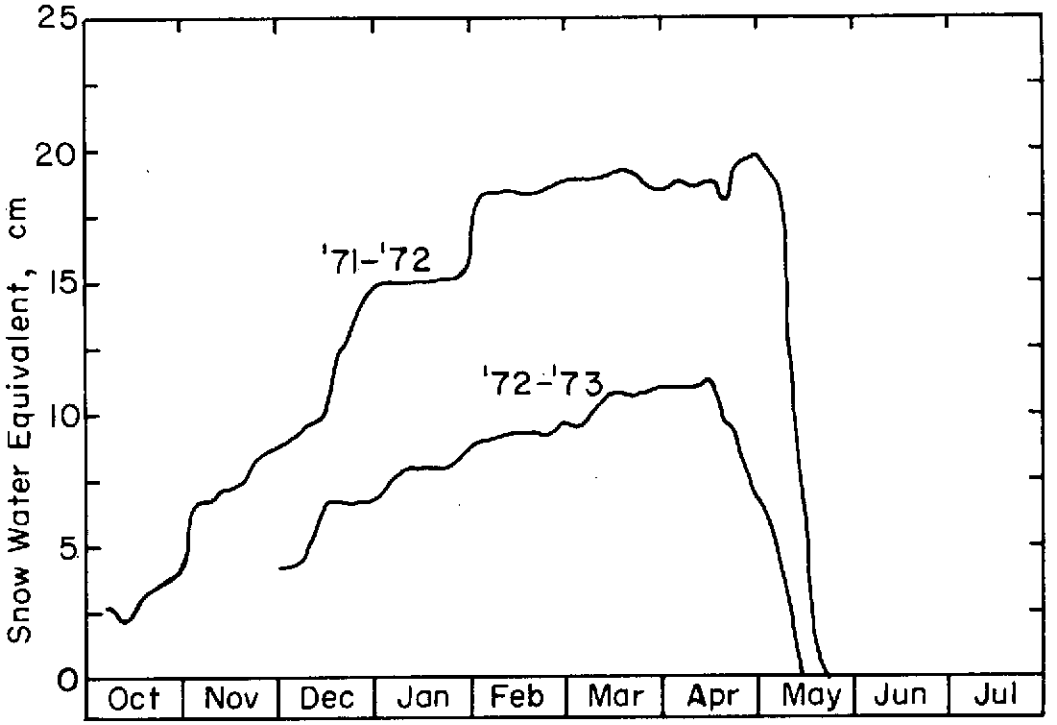

Figure 32. Snow pillow data for '71-'72 and '72-'73 seasons in the Caribou Creek Valley.

Table 5. Mean depths (cm) and mean water equivalents (cm) along Soil Conservation Service snow courses, Caribou-Poker Creeks research watershed.

	Course #102 Haystack Mountain (Elev. 591 m)		Course #103 Caribou Creek (Elev. 436 m)		Course #104 Snow Pillow (Elev. 311 m)	
Date	Mean depth	Mean Water equiv.	Mean depth	Mean water equiv.	Mean depth	Mean water equiv.
30 Jan 73	83.8	20.3	55.8	10.4	50.8	11.1
28 Feb 73	78.7	18.0	55.8	12.7	50.8	11.1
29 Mar 73	83.8	17.7	53.3	12.7	50.8	10.4
2 May 73	60.9	23.6	(no data)		5.0	1.7

Table 6. Snow depths at time of maximum seasonal accumulation at four snow transects: data summary, 1973.

Location	Date	No. of sample pts.	Mean snowpack depth (cm)	Standard deviation (cm)	Mean water equivalent (6 samples) (cm)
636 m MSL Subdrainage C-2	4 Apr 73	32	61.4	14.0	12.3
485 m MSL Subdrainage C-2	6 Apr 73	35	58.3	8.7	12.9
636 m MSL Subdrainage C-3	26 Apr 73	31	77.5	10.5	19.6
485 m MSL Subdrainage C-3	26 Apr 73	36	68.9	12.3	16.3

in early to mid-April for all sampling points at upper elevations. ERTS observations together with the snow pillow data indicate that ablation began at lower elevations in early April, at higher elevations in early May.

3.3.3 Imagery Analysis

Cloud free ERTS imagery acquired on 3 November 1972 (image 1103-20502), 27 March 1973 (image 1247-20505), 3 May 1973 (image 1284-20562) and 20 May 1973 (image 1301-20503) was reviewed. The distinction between snow, snow-free areas and forest was most apparent in band 5 (Wendler et al. 1973 report similar findings). The 9.5 inch positive transparencies of band 5 were enlarged and an accurate outline of the research watershed was transferred from a topographic map to the photographic enlargements with a Bausch and Lomb Zoom Transfer Scope (Fig. 33). Snow cover (4) was readily observable in the alpine zone and in the treeless valley bottoms along the Poker (1) and Caribou (2) Creeks. The alpine zone and bottom lands comprise approximately 35 percent of the total watershed area. Snow was obscured on densely forested slopes (5) and also in the shadowed areas (3) of the watershed. To accomplish the analysis it was assumed that changes observed in the treeless areas were representative of the basin as a whole. This assumption is considered reasonable because the treeless areas include both the highest and lowest areas within the watershed.

3.3.4 Comparison of ERTS imagery analysis to snow pillow data

An extensive snow cover was observed on the ERTS imagery from 3 November 1972 to 27 March 1973 and also recorded by the snow pillow (Fig. 32). Significant changes in snow cover were first evident in the valley bottoms while minor differences were observed in the alpine areas. Ablation was well advanced by 3 May 1973; the areal extent of the snow cover within the watershed appeared by then rather similar to that on 3 November 1972, although there was considerably more snow remaining in the Caribou Creek Valley. The most striking indication of ablation was observed between 3 and 20 May. Snow remaining in late May was restricted to the high alpine areas of the watershed.

Snow covered areas were measured as a fraction of the total watershed area using an Antech A-12 color densitometer with an electronic planimeter attachment. These measurements were then compared to the snow pillow data, the only continuous data available for the watershed during the winter months, in a search for correlations. Since the snow pillow provides a measure of water equivalency of the snow cover at a single point within the watershed, it is not directly comparable to the areal snow cover measurements as obtained from ERTS imagery. To facilitate comparison, water equivalency and areal coverage of the snow pack were converted to a percentage difference from the maximum values measured

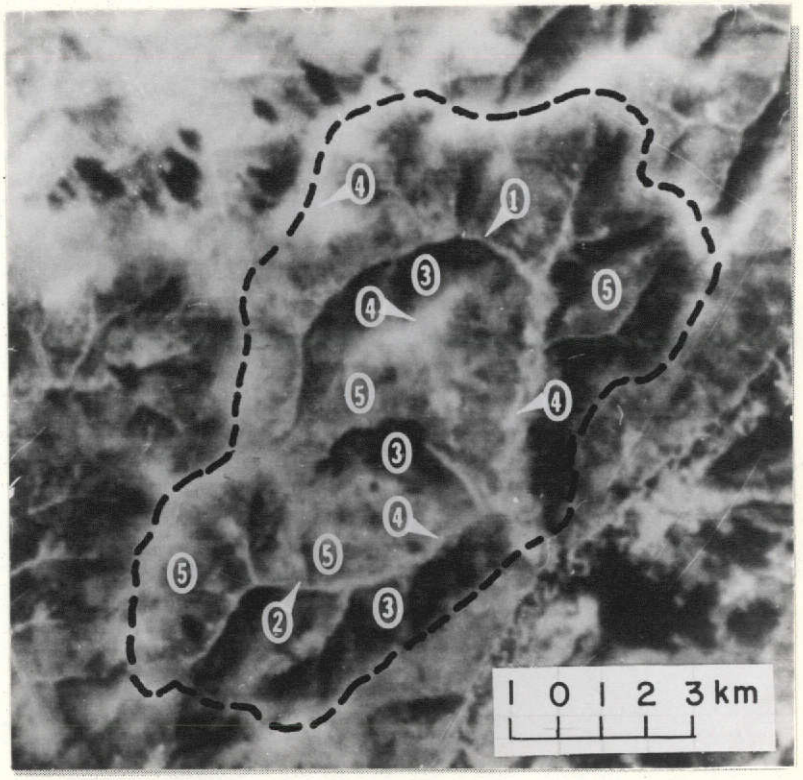

Figure 33. Caribou-Poker Creeks watershed (outlined) on 27 March 1973; 6 x enlargement from ERTS band 5 image 1247-20505; scale approximate.

for each. These are plotted in Figure 34. Line A shows changes in the areal extent of the snow cover for the entire watershed as measured on the four ERTS scenes. The maximum cover measured was on the 27 March 1973 scene; this, therefore, is taken to be the 100% reference value. The remaining three areal snow cover measurements are expressed as a percentage of this value. Line B shows the snow pillow data from Figure 32. Line C is a plot of ERTS-derived snow cover data for the Caribou Creek Valley portion of the watershed; these data correspond more closely to the snow pillow data.

On 3 November, 27% of the maximum snow cover observed on the ERTS imagery during the '72-'73 season was found to be in Caribou Creek Valley, while approximately 77% of the maximum value was observed for the entire watershed. Snow cover distribution from 27 March to 3 May decreased from the maximum value to 80% in the entire watershed, and to 62% in the Caribou Creek Valley. By 20 May snow cover was virtually gone according to both data sources.

Data on stream discharge were acquired at the gaging stations near the confluence of the Caribou and Poker Creeks (Fig. 31) and were available in April 1974. Figure 35 shows the discharge through the time of maximum snow melt. The rapid melting that began in mid-April (Fig. 34) was recorded initially at the Poker Creek station; discharge increased from 7 to 9 ft^3/sec between 15 April and 1 May. Melt continued through April and early May and discharge reached a peak in mid-May. Discharge dropped to near normal summer levels at the end of May. The sudden increase in discharge in early June may have been a result of rapid precipitation. The lag time between the time of melting and the time the water passes the gaging stations is approximately 10 days. The maximum discharge at 15 May probably corresponds to the arrival of the water resulting from the rapid increase in snow melt beginning at the beginning of May.

The following relationships were recognized during this preliminary analysis: changes in water equivalents recorded by the snow pillow and changes in areal snow cover measured on ERTS imagery appear to correlate; the general regime of snow accumulation and ablation is observable on ERTS imagery; and, significant decreases in the areal extent of snow cover observable on ERTS imagery are reflected in increased stream runoff measured at gaging stations. These findings suggest that sequential satellite imagery can be used to monitor snow regime and forecast times of maximum runoff.

3.4 Icings

Icings (naleds, aufeis) are masses of surface ice formed during the winter by continual or successive freezing of ground water that makes

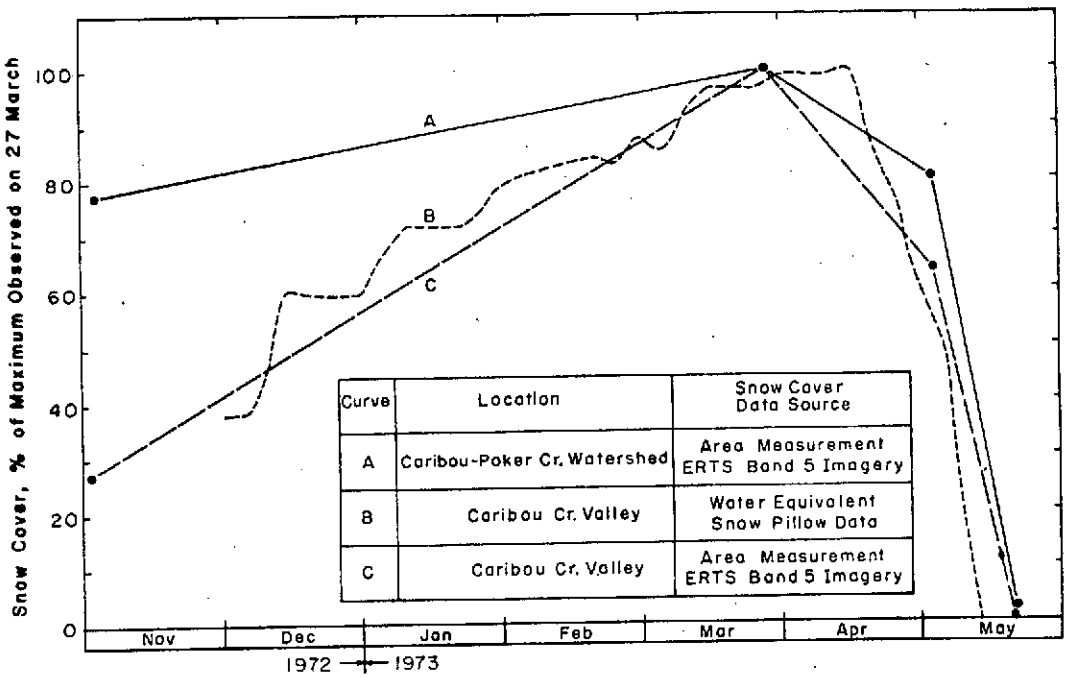

Figure 34. Percent snow cover from densitometer measurements on ERTS imagery versus percent snow accumulation from snow pillow data.

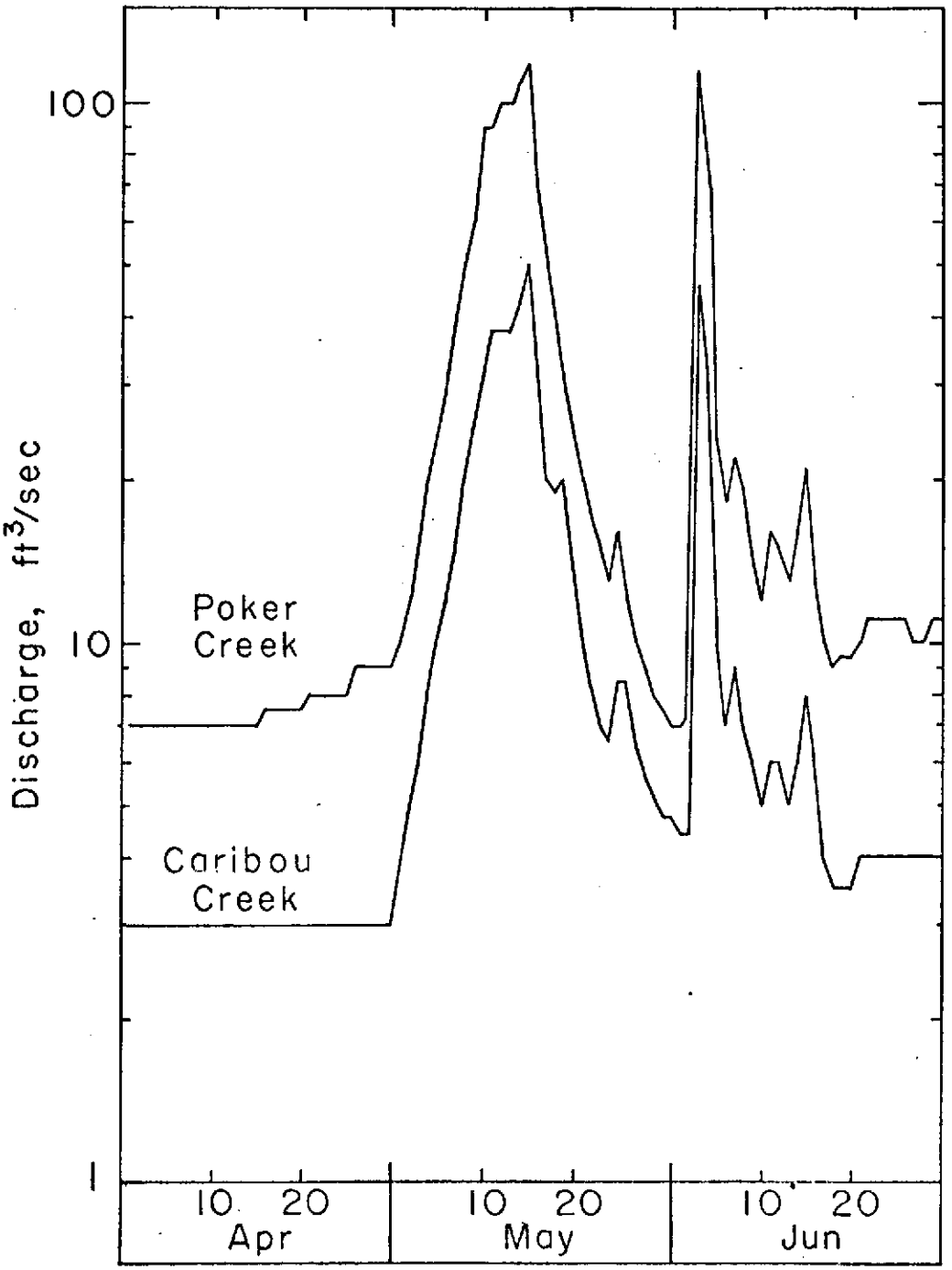

Figure 35. Discharge at the watershed gaging stations through the time of maximum snow melt.

its way to the surface (Muller 1947). Repetitive overflows form layers of stratified ice that often create massive deposits. During the late stages of formation the ice build-up often extends considerably beyond the normal boundaries of the stream channels. In such cases, icings may become hazardous. Icings may spread over or encroach upon roads, for example, and ice blocked drainageways may lead to washout of embankments during spring thaw (Carey 1973). Although the amount of build-up varies considerably, icings tend to occur at the same locations from year to year. The ability to survey and monitor the occurrence of icings by means of sequential satellite imagery in uninhabited or little known areas provides information of great value on route and site selection, etc.

Briefly stated the principal environmental factors influencing the development of icings are precipitation, immediately prior to freeze up, which influences streamflow during the winter, the depth of snow during the winter which influences the depth of frost penetration in the ground, and the temperature regime during late winter and early spring when icing formations usually experience rapid growth.

3.4.1 Chena River

The Chena River watershed was selected initially as a convenient site for judging the effectiveness of ERTS imagery for the identification and inventory of stream icings. Beginning in January, the Chena watershed was monitored for icing formation on a monthly basis, by ground observations along the Chena Hot Springs Road, and by several aircraft overflights. No indication of icing build-up was observed until late March when a few small icings were observed on the Upper Chena River. These were all located within the stream channels however and had not developed great thicknesses. The largest icing in the watershed occupied about a mile of the main stream of the Chena; another delta-shaped icing of considerable areal extent occurred at a highway bridge crossing the Chena. These two icings are shown on oblique aerial photography in Figure 36. Both of these icings are large enough to be visible on ERTS imagery. The bright bluish ice surface would be expected to have sufficent contrast against the background to be observable on MSS band 7 at this time. Unfortunately, it was not possible to validate this hypothesis because snow cover and/or cloud cover obliterated the blue ice surface in the scene until after break up. ERTS image 1247-20505 acquired on 27 March 1973 is cloud free but snow cover obscures the icings viewed from the aircraft. The ERTS image, 1265-20505, acquired on 14 April 1973 was very hazy and cloud covered; the watershed was obscured. The first usable ERTS scene of the Chena River subsequent to the underflight observation of icing formation was acquired on 2 May 1973 (MSS scene 1283-20504). By this time the valley bottom was snow free so that any ice remaining would have been clearly visible against the dark background. A careful examination of this image failed to

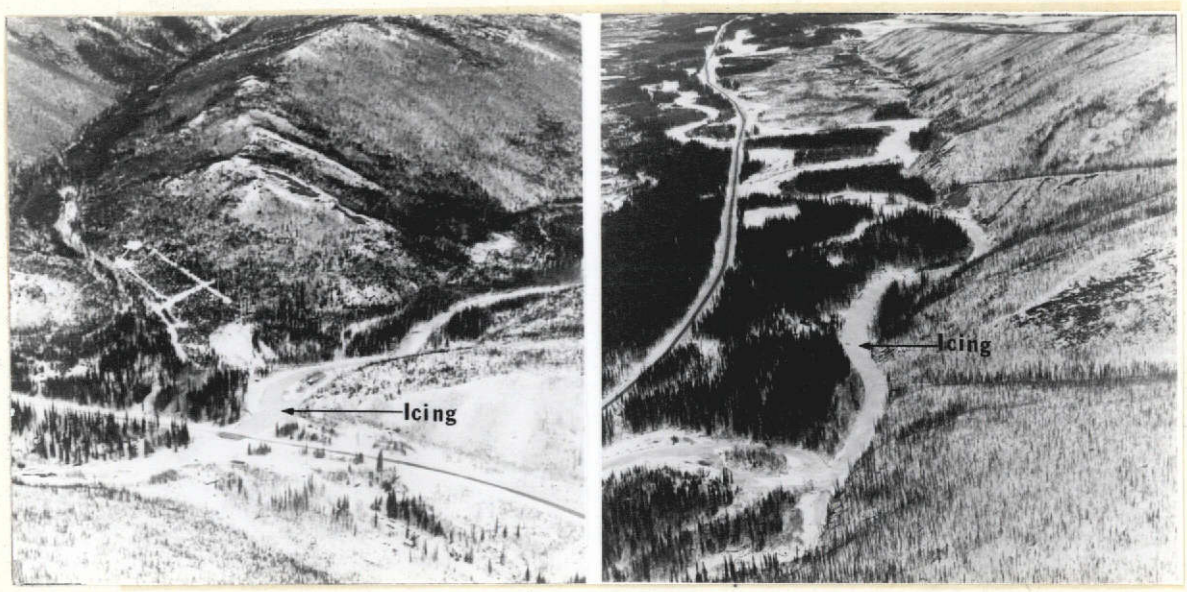

Figure 36. Oblique aerial photographs of the two largest icings observed on the Chena River during the 1972-73 winter; acquired 31 March 1973.

reveal any evidence of these icings, suggesting that the accumulated ice was carried away at the time of break-up.

3.4.2 North Slope

Large river icings did not develop in the interior of Alaska during the 1972-73 season, but on the North Slope of the Brooks Range many icings were located, identified and monitored through two or more satellite passes. During icing formation in late winter, and also in the spring, water often overflows the ice resulting in very dark tones in MSS band 7 against the surrounding white snow background. Later, after the snow cover has disappeared, icings appear white in all bands contrasting sharply with the surrounding landscape. A number of icings were observed along the proposed Alaskan pipeline route from Prudhoe Bay to the Brooks Range (Fig. 37). Along the Echooka River, a tributary of the Sagavanirktok River, an icing some 5 m in thickness is visible. Other icings are identified on the Kuparuk (1), Toolik (2), Sagavanirktok (3), Ivishak (4), Echooka (5) and Shaviovik (6) Rivers. Many of these were seen to persist throughout the year. A knowledge of their location and annual regimes will obviously be useful in laying out routes, and selecting the sites of and scheduling the various construction activities in this region.

3.5 Identification and interpretation of geomorphic, vegetation and cultural features*

Nineteen ERTS-1 MSS images have been studied in detail to test our ability to provide characteristic interpretations of the variety of features indigenous to the physiographic provinces representative of Alaska. The location of each of these scenes is shown in Figure 1. Most of the annotated features are readily apparent in the reproductions given here but there are a few cases where subtle tones and textures of a feature visible in the first generation image have been obscured in the offset reproduction processes. Where this is the case, it is necessary to consult a better photographic reproduction to confirm our interpretation. High quality reproductions of all imagery referred to in this report can be purchased at nominal cost from the EROS Data Center, Sioux Falls, S.D., or can be viewed at USACRREL.

Figure 38 shows the northern coast of Alaska, including Prudhoe Bay (1). An open ice edge (2) separates a shore lead (3) from close pack ice (4). Numerous oriented thaw lakes (5) dot the Arctic Coastal Plain province. The Jones Islands (6) and the Colville Delta (7) are north of the coastline. Clouds cover 60% of this scene.

---

* Circled numbers indicate that an area is being referred to; arrows indicate specific features.

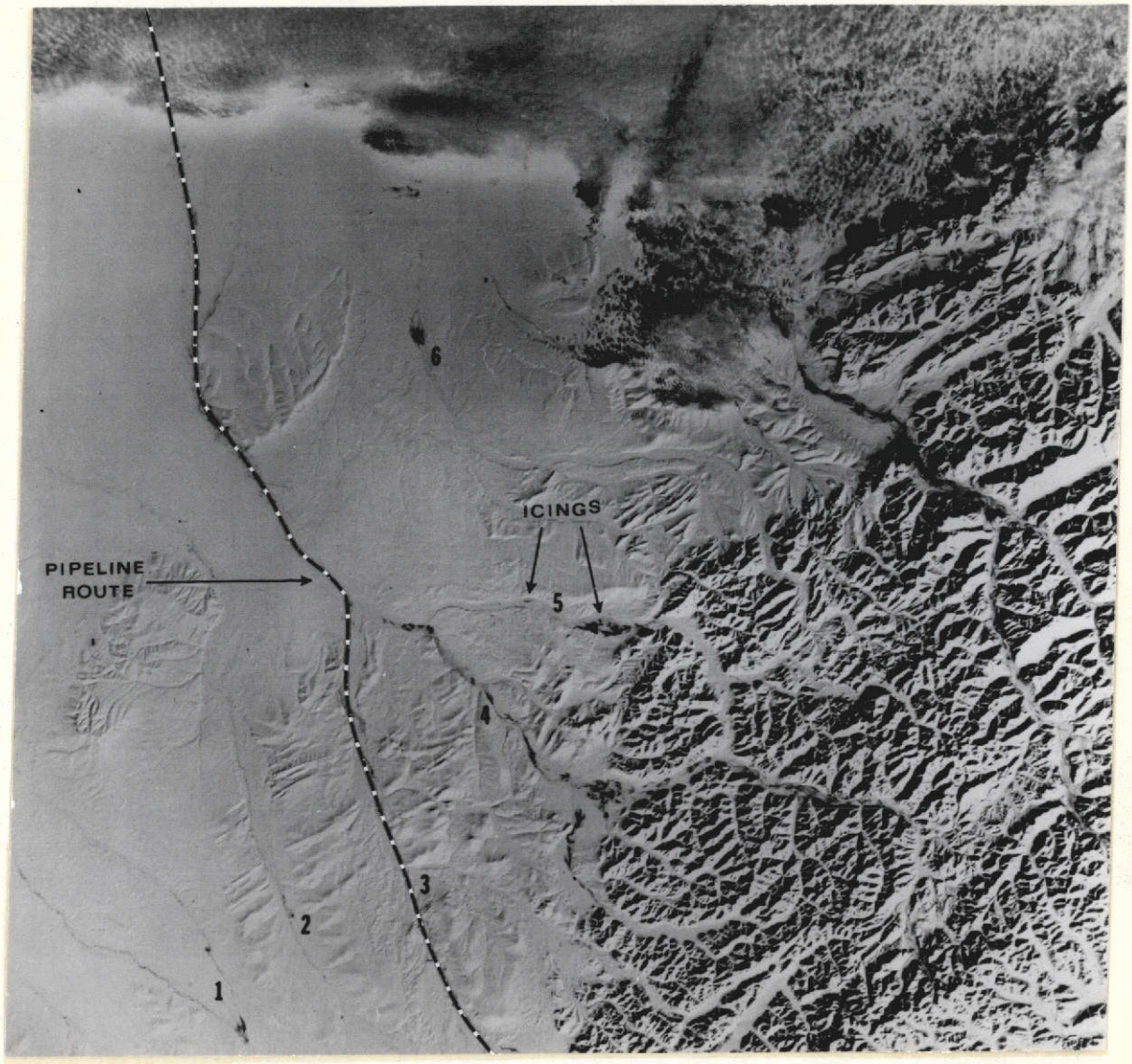

Figure 37. Proposed pipeline route in relation to known icings on the foothills north of the Brooks Range. MSS band 7, image 1251-21123, acquired 31 March 1973.

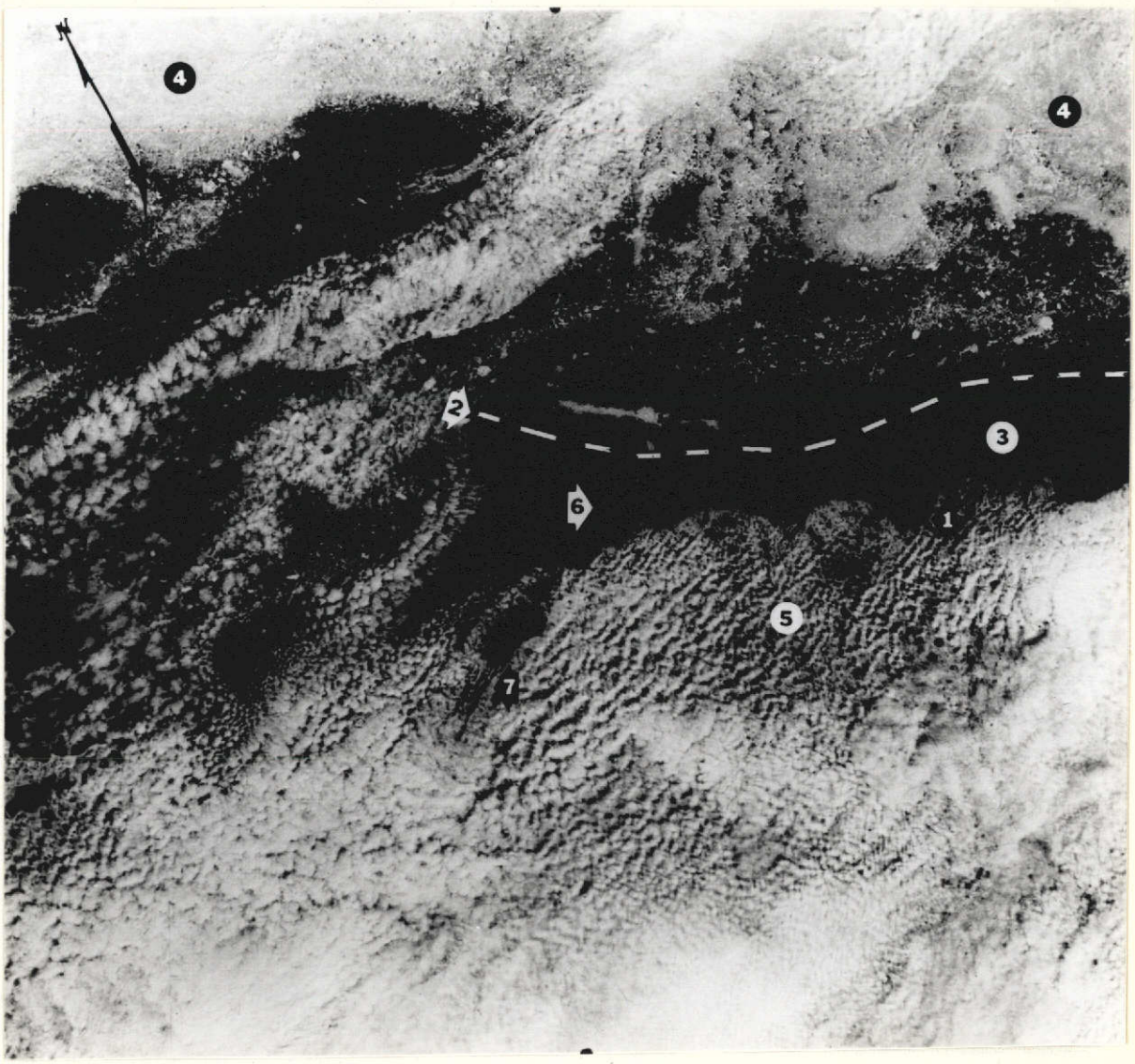

Figure 38. Coastal area near Prudhoe Bay. MSS band 7, image 1020-21281, acquired 12 August 1972.

Over 95% of the image shown in Figure 39 is close pack ice (1) which has numerous characteristic features such as ice openings (2), pressure ridges (3) and leads (4). Gray tone variations are related primarily to ice thickness. Black indicates open water, dark gray tones indicate thin ice, and the lighter gray tones indicate thicker ice. Clouds obscure the pack in the northwest and southeast corners of this image.

A striking example of inverted topography, with anticlinal valleys and synclinal hills, is located east of Cape Beaufort (1) in Figure 40. The bedding planes in most of the structures between Cape Beaufort on the Chukchi Sea (3) and the DeLong Mountains (2) have east-west orientations. The Kukpowruk (4) and Kokolik (5) Rivers, that cut across the geological structures, are probably superimposed streams (Atwood and Atwood 1938). The thaw lakes in the north central portion of the scene are indicative of an area of low topographic relief, fine-grained alluvium and permafrost with high ice contents.

The interrelationship of coastal morphology and near shore currents is well illustrated in Figure 41; this scene shows the west coast of the Seward Peninsula. Cape Prince of Wales (1) in the Bering Strait (2), Point Spencer (3) in Port Clarence (4), Big Diomede (5), Little Diomede (6) and King (7) Islands are all visible. The predominant direction of currents along this coast clearly is northerly. This is inferred from the orientation of the Point Spencer Spit (8), baymouth bars (11) and cuspate forelands (10) along the shore. Jones Point Spit (9) is indicative of a circular flow within Port Clarence. Baymouth bars built up along the present coastlines have formed Breving (12), Lopp (13) and Arctic (14) Lagoons.

Figure 42 shows the Norton Sound area. The Kigluaik Mountains (1) are a prominent feature composed primarily of Paleozoic metamorphic rocks (Dutro and Payne 1954). An open ice pack (2) with many ice openings (3) covers Norton Sound in this winter scene. The fast ice boundary is clearly delineated (4). Fast ice (5) occurs along the coast and extends seaward to Sledge Island (6). The Sinuk River (9) enters the sound and flows under the fast ice. Grease ice (10) is observed south of Rocky Point (11) and Golovnin Bay (12). Port Safety (7) and Nome (8) are icebound in this image.

The Yukon River Delta (1) on the western coast of Alaska projects into the Bering Sea (Fig. 43). Fast Ice (2) extends 5 to 11 km seaward. New ice (3) occurs along the fast ice boundary (4). Grease ice (5) covers a major portion of the area between the fast ice boundary and open ice pack (6). The open pack ice in the Bering Sea contains ice fragments varying in length from tens to hundreds of meters.

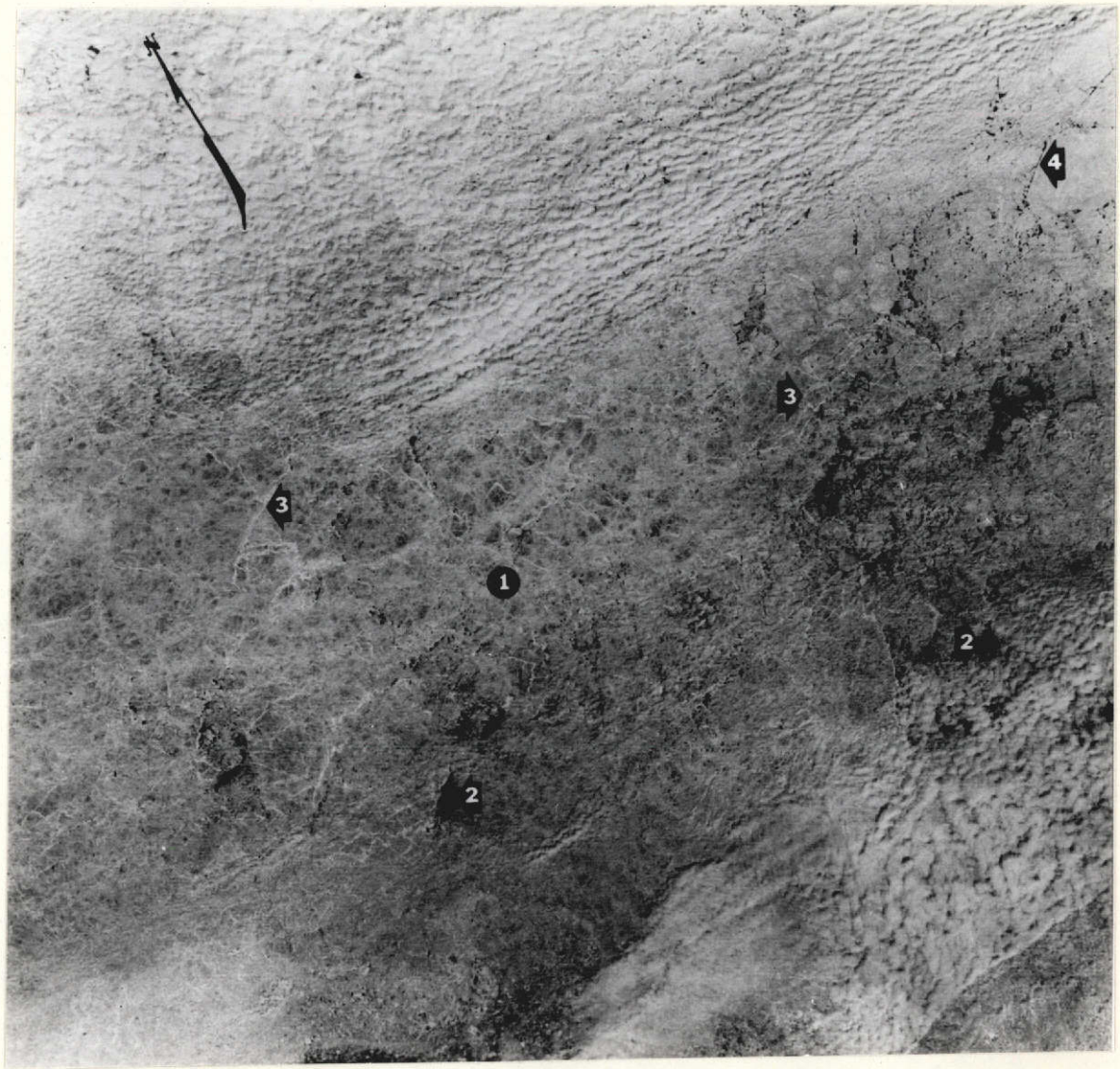

Figure 39. Sea ice north of Prudhoe Bay. MSS band 7, image 1020-21274, acquired 12 August 1972.

Figure 40. Structural features near Cape Beaufort. MSS band 7, image 1010-22142, acquired 2 August 1972.

Figure 41. Coastal features along the west coast of Seward Peninsula. MSS band 7, image 1010-22153, acquired 2 August 1972.

Figure 42. Sea ice in Norton Sound. MSS band 7, image 1205-21595, acquired 13 February 1973.

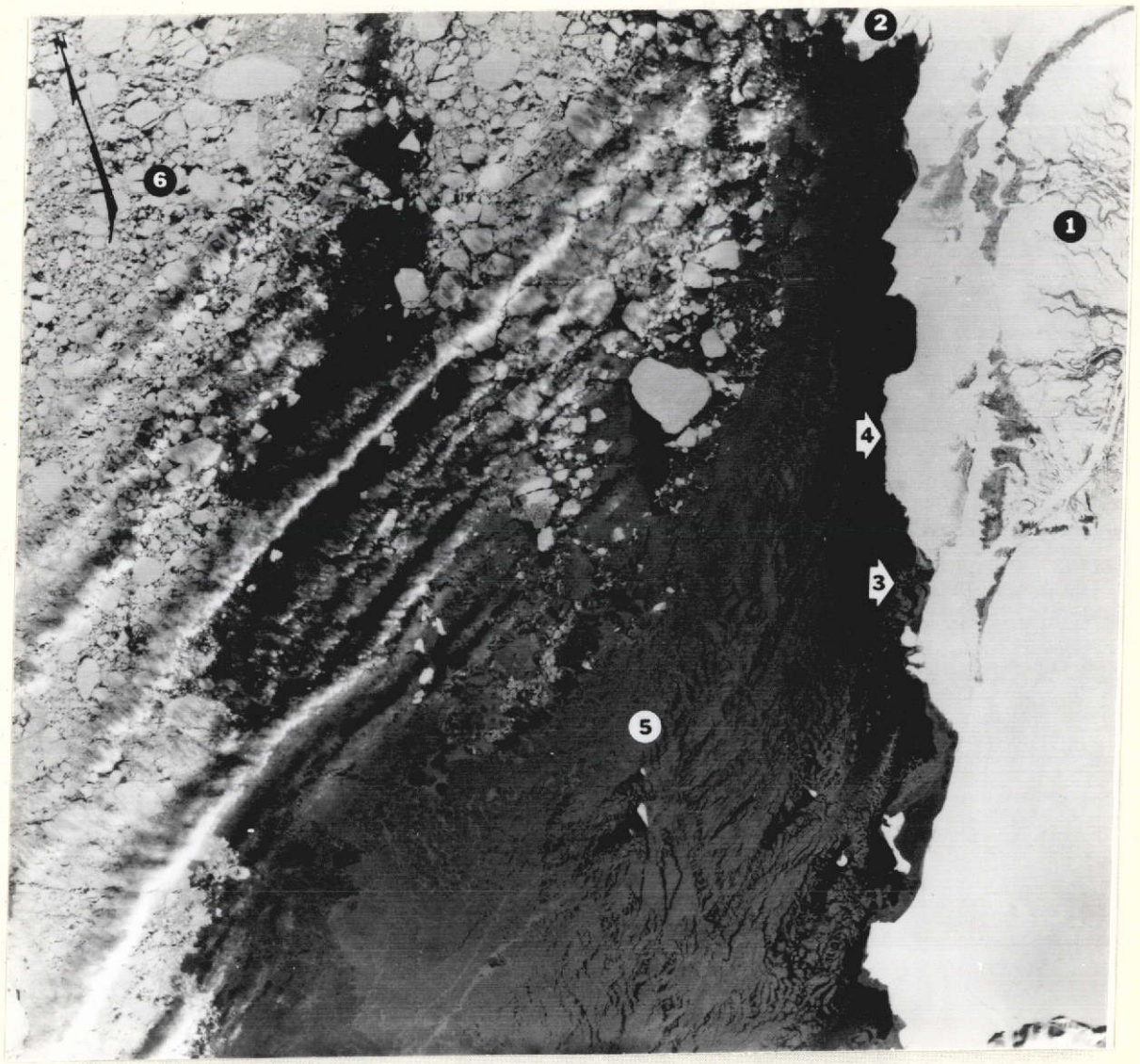

Figure 43. Sea ice in the Bering Sea near the Yukon River Delta. MSS band 7, image 1205-22001, acquired 13 February 1973.

The northwest portion of Figure 49 shows Pastol Bay (1), Stuart (2) and St. Michael (30) Islands, and the southern coast of Norton Sound. The patterned ground discussed earlier (4) is widespread in the swampy Yukon Delta lowlands. The individual polygonal blocks are 300 to 500 m across, and occur in a region generally underlain by moderately thick permafrost. The drainage patterns of the Andreafsky (5) and East Fork (6) Rivers, in the hilly areas, are structurally controlled trellis networks oriented northeast-southwest.

Figure 45 shows the Yukon River (1) 160 km northeast of Bethel, Alaska. Old meander scars (2), oxbow lakes (3), mid-channel bars (5), point bars (6), sloughs (7) and chutes (8) are easily identified. The headward portions of many of the streams exhibit dendritic drainage patterns (4). Numerous thaw lakes occur here, a certain indication of underlying permafrost. The Innoko River (10) is a small, meandering tributary of the Yukon River. The Kuskokwim River (9) lies south of the Yukon and empties into Kuskokwim Bay south of Bethel.

Vegetation associations were studied in the Holy Cross (8) area along the Yukon River (9) in Figure 46. Ground truth for the interpretation of vegetation patterns was obtained primarily from Alaska vegetation maps by Spetzman (1963) and Viereck (1972). Eight associations are recognizable here: Wet tundra (1) is characterized by sedges, grasses and aquatic plants 0.3-0.6 m high with higher willow brush along stream banks. Many thaw lakes and thermokarst depressions are present. The depth of seasonal thaw over the continuous permafrost is shallow in this lowland area. Thaw lakes (2) show light and dark tones which reflect varying water depths and turbidity. Several lakes are similar in tone to the sediment laden Yukon River, while other lakes are very dark. In some cases there is evidence of patterns due to variations in surface reflectance. Moist tundra (3) has cottongrass tussocks associated with mosses, lichens, low heath shrubs and higher willows along stream banks. These are interspersed with stunted trees near forest margins. This area is gently sloping and also has a shallow seasonal thaw depth. Upland white spruce, birch, and aspen forest (4) is intermixed with moist tundra in the valleys (lighter tones). Depth to permafrost in this association is large on south-facing slopes but shallow in the valleys. Closed white and black spruce forest mixed with high brush (5) contains sloughs and small lakes with aquatic vegetation. It is an active floodplain area with generally unfrozen alluvial materials. Closed white spruce forest (6) occurs mainly on well-drained slopes and in hilly areas grades to alpine tundra at elevations over 300 m. Open black spruce forest (7) is mixed with birch, aspen, poplar and willow. The undercover plants are shrubs and the ground cover is cottongrass tussocks, mosses and lichens. Dense spruce-deciduous forest (10) and high brush border the Kuskokwim River.

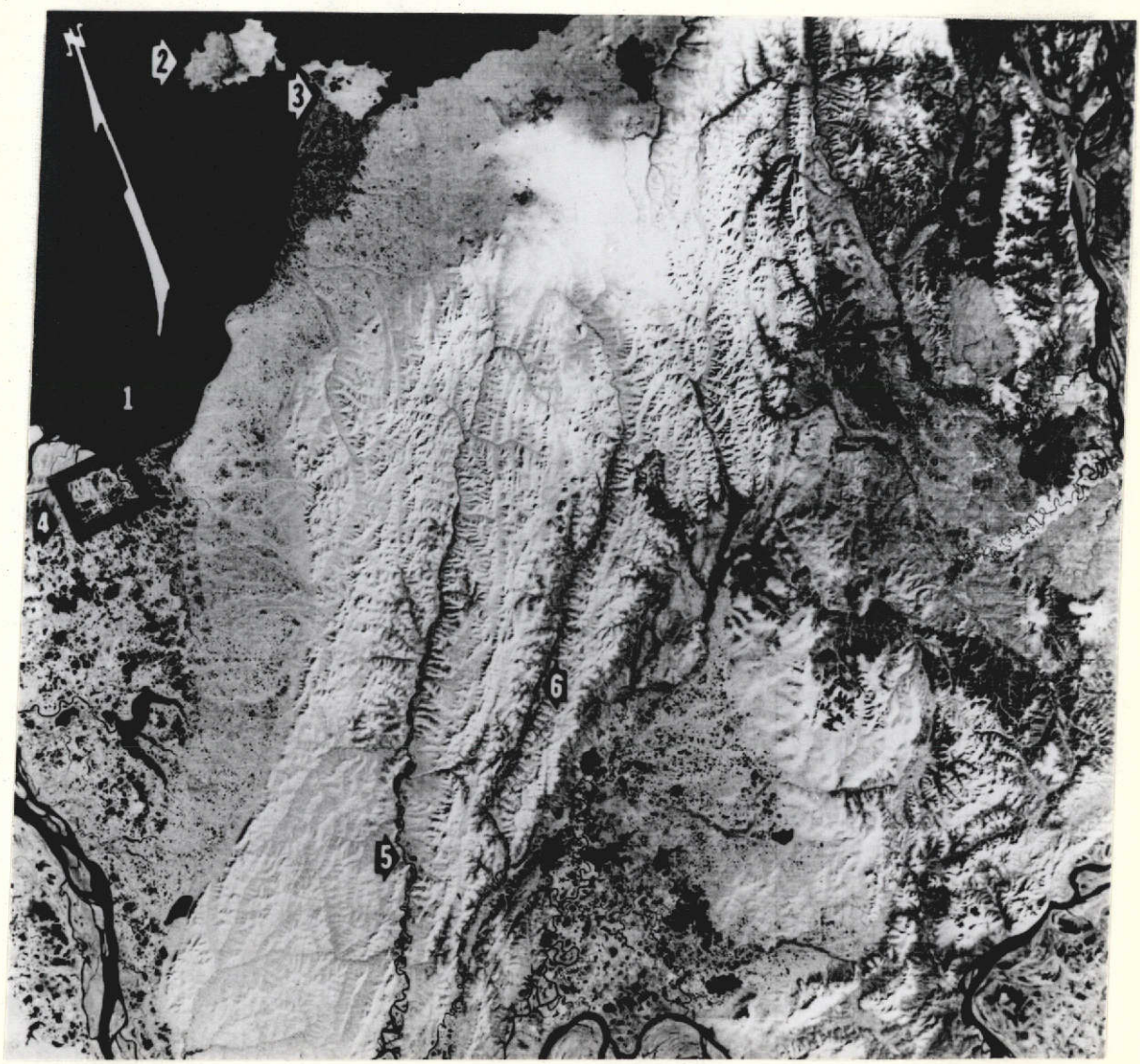

Figure 44. Southern coast of Norton Sound. MSS band 7, image 1058-21421, acquired 19 September 1972.

C-2

Figure 56. Yukon-Tanana Uplands, Canadian border. MSS band 5, image 1081-20272, acquired 12 October 1972.

Figure 46. Vegetation distribution along the Yukon River in the Innoko Lowlands. MSS band 5, image 1002-21324, acquired 25 July 1972.

The Ahklun Mountains (1) and the surrounding mountains shown in Figure 47 are predominantly undifferentiated marine and nonmarine rocks of Lower Cretaceous, Jurassic and Triassic age. The lowlands, marked with numerous lakes, are predominantly undifferentiated Quaternary glacial and glaciofluvial deposits (Dutro and Payne 1954). The Togiak River (2) follows the western portion of the Denali fault zone which extends out into Togiak Bay (13). Ualik (3), Amanka (4) and Nunavaugaluk (5) Lakes occupy abandoned glacial valleys. This entire area was extensively glaciated from early to late Pleistocene. The late Pleistocene glaciers terminated south and east of these lakes (Coulter et al. 1962). Wood River (6) originates in Lake Aleknagik, partially shown on the north side of the image. The Iowithla (7) and Nushagak (8) Rivers drain a large glacial floodplain. Well-defined meanders and oxbows occur along the Nushagak River. Flood tides in Bristol Bay inundate the lower portion of this river; points where the meanders abruptly terminate mark the upstream limits of the tidal waters.

Dillingham (9) is located on Nushagak Bay (17). Rapid siltation in Dillingham harbor causes difficulties in its use during low tide cycles (U.S. Army Corps of Engineers 1971). The high sediment load in the bay is contributed from the Iowithla, Nushagak, Wood, Snake (10) and Igushik (11) Rivers. The Snake and Igushik Rivers originate in the glacial valleys and lakes to the north. Kulukak (12) and Togiak (13) Bays mark areas where middle to late Pleistocene glaciers extended seaward of present dry land areas. The locations of their termini are marked by submarine features not visible on this image (Coulter et al. 1962). Tongue Point (14) is a well developed spit indicating local westwardly current directions between the mainland and Hagemeister Island (15). The linear southeast coast of the island marks the offshore location of the Denali fault zone (Dutro and Payne 1954). Nushagak Peninsula (16) is composed of Quaternary glacial deposits and is marked by arcuate terminal moraines (lighter in tone) of middle to late Pleistocene glaciers. Spit morphology on the lower east shore of the peninsula indicates predominantly northward currents in this area. Extensive tidal flats are visible along the shore of Nushagak Bay (17). Etolin Point (18) and Cape Constantine (19) mark the entrance to the bay.

Figure 48 includes Seward (1), located at the head of Resurrection Bay (2) in Blying Sound (3) on the north shore of the Gulf of Alaska. The area is in the rugged and extensively glaciated Kenai Mountains. Harding Icefield (4) has numerous valley glaciers, including Bear (5), Aialik (6), Holgate (7) and McCarty (8) Glaciers, which terminate in local fiords. The medial moraine in Bear Glacier is well defined. North of Seward, Kenai Lake (9) occupies one of many abandoned glacial valleys (10) in this area. Northeast of Seward, the Ellsworth (11) and Excelsior (12) Glaciers have proglacial lakes at their termini. Prince William Sound (13) and Montague Island (14) are located in the eastern portion of the scene. Altocumulus clouds (15) may be seen in the southeast portion.

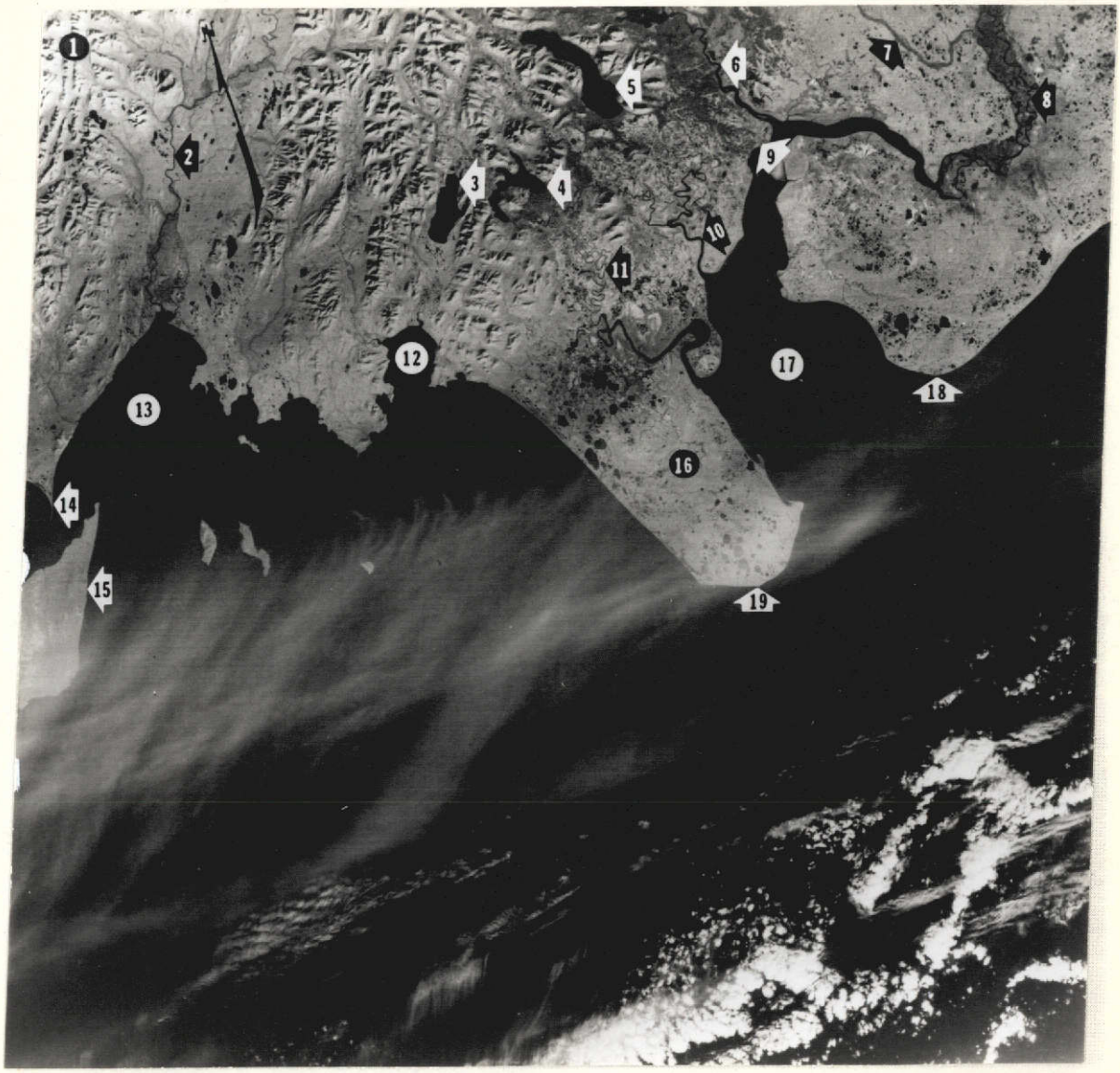

Figure 47. Nushagak Peninsula and the Dillingham area on the northern coast of Bristol Bay. MSS band 7, image 1072-21203, acquired 3 October 1972.

Figure 48. The Seward area in south central Alaska. MSS band 6, image 1101-20403, acquired 1 November 1972.

Figure 49 shows Valdez (1) located at the head of Valdez Arm (2) in the northern part of Prince William Sound (3). It is surrounded by the glaciated Chugach Mountains (4). The multitude of valley glaciers and abandoned glaciated valleys (5) illustrates the extensive glaciation of this area. Columbia (6), Yale (7) and Harvard (8) Glaciers with their well defined lateral and medial moraines terminate in the fiords west of Valdez. Many of the glaciers are snow covered in the higher elevations. The snowline, an important climatic indicator, here is quite distinct. At the terminus of Columbia, a concentration of recently calved floating glacial ice is visible. Nelchina (9) and Tazlina (10) Glaciers flow northward into the flatlands and Tazlina Lake (11), respectively. Klutina Lake (12) is in an abandoned glacial valley of the Klutina Glacier, which at one time extended much farther down the valley. Cordova (13) is located on the mainland east of Hawkins Island (14). The Chugach Mountains north of this town have many piedmont glaciers which terminate in the Copper River (15) lowland. Examples are the Sheridan (16), Childs (17), and Allen (18) Glaciers. The large quantity of glacial sediment in the Copper River is eventually deposited in the Gulf of Alaska where it has formed a large delta (19) and tidal flats (20). Altocumulus clouds (21) obscure the northwest portion of Prince William Sound.

Figure 50 shows a portion of the Chitina River (1) 370 km east of Anchorage. The Wrangell Mountains (2) are to the north and the Chugach Mountains (3) to the south. In the Chugach Mountains, Bagley Icefield (4) and Brenner (5) and Tana (6) Glaciers have well developed medial (7), terminal (8) and recessional moraines. Kennicott (10) and Bernard (11) Glaciers also have well defined medial and lateral moraines. Two abandoned glacial valleys (9) may be seen.

Malaspina Glacier (1), a large (approximately 75 km across) piedmont glacier fed by numerous valley glaciers originating in the Saint Elias Mountains dominates the landscape in Figure 51. Snow cover and the rugged topography of the stagnant area and the thrust moraines at the terminus are easily distinguished. Braided streams and proglacial lakes border the glacier terminus. Yahtse (2), Columbus (4) and Seward (5) Glaciers are valley glaciers flowing from or forming part of the Bagley Icefield (3) in the Chugach and Saint Elias Mountains. There is a high concentration of suspended sediment near the terminus of Yahtse Glacier in Icy Bay (8). Hubbard Glacier (6) is a large glacier in the St. Elias Mountains which drains into Disenchantment Bay (outside this frame) at the northern end of Yakutat Bay (7). Mt. Logan (6050 m) (10) and Mt. King George (3750 m) (11) are two of the highest peaks in the St. Elias Mountains. North of Point Riou (9) is a clearly visible spit-like feature which may be a reef formed from an old terminal moraine of the Malaspina Glacier. The Duktoth River (12) drains a portion of the Robinson Mountains located west of Icy Bay (8). The area around the

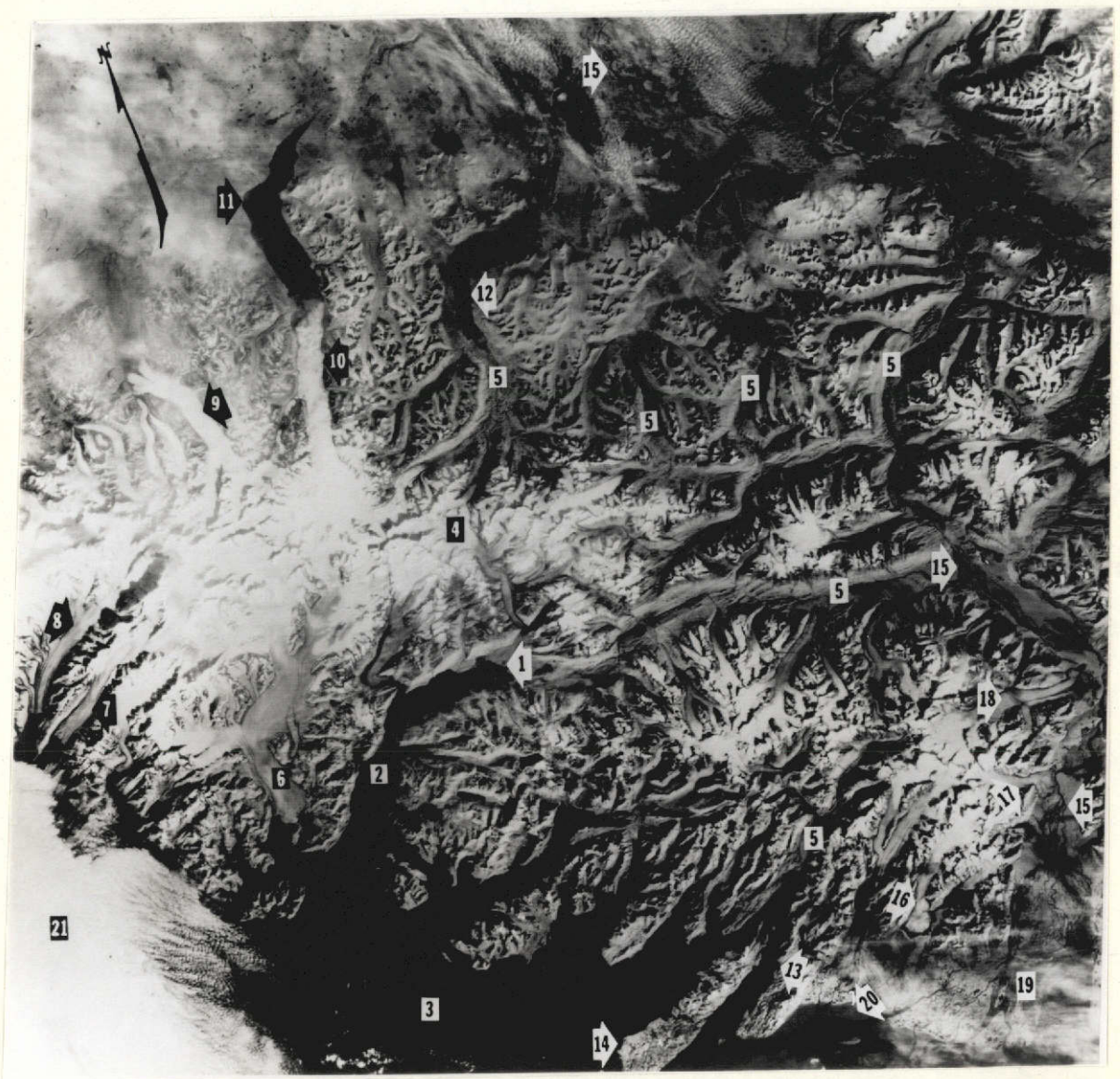

Figure 49. The Valdez area along the northern coast of Prince William Sound. MSS band 7, image 1064-20334, acquired 25 September 1972.

Figure 50. Glacial features in the Wrangell Mountains. MSS band 7, image 1062-20221, acquired 23 September 1972.

Figure 51. Malaspina Glacier in southern Alaska. MSS band 7, image 1204-20120, acquired 12 February 1973.

river mouth is a portion of the glacial floodplain of the Bering Glacier (to the left of this scene).

The eastern extension of the Denali fault zone through the highly glaciated Saint Elias Mountains of southeastern Alaska and northern Canada is seen in Figure 52. The Denali fault is a major structural feature of Alaska, arcing across the state from the northern coast of Bristol Bay to the international border between the United States and Canada. The White River (1) flows through extensive glacial deposits of late Pleistocene age near the border (Dutro and Payne 1954). This river originates from glaciers in the Wrangell Mountains and is fed by meltwaters from Klutlan Glacier (5) in the northern St. Elias Mountains. Meltwaters from Donjek Glacier (6) and Kluane Glacier (7) form the head of the Donjek River (2) which flows north across the Denali fault zone and joins the White River. The Kluane River (3) flows from Kluane Lake (4) through glacial and glaciofluvial deposits in an abandoned glacial valley. A thin cloud haze obscures the western end of Kaskawulsh Glacier (8), a large valley glacier that drains into Kluane Lake and forms the Kaskawulsh River. Hawkins Glacier (9), Barnard Glacier (10), Anderson Glacier (11), Chitina Glacier (12), and Logan Glacier (13) are valley glaciers which terminate in the Chitina River valley and their meltwaters form the Chitina River.

The Alaska Range (1) and the Wrangell Mountains (2), 170 km northeast of Valdez, are shown in Figure 53. Volcanic features include Mt. Wrangell (3) with caldera and side vent, and Mt. Drum (4) and Mt. Sanford (5), volcanic cones. Many of these volcanic features have been modified by glacial activity. Radial drainage patterns are evident on Mt. Sanford and Mt. Drum. Snow-covered glaciers (6), a possible small volcanic cone (7), and a fault (8) extending 160 km across the northern portion of the image are also seen in the vicinity.

Vegetation associations were studied again in the scene shown in Figure 54. Minto Flats (1), west of Fairbanks (17), is covered by low brush muskeg interspersed with stunted black spruce, birch and aspen that border numerous small thaw lakes and meandering streams. The thick ground cover also includes sedges and mosses, and floating mats of aquatic vegetation cover portions of many of the lakes. Permafrost is found near the surface here except in the immediate vicinity of larger lakes and active stream courses. The extensive flats south of Fairbanks are locally known as the Bombing Range. Vegetation in this area is primarily low brush muskeg, with linear developments of black spruce, birch and aspen stands along active or abandoned stream courses. The Wood River Buttes (2), Blair Lake Buttes (3) and Clear Creek Buttes (4) areas are well drained and have a well developed mixed spruce, aspen and birch forest. Shallow, continuous permafrost occurs throughout this area except for the well drained buttes and areas adjacent to large

Figure 52. The Denali fault zone and major glaciers in the St. Elias Mountains of southeastern Alaska. MSS band 5, image 1204-20114, acquired 12 February 1973.

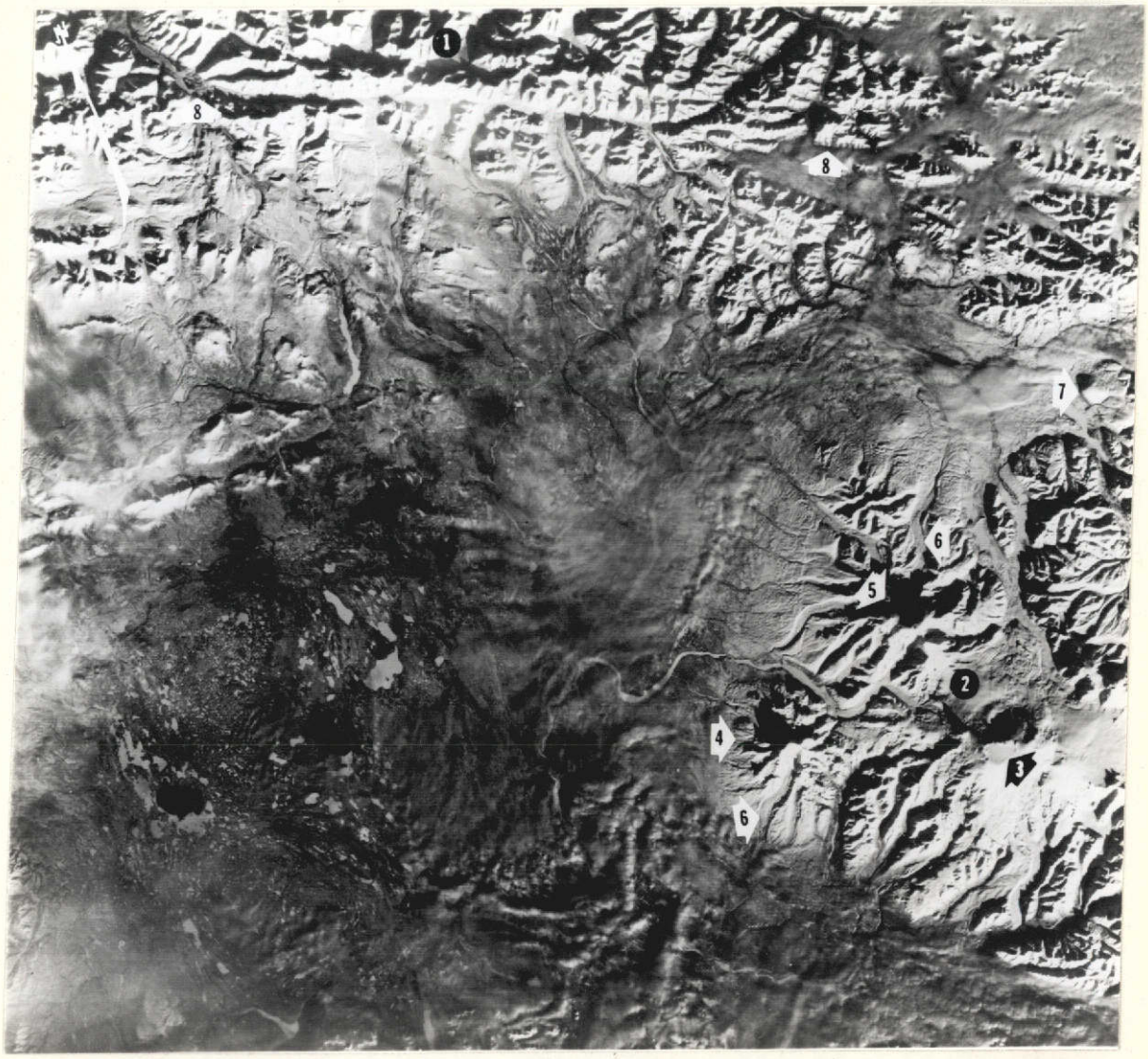

Figure 53. Alaska Range and the Wrangell Mountains in southeastern Alaska. MSS band 5, image 1100-20335, acquired 31 October 1972.

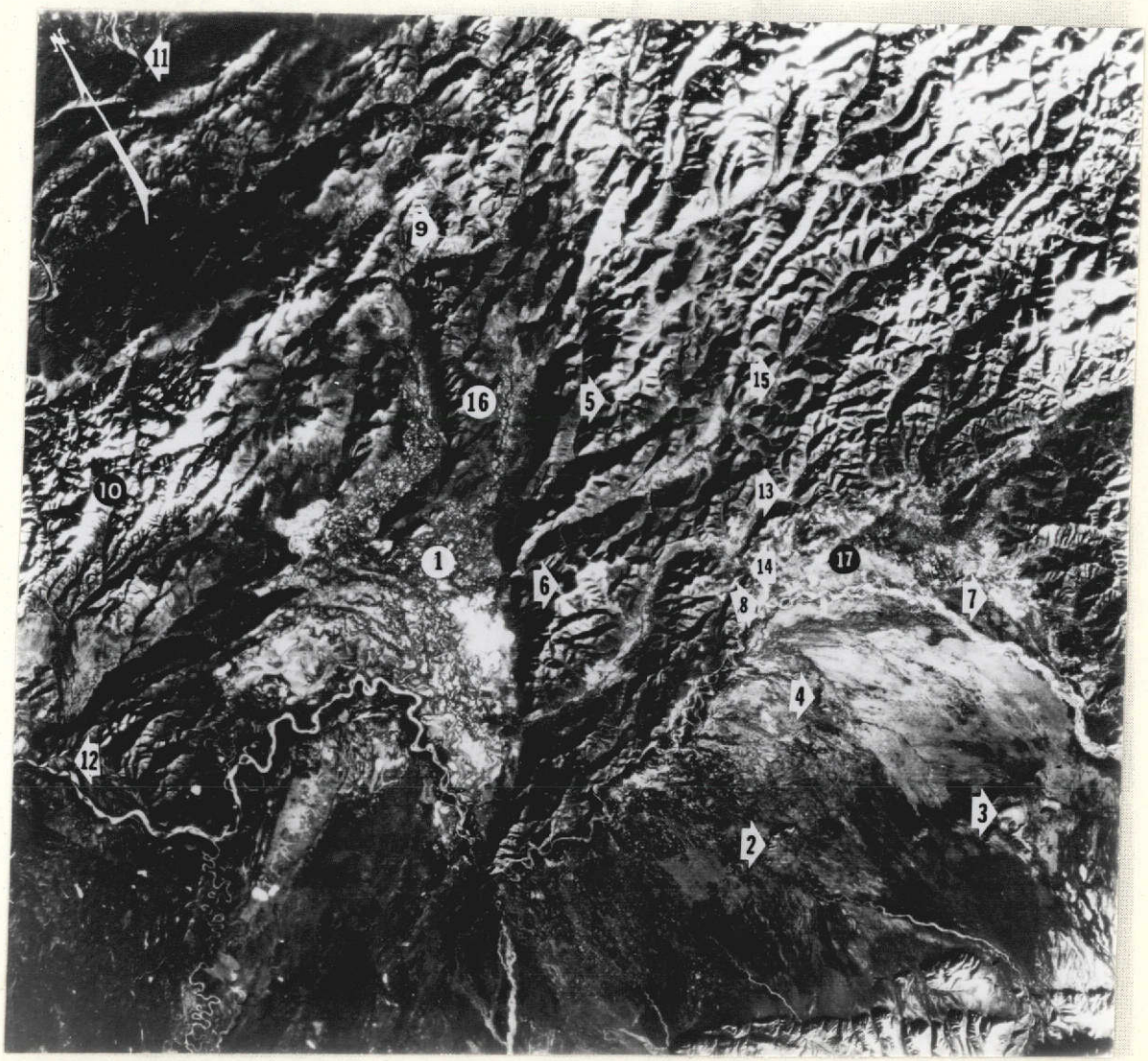

Figure 54. Fairbanks and the Yukon-Tanana Uplands. MSS band 7, image 1102-20560, acquired 2 November 1972.

streams or lakes. Closely spaced white spruce forest (16) covers most of the moderately to well drained upland portions of this scene. The timberline ranges from 750 m elevation in the western part of the scene to about 1000 m in the eastern part. The alpine tundra is snow covered in this scene. This association, however, is known to consist of willows and alders 2.5-4.0 m high near the timberline changing to dwarf willows and alders, herbs, and lichens at higher elevations. The alpine zone is barren above about 1200 m. Wickersham (5), Murphy (6) and Livengood (9) Domes, Eielson AFB (7) and Fairbanks International Airport (8) are easily identified. The Yukon River and Rampart Canyon (11) are located in the northwest corner of this image; Manley Hot Springs (12) to the south of Sawtooth Mountain (19) is included. Evidence of gold dredging operations can be seen in the Goldstream valley near Fox (13) and at Ester Creek (14). "Tailings" left after dredging cover the floodplains and since they are for the most part unvegetated, they are highly reflective. Extensive tailing piles near Chatanika (15) , on the other hand, have been overgrown with vegetation and are distinguishable with difficulty only on very close examination.

In Figure 55 the Chena (1), Salcha (2) and Goodpaster (3) Rivers head in the Yukon-Tanana Uplands and drain a large portion of this province. The Tanana River (4) and its tributaries drain a major portion of east central Alaska. The river itself is a major tributary to the Yukon River. The road networks and development patterns of the Delta Junction and Fort Greely area (5) are distinct at the confluence of the Delta River (6) and the Tanana. The Alaska Highway (7) traverses the entire frame. Alpine tundra (10) is present on Donnelly Dome (8) and other high elevations. Here the alpine tundra unit consists of low flowering plants, lichens, willow, alder, and birch 3-4 m high near the timberline with low dwarf varieties at upper elevations. This area is generally underlain by permafrost except on some of the steepest, south-facing slopes. Vegetation gives way to barren ground at upper elevations. White spruce forests (9) consist of closely spaced white spruce mixed with scattered birches and aspen on moderately to well drained sites. The ground cover consists of alder and willow shrubs, grasses, herbs and mosses. Cottongrass is the dominant plant in the moist tundra (11); willow and alder shrubs occur at lower elevations, grading to open black spruce forest in lowlands where depths to permafrost are shallow. The Shaw Creek Flats (12) is a wet, treeless, boggy area with a cover of willow, alder, and dwarf birch 1-1.5 m high. Ground cover here consists of cottongrass tussocks and sphagnum moss grading to widely spaced black spruce at the margins. Permafrost is shallow. Areas of open black spruce forest (13), mixed with birch and aspen, cover much of the moderately well drained lowland portions of the Tanana valley, grading to high closed spruce forest near the Alaska Range. The ground cover consists of shrubs, cottongrass tussocks and

Figure 55. Junction of the Tanana and Delta Rivers. MSS band 5, image 1029-20383, acquired 21 August 1972.

mosses. Permafrost is at a shallow depth. Areas of shrubs and muskeg (14) are similar to those in the Shaw Creek Flats area.

The Alaska-Canada border (1) crosses the eastern part of Figure 56 although the cleared swath marking the border is not visible due to the lack of contrast between the cleared area and the forested surroundings in this summer scene. In Yukon Territory, Canada (2), the Yukon River (3) and the Sixtymile River (4) are easily recognized. In the Yukon-Tanana Uplands, the alpine zone of Mt. Fairplay (5), portions of the Taylor Highway, a gravel road (6), the Alaska Highway (8), and the Tanana River and floodplain (7) are also clearly visible. The town and airport at Tok (9) are seen adjacent to the Alaska highway. Some of the highest peaks (>1800 m) (10) occur in the northwest corner of the scene. Glacier Mountain (11) to the east is located in another group of very high peaks. Although the uplands never have been modified by continental glaciation, local valley glaciers have eroded cirques in the highest peaks (10 and 11). These glacial features contrast sharply with the rounded ridges and V-shaped valleys (12) of the lower, unglaciated portions of the uplands. The regional vegetation consists of three major associations: alpine tundra, closed mixed spruce-hardwood forest in the uplands, and brush-muskeg thickets in the lowlands. The white spruce timberline reaches an elevation of about 1200 m in the vicinity of the Canadian border.

Although this area abounds with geomorphic features formed by permafrost, such as solifluction terraces, etc., none of these are apparent in the imagery. Numerous pingos varying from 3 to 30 m high and from 8 to 360 m in diameter also are present in this scene. Many pingos have been identified in the area (13) along the Ladue River (14) and the area (15) near Prindle Volcano (16) also contains many pingos easily identified in aerial photography. Still others are present in the Mt. Fairplay (5) and Mosquito Flats (17) areas. They do not show up as clearly identifiable features in the ERTS imagery however.

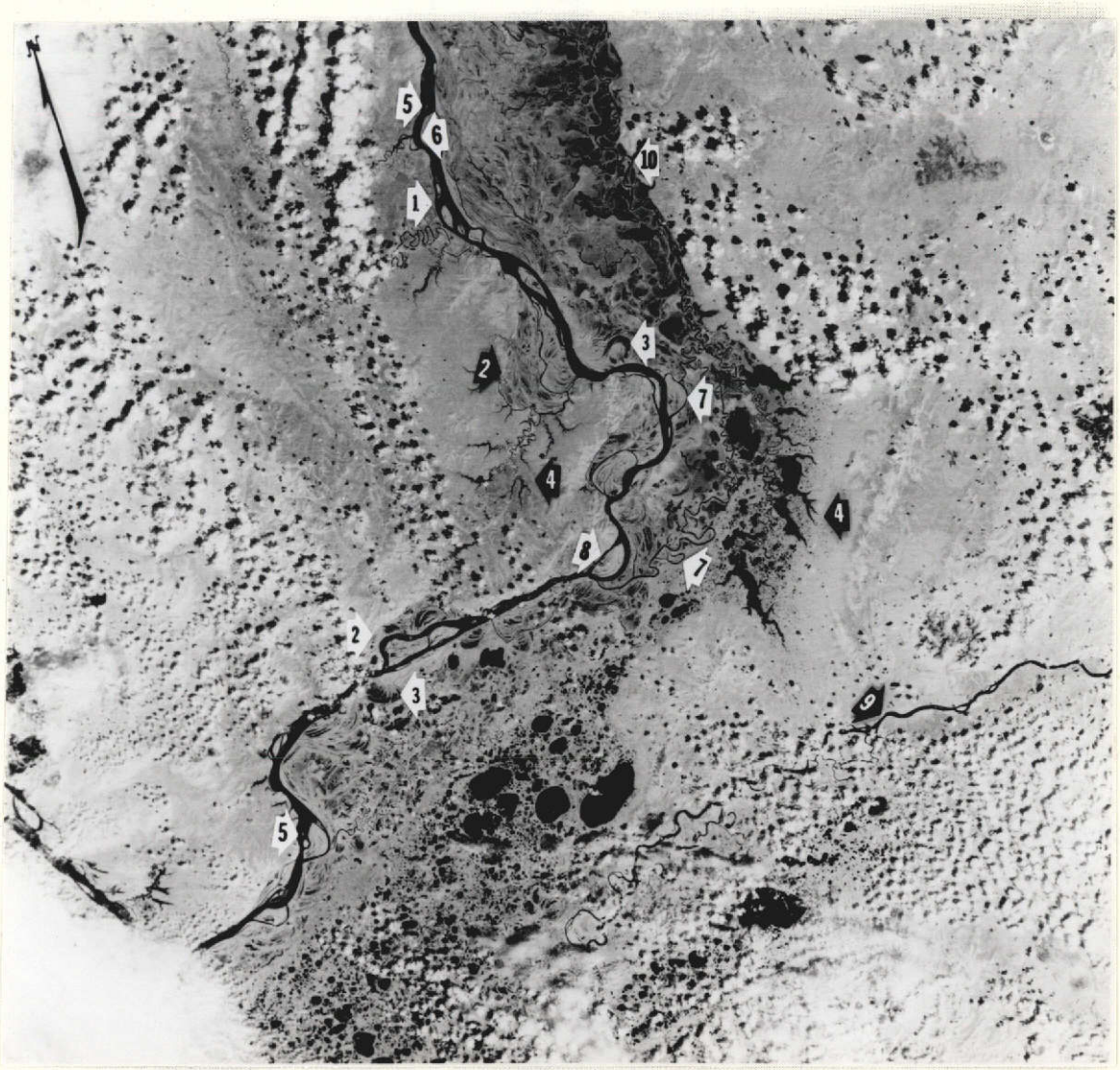

Figure 45. The Yukon River in the Innoko Lowlands. MSS band 7, image 1002-21324, acquired 25 July 1972.

4.0 Applications

4.1 Potential applications

A number of applications utilizing sequential ERTS-1 imagery in earth resources studies have been recognized during this investigation (Table 7). The potential uses listed here are those directly applicable to the requirements of the various Congressional Acts which form the basis for the principal civil works mission responsibilities of the Corps of Engineers. These are responsibilities relating to: maintenance of waterways, water and land conservation, environmental impacts, inspection and management of dams, urban and land use planning, shoreline erosion, flood plain inventories, management and assessment, and recreation projects, to name a few.

Specific examples of results from this and other ERTS investigations known to us that contribute to Corps of Engineers activities presently being performed in one or more of these areas include: snow and ice surveys, attempts to relate snowmelt to stream runoff; the delineation of areas where ice creates engineering problems and hazards; floodplain and land use mapping; monitoring of aquatic pollution and relating the measured parameters to land use practices; preparation of microzonation maps for seismic risk evaluations in areas where planning is preliminary to construction activities; compiling baseline data for maritime projects and coastal zone management programs; and, the interpretation of coastal processes.

4.2. Applications achieved

The application of satellite imagery in describing and interpreting aspects of arctic and subarctic environments for proper utilization and management of earth resources was addressed in this investigation. ERTS imagery has been used to improve thematic mapping of estuarine processes, vegetation and geomorphic and geologic features. Major estuarine circulation patterns, water masses, areas of sediment deposition and the distribution of tidal flats were identified and mapped in Cook Inlet. This information is being used to augment an existing data base needed in regional planning and in the development of management programs as required by the Coastal Zone Management Act of 1972. It also will aid local groups, such as the fishing industry, for example, by augmenting currently available hydrologic and navigation charts.

The distribution of permafrost terrain was mapped for a 153,400 km^2 area in north central Alaska. The methods employed were similar in many respects to those of previous workers but the resulting regional scale map was produced in considerably greater detail. As a part of the permafrost mapping, more detailed surficial geology and vegetation maps than previously available were also made and the location and monitoring

	Applications	Limitations*
Sediment Deposition in Cook Inlet	A. Data Base 1. Preliminary site selection 2. Coastal Zone Management decisions B. Augment preparation and revision of hydrographic and navigation charts C. Monitor estuarine circulation 1. Dispersion of pollutants 2. Movement of sea ice D. Fisheries E. Channel and harbor maintenance F. Ecosystem protection	A. Thermal patterns not visible B. Only circulation patterns with suspended material, floating debris, or sea ice are visible C. Small scale changes (<70m) in circulation, tidal flats and coastal landforms are not detectable
Permafrost Mapping	A. Route/site selection B. Regional environmental interpretation C. Identification and inventory natural resources D. Urban and land use planning E. Land use regulation and management F. Improved thematic mapping	A. Criteria not obtainable 1. Air and land temperature 2. Depth B. Feature not identifiable 1. Pingos (palsas) 2. Ice wedge polygons 3. Solifluction lobes 4. Nivation terraces 5. Stone polygons and stripes
Pack Ice and Shore-fast Ice Surveys	A. Quantifying formation, ablation, movement and deformation of sea and lake ice B. Ice surveys C. Shoreline and beach erosion D. Navigation route and offshore site selection E. Engineering design criteria	A. Not daily coverage of same area B. Significant deformation/movement not coincident with satellite overpass
Snow Cover - Runoff Relationships	A. Runoff/flood predictions B. Snow surveys C. Reservoir management	
Stream Icings	A. Route selection B. Potential fresh water source	A. Resolution of imagery B. Contrast

*General Limitations:
1. Atmospheric attenuation reduces tonal and textural contrast
2. Cloud cover obscures all features
3. Snow cover obscures some small scale topographic features, low-lying vegetation and decreases accuracy of slope determinations

of large river icings in northern Alaska was accomplished. These results will be directly applicable to route and site selection, for example in route selection for the Nome to Kobuk Road in western Alaska. Permafrost mapping will also be useful in regional environmental interpretation, in urban and land use planning, and in the regulation and management of developing areas of the state.

The anticipated need for information on ice patterns and movements for purposes of selecting north sea navigation routes and construction of offshore docking facilities led to an analysis of shore-fast ice accumulation and breakup along the western coast of Alaska. Pressures for the development of the North Slope oil reserves also generated the need for an experimental test of a rapid method of assessing sea ice deformation and drift. An evaluation of the ERTS imagery from the northern Alaska coast has shown that the repetitive, multispectral imagery available from this system is adequate to perform many detailed ice dynamics studies. In this ancillary investigation a spatial deformation analysis was done for a portion of the Beaufort Sea during a four day period in March 1973. It was shown to be possible to track sequential positions of grid points (fiducial marks) on the deforming pack. The data collected during this four day deformation at the shear zone northeast of Point Barrow, Alaska suggest that the pack here behaves as a relatively cohesive mass (i.e. highly viscous) with slippage over a narrow region (~50 km) at the boundaries. This invalidates the common assumption of no slip at the boundary. Thus the no slip assumption coupled with a single viscosity model is not adequate in general for the arctic pack. Measurements like these are needed in the formulation of realistic prediction models. Three particular types of data are especially needed: 1) data on ice deformation across the shear zone region where the moving pack impacts and grinds against stationary shore-fast ice, 2) the formation, distribution and persistence of the shore-fast ice, and 3) sequential deformation measurements on a variety of spatial scales at representative locations to determine the regional characteristics of the ice velocity field. The most serious limitation of the ERTS system in obtaining this type of information is the difficulty of obtaining sequential, cloud free imagery coincident with the occurrence of significant deformation wherever and whenever it occurs. The experiment described here represents the first successful application of satellite imagery for this purpose (Crowder et al. 1973).

Another direct application of ERTS imagery to an operational requirement of the Corps of Engineers also was achieved during this investigation in response to a specific and pressing need. The Corps of Engineers was required to institute rapidly a program for the inspection and inventory of dams throughout the United States as a result of public law 92-367, passed on 9 August 1972. In response, members of this ERTS investigation team were requested by the Office of the Chief of

Engineers to publish a manual on "The Use of ERTS-1 Imagery in the National Program for the Inspection of Dams". This manual (McKim et al. 1972) described a photointerpretation technique for quickly identifying and inventorying water bodies six acres or larger directly from ERTS imagery. This approach was shown to be the most practical and economical method for rapidly fulfilling the requirements of this law as set forth by the Congress on the Corps of Engineers.

5.0 Conclusions

The ERTS-1 systems performance has exceeded expectations and has made possible analyses of regional phenomena previously not feasible due to inaccessibility or prohibitive expense. The 70 meter resolution of the multispectral scanner system makes possible the identification of all major geomorphic features such as floodplains, moraines, alluvial fans, terraces, thaw lakes, bars, spits, sand dunes, etc. Using stereographic mapping techniques, it was immediately apparent that more detail can be seen on the ERTS-1 imagery than can be mapped at a scale of 1:1,000,000. Observable detail on the imagery was found to be affected by such factors as sun angle, atmospheric haze, cloud cover and snow cover. Low sun angles tend to enhance some topographic expression and accentuate geomorphic features while adversely affecting oceanographic and lacustrine analyses by rendering water surfaces and sedimentation patterns very dark. A heavy snow cover (> 22 cm) accentuates major structural features whereas a light dusting (< 2 cm) accentuates more subtle topographic expressions (Wobbler and Martin 1973). Also snow cover obscures low vegetation but enhances forest boundaries. Such effects enhance the value of sequential as opposed to "one pass" imagery.

Oceanographic investigations have been undertaken at a number of specific sites in the Cook Inlet area by various governmental and private agencies for many years. ERTS-1 imagery was shown to provide, for the first time, a means of monitoring estuarine circulation patterns, water masses, areas of sediment deposition, and tidal flat distribution on a regional basis. It has shown that a tongue of clear ocean water moves into the inlet along the east shore to the approximate location of Ninilchik where extensive mixing occurs with sediment laden inlet water. Turbid inlet water was shown to occur in the western portion of the inlet and generally moves south along the shore towards the inlet mouth. It is clear that changes in the relative load of these water masses and of rivers discharging into the inlet can be inferred from the tonal variations in the MSS imagery between successive passes. Several local patterns not recognized before were identified: the clockwise back eddy observed during flood tide in the slack water area between Cape Ninilchik and Kenai offshore from Clam Gulch and the counterclockwise current that forms north of the Forelands during ebb tide. The movement of sediment laden, ebbing water west of Augustine Island and out the inlet past Cape Douglas and through Shelikof Strait was clearly established on the basis of visual evidence. Thus the use of satellite imagery in this application is definitely established.

It was shown that ERTS-1 imagery can be used to rapidly produce accurate thematic maps for arctic and subarctic regions. Permafrost terrain, surficial geology, and vegetation were quickly and efficiently

mapped at a scale of 1:1,000,000 for 153,400 km^2 in north central Alaska and at a scale of 1:250,000 for an area south of Fairbanks. The detail mapped compared favorably with that shown on U.S. Geological Survey Miscellaneous Geologic Investigation Maps 290,437,459, and 554 at a scale of 1:250,000. Physical boundaries mapped from ERTS-1 imagery in combination with ground truth obtained from existing small scale maps and other sources resulted in improved and more detailed delineation of permafrost terrain and vegetation units for these areas. Surveys of shore-fast ice and off shore permafrost have been given high priority in connection with permafrost mapping. It was clearly established that the formation and persistence of shore-fast ice is easily monitored with ERTS sequential imagery. When compiled in an atlas of shore-fast ice distribution as a function of season, such data will be very valuable in guiding the planning and construction of navigational and shore facilities.

Recent evidence from Mariner 9 has indicated the high probability of permafrost and massive ground ice on Mars. Large scale slump features on the Martian surface have been attributed to degradation of ground ice and permafrost. In some respects these features appear to be analogous to certain permafrost terrain features seen on the ERTS imagery. Polygonal patterns on the Yukon River delta, although probably not of a similar origin, compare in size to polygonal patterns identified on Mariner imagery. Also, a large area of thermokarst terrain on the North Slope and the alas topography of the Yakutian region of Siberia, appears analogous to the fretted terrain of Mars.

Accumulation and ablation of snow cover in a relatively small watershed can successfully be monitored with ERTS imagery. Comparison of imagery with observed ground truth measurements shows good correlation, and indicates that satellite imagery can be used to study the snow melt in watersheds where little or no hydrological or climatological data are presently being collected. Location and monitoring of large icings can be efficiently and effectively accomplished by means of sequential ERTS imagery. It was shown that during the formation of icings in late winter and spring, overflowing water appears as a very dark tone against the white snow background in MSS band 7. With certain reservations, ablation of icings can be monitored after the snow cover has disappeared because in this circumstance the icings appear white in all bands in comparison with the surrounding landscape.

Anticipated needs for information on sea ice movement for purposes of navigation and construction of off-shore facilities led to an analysis of sea ice deformation in the Beaufort Sea. The results demonstrate that with certain limitations, satellite imagery often can be used to advantage in following formation and drift of the arctic pack. An important advantage is the synoptic view while the major limitation is the difficulty of obtaining sequential cloud free imagery coincident with the occurrence of significant deformation.

6.0 Recommendations

Based on the experience of this investigation it is considered appropriate to make some general recommendations relative to future NASA satellite applications programs. First, we recommend that ERTS-1 should be fully utilized as long as it is operational. Second, our experience has convinced us that there is a need to emphasize and improve provisions for technology transfer within user organizations. Greater awareness and participation from the operational personnel of user agencies is needed. This, of course, is a responsibility of the user agencies but NASA should recognize this need and take the lead in stimulating a greater awareness of this requirement and aid in devising means for implementing effective programs. Third, a provision for direct downlink for users of DCP's would enhance the utility of this system for many present and potential users by streamlining the data handling system. We recommend that direct downlink instrumentation be provided to users who are willing to bear the burden of acquiring and operating the system. Finally, the logical culmination of the ERTS program would be the establishment of geostationary operational satellites, as have been proposed in the SEOS program, in addition to a family of polar orbiting low altitude satellites of the ERTS type. These satellites should be specialized for distinct disciplines and carry active and passive sensors (e.g. high resolution MSS imaging devices with directable zoom capability for coverage of localized phenomena), have data relay and direct downlink capability for users of the data collection system, and orbit at altitudes appropriate for separate or related disciplines.

7.0 Bibliography

Alaska Construction and Oil. (1973) Big Anchorage sewer job nears completion, November, p. 45-48.

Anderson, D.M., L.W. Gatto, H.L. McKim, and A. Petrone. (1973) Sediment distribution and coastal processes in Cook Inlet, Alaska, Proceedings of the ERTS-1 Symposium, Goddard Space Flight Center, 5-9 March, p. 1323-1339.

Atwood, W.W. Sr. and W.W. Atwood Jr. (1938) Working hypothesis of the physiographic history of the Rocky Mountain regions, Bull. Geol. Soc. Amer., vol. 49, p. 957-980.

Barnes, J.C. and C.J. Bowley. (1973) Mapping sea ice from the Earth Resources Technology Satellite, Arctic Bulletin, vol. 1, no. 1, p. 6-13.

Blenkarn, K.A. (1970) Measurement and analysis of ice forces on Cook Inlet structures, Offshore Technology Conference, 22-24 April, p. 365-378.

Bowden, K.F. (1967) Circulation and diffusion, Estuaries, Amer. Assoc. for the Advancement of Science, Washington, D.C., Publ. No. 83, p. 15-36.

Brown, R.J.E. (1969) Factors influencing discontinuous permafrost in Canada, in The Periglacial Environment, Past and Present (T.L. Péwé, Ed.). Montreal: McGill-Queens University Press, p. 11-53.

Bryson, R.A. (1966) Air masses, streamlines and the boreal forest, Geographical Bulletin, vol. 8, p. 228-269.

Burrell, D.C. and D.W. Hood. (1967) Clay-inorganic and organic-inorganic association in aquatic environments, Part II. Institute of Marine Science, University of Alaska, Fairbanks, Alaska.

Campbell, W.J., P. Gloersen, W. Nordberg and T.T. Wilheit. (1973) Dynamics and morphology of Beaufort Sea ice determined from satellites, aircraft, and drifting stations, NASA Report No. X-650-73-194.

Carey, K.L. (1973) Icings developed from surface water and ground water, U.S. Army Cold Regions Research and Engineering Laboratory Monograph III-D3.

Cass, J.T. (1959) Reconnaissance geologic map of the Melozitna quadrangle, Alaska, U.S. Geological Survey Misc. Geol. Inv. Map I-290, scale 1:250,000.

Coulter, H.W., D.M. Hopkins, T.N.V. Karlstrom, T.L. Péwé, C. Wahrhaftig and J.R. Williams. (1962) Map showing extent of glaciations in Alaska, U.S. Geological Survey Misc. Geol. Inv. Map I-415, scale 1:2,500,000.

Crick, R.W. (1971) Potential petroleum reserves, Cook Inlet, Alaska, in Future Petroleum Provinces, North America, Amer. Assoc. Pet. Geol. Memoir 15, vol.1. p. 109-119.

Crowder, W.K., H.L. McKim, S.F. Ackley, W.D. Hibler, and D.M. Anderson. (1973) Mesoscale deformation of sea ice from satellite imagery, Symposium on Advanced Concepts and Techniques in the Study of Snow and Ice Resources, 2-8 December, Monterey, California, p. 563-573.

Czudek, T. and J. Demek. (1970) Thermokarst in Siberia and its influence on the development of lowland relief, Quaternary Research, vol. 1, no. 1, p. 103-120.

Dutro, V.I. and T.G. Payne (1954) Geologic map of Alaska, U.S. Geological Survey, scale 1:2,500,000.

Environmental Currents. (1972) Environmental Science and Technology, vol. 6, no. 12, p. 965.

Evans, C.D., E. Buch, R. Buffler, G. Fisk, R. Forbes and W. Parker. (1972) The Cook Inlet environment, a background study of available knowledge, Resource and Science Service Center, University of Alaska, Anchorage, Alaska.

Ferrians, O.J. (1969) Permafrost map of Alaska, U.S. Geological Survey Misc. Geol. Inv. Map I-445, scale 1:2,500,000.

Ferrians, O.J., R. Kachadoorian and G.W. Greene. (1969) Permafrost and related engineering problems in Alaska, U.S. Geological Survey Prof. Paper 678, 37 p.

Glen, J.W. (1970) Thoughts on a viscous model for sea ice, AIDJEX Bulletin No. 2, October, p. 18-27.

Hibler, W.D. III, W.F. Weeks, S.F. Ackley, A. Kovacs and W.J. Campbell (1973) Mesoscale strain measurements on the Beaufort Sea pack ice (AIDJEX 1971), J. Glaciol., vol.12, no. 65, p. 187-206.

Hibler, W.D. III, W.F. Weeks, A. Kovacs and S.F. Ackley. (1973) Spatial and temporal variations in mesoscale strain in sea ice, AIDJEX Bulletin No. 21, p. 79-114.

Hibler, W.D. III. (1973) Comparison of mesoscale strain measurements with linear drift theory predictions, AIDJEX Bulletin No. 21, p. 115-138.

Holmes, G.W., H.L. Foster, and D.M. Hopkins. (1963) Distribution and age of pingos of interior Alaska, in Proceedings of the Permafrost International Conference, 11-15 November, Lafayette, Indiana, p. 88-93.

Hopkins, D.M., T.N.V. Karlstrom and others (1955) Permafrost and ground water in Alaska, U.S. Geological Survey Prof. Paper 264-F, p. 113-146.

Horrer, P.L. (1967) Methods and devices for measuring currents, Estuaries, Amer. Assoc. for the Advancement of Science, Washington, D.C., Publ. No. 83, p. 80-89.

Karlstrom, T.N.V. and others. (1964) Surficial geology of Alaska, U.S. Geological Survey Misc. Geol. Inv. Map I-357, scale 1:1,584,000.

Kinney, P.J., D.K. Button, D.M. Schell, B.R. Robertson and J. Groves. (1970a) Quantitative assessment of oil pollution problems in Alaska's Cook Inlet, Report R-169-16, Institute of Marine Sciences, University of Alaska, College, Alaska, 116 p.

Kinney, P.J., J. Groves and D.K. Button. (1970b) Cook Inlet environmental data: R/V Acona cruise 065-May 21-28, 1968, Report R-70-2, Institute of Marine Sciences, University of Alaska, Fairbanks, Alaska, 120 p.

Lachenbruch, A.H. (1968) Permafrost, in Fairbridge, R.W., ed. The Encyclopedia of Geomorphology: New York, Reinhold Publishing Corp., p. 833-839.

MacKay, R.S. (1972) The world of underground ice, Annals of the Association of American Geographers, vol. 62, no. 2, p. 1-22.

McKim, H.L., T.L. Marlar and D.M. Anderson. (1972) The Use of ERTS-1 Imagery in the National Program for the Inspection of Dams. USACRREL Special Report 183, 20 p.

Muller, S.W. (1947) Permafrost or permanently frozen ground and related engineering problems. Ann Arbor, Michigan: J.W. Edwards, Inc., 231 p.

Murphy, R.S. and R.F. Carlson. (1972) Effect of waste discharges into a silt-laden estuary, a case study of Cook Inlet, Alaska, Report IWR 26, Institute of Water Resources, University of Alaska, Fairbanks, Alaska, 42 p.

NASA. (1972) NASA Earth Resources Technology Satellite. ERTS-1 Data Users' Handbook, Goddard Space Flight Center, Document No. 715D4249.

Patton, W.W., Jr. (1966) Regional geology of the Kateel River quadrangle, Alaska, U.S. Geological Survey Misc. Geol. Inv. Map I-437, scale 1:250,000.

Patton, W.W., Jr. and T.P. Miller. (1966) Regional geologic map of the Hughes quadrangle, Alaska. U.S. Geological Survey Misc. Geol. Inv. Map I-459, scale 1:250,000.

Patton, W.W., Jr., T.P. Miller and I.L. Tailleur. (1968) Regional geologic map of Shungnak and southern part of the Ambler River quadrangles, Alaska, U.S. Geological Survey Misc. Geol. Inv. Map I-554, scale 1:250,000.

Péwé, T.L. (1966) Paleoclimatic significance of fossil ice wedges, Biuletyn Peryglacjalny, no. 15, p. 65-73.

Péwé, T.L. (1967) Permafrost and its effects on life in the north, in Arctic Biology, H.P. Hansen, ed., Corvallis, Oregon: Oregon State University Press, p. 27-65.

Rosenberg, D.H., D.C. Burrell, K.V. Natarajan and D.W. Hood. (1967) Oceanography of Cook Inlet with special reference to the effluent from the Collier carbon and chemical plant, Report R67-5, Institute of Marine Sciences, University of Alaska, College, Alaska, 80 p.

Rothrock, D.A. (1973) The steady drift of an incompressible arctic ice cover, AIDJEX Bulletin No. 21, p. 49-78.

Selkregg, L.L., E.H. Buck, R.T. Buffler, O.E. Coté, C.D. Evans and S.G. Fisk (Editors). (1972) Environmental atlas of the greater Anchorage area borough, Alaska, Resource and Science Service Center, University of Alaska, Anchorage, Alaska, 105 p.

Sharma, G.D. and D.C. Burrell, (1970) Sedimentary environment and sediments of Cook Inlet, Alaska, Amer. Assoc. Pet. Geol., vol. 54, no. 4, p. 647-654.

Shepard, F.P. and H.R. Wanless. (1971) Our changing coastlines, New York: McGraw-Hill Book Co., 579 p.

Spetzman, L.A. (1963) Terrain study of Alaska, Part V: Vegetation. Military Geology Branch, U.S. Geological Survey.

Thorndike, A.S. (1972) Analysis of position measurements-AIDJEX, 1972. abstract in EOS, vol. 53, no. 11, p. 1018.

Trytikov, A.P. (1959) Perennially frozen ground and vegetation, in Principles of Geocryology, Part II, Engineering Geocryology, Chapter XII, Academy of Sciences of the U.S.S.R., V.A. Obruchev Institute of Permafrost Studies, Moscow, p. 399-421.

U.S. Army Corps of Engineers, Alaska District. (1971) Water resources development, Anchorage, Alaska.

Viereck, L.A. (1972) Alaska - vegetation types, map for Alaska trees and shrubs, Forest Service, U.S. Department of Agriculture, Agriculture Handbook 410.

Wagner, D.G., R.S. Murphy and C.E. Behlke. (1969) A program for Cook Inlet, Alaska for the collection, storage and analysis of baseline environmental data, Report No. IWR-7, Institute of Water Resources, University of Alaska, Fairbanks, Alaska.

Wahrhaftig, C. (1965) Physiographic divisions of Alaska, U.S. Geological Survey Prof. Paper 482.

Weber, F.R. and T.L. Péwé. (1970) Surficial and engineering geology of the central part of the Yukon-Koyukuk Lowland, Alaska, U.S. Geological Survey Misc. Geol. Inv. Map I-590, scale 1:125,000.

Wendler, G. (1973) Sea ice observation by means of satellite, J. Geophys. Res., vol. 78, no. 9, p. 1427.

Wendler, G., R. Carlson and D. Kane. (1973) Break-up characteristic of the Chena River watershed, central Alaska, in Advanced Concepts and Techniques in the Study of Snow and Ice Resources, An Interdisciplinary Symposium, 2-6 December, Monterey, California, p. 523-532.

Williams, J.R. (1970) Groundwater in the permafrost regions of Alaska, U.S. Geological Survey Prof. Paper 696, p. 18-20.

Wobber, F.V. and K.R. Martin. (1973) Exploitation of ERTS-1 imagery utilizing snow enhancement techniques, in Abstracts for Symposium of Significant Results, ERTS-1, 5-9 March, p. 38.